ACCELERATED CO_2 REMOVAL FOR ARTIFICIAL LUNG APPLICATIONS

by

David Takashi Arazawa

B.S. in Bioengineering, The Pennsylvania State University, 2008

Submitted to the Graduate Faculty of

Swanson School of Engineering in partial fulfillment

of the requirements for the degree of

Doctor of Philosophy

University of Pittsburgh

2018

UNIVERSITY OF PITTSBURGH

SWANSON SCHOOL OF ENGINEERING

This dissertation was presented

by

David Takashi Arazawa

It was defended on

July 19, 2018

and approved by

Jeremy D. Kimmel, Ph.D.
Adjunct Assistant Professor, Department of Bioengineering

Sanjeev G. Shroff, Ph.D.
Distinguished Professor and Gerald E. McGinnis Chair, Department of Bioengineering

Alan J. Russell, Ph.D.
Highmark Distinguished Career Professor, Department of Chemical Engineering
Director, Disruptive Health Technology Institute, Carnegie Mellon University

William R. Wagner, Ph.D.
Director, McGowan Institute for Regenerative Medicine, and Professor of Surgery,
Departments of Bioengineering and Chemical Engineering

Dissertation Director: William J. Federspiel, Ph.D.
William Kepler Whiteford Professor, Departments of Bioengineering, Critical Care Medicine,
and Chemical Engineering

ACCELERATED CO_2 REMOVAL FOR ARTIFICIAL LUNG APPLICATIONS

David Takashi Arazawa, Ph.D.

University of Pittsburgh, 2018

Acute and chronic lung disease remains a major problem within the healthcare industry, accounts for one in seven deaths, and places lung disease as the third leading cause of death within the United States. Carbon dioxide removal (CO_2R) devices are a viable alternative or adjuvant therapy to invasive mechanical ventilation, which can initiate and exacerbate lung injury, substantially contributing to patient mortality. The complexity and invasiveness of current respiratory assist devices used for extracorporeal CO_2R has limited widespread use in ICUs. In this work we developed a bioactive hollow fiber membrane (HFM) which accelerates CO_2 removal to facilitate the next generation of highly efficient CO_2 respiratory assist devices.

Since over 90% of blood CO_2 is transported as bicarbonate (HCO_3^-), CO_2R devices must overcome the small CO_2 partial pressures (50mmHg) across HFMs limiting CO_2 removal. Bioactive HFMs improve CO_2 removal efficiency by converting bicarbonate to CO_2 directly at the HFM surface. A 36% increase in the blood CO_2 removal rate was achieved using CA-immobilized HFMs. Thromboresistance of CA-modified HFMs demonstrated 95% less platelet deposition compared to unmodified HFM.

We characterized the CO_2 mass transport processes within these biocatalytic devices to develop approaches towards improving bioactive HFM efficiency. The diffusional resistance from the liquid boundary layer was observed as the primary impediment to CO_2 transport by both unmodified and bioactive HFMs under clinically relevant conditions. Strategies to increase CA loading on HFMs are not ideal avenues for improved efficiency of biocatalytic CO_2R devices.

Based on our findings, we proposed a bicarbonate/CO_2 disequilibrium hypothesis to describe performance of CA-modified devices in blood.

Improvement in CO_2 removal rates using CA-modified devices in blood was realized by maximizing bicarbonate/CO_2 disequilibrium at the fiber surface via blood acidification. Dilute acidic sulfur dioxide (SO_2) sweep gas created an acidic microenvironment within the diffusional boundary layer adjacent to the HFM surface, and when used in combination with bioactive CA-HFMs had a synergistic effect to more than double CO_2 removal efficiency while maintaining physiologic pH. Overall these findings revealed increased CO_2 removal can be achieved through bioactive HFMs, enabling a next generation of more efficient CO_2 removal intravascular and paracorporeal respiratory assist devices.

TABLE OF CONTENTS

LIST OF TABLES

LIST OF FIGURES

ACKNOWLEDGMENTS

I would like to thank my mentor and advisor, Dr. William J. Federspiel, for his absolute dedication and guidance throughout my time at the University of Pittsburgh. My experience in the Medical Devices Laboratory has enabled me with a depth of critical thinking, curiosity to continuously question, and wisdom that in the face the unexpected challenges lie the magic of scientific discovery. Thank you for setting the bar high, challenging each facet of my scientific journey and reshaping the lens through which I view the world. I leave inspired, hopeful and driven to advance the field of medical device technology.

I would like to thank the collaborators throughout the university who shared their time, expertise, and equipment with me. Thank you to the members of the Medical Devices Laboratory for being great colleagues and friends. The team environment and continuous collaboration was inspirational. I am privileged to have spent my time with an exceptional group of students, staff and mentors.

I would also like to acknowledge and thank my funding sources. Without support from the National Institutes of Health (NIH) and National Heart, Lung, and Blood Institute (NHLBI) (5R01HL070051-08, 5R01HL117637-05), the University of Pittsburgh CBTP training grant (NIH T32-HL076124) and Department of Bioengineering, The McGowan Institute for Regenerative Medicine, and the Commonwealth of Pennsylvania, none of this work would have been possible.

1.0 INTRODUCTION

Acute and chronic lung disease remains a major problem within the healthcare industry. In the United States alone over 350,000 Americans die of lung related illness [1]. The lifesaving efforts of traditional therapy such as mechanical ventilation (MV) are often marred by unfavorable effects which initiate and more often exacerbate lung injury, substantially contributing to patient morbidity and mortality [2]. Breathing support independent of the lungs through low blood flow CO_2 removal devices are needed as a tool for the management of acute and possibly chronic respiratory insufficiency [3–9]. Several novel respiratory assist devices which mechanically enhance gas exchange have been developed and proposed, however further improvement in efficiency is still desired. The objective of this thesis was to develop and characterize a novel bioactive approach to substantially increase CO_2 exchange in blood. This chapter describes two common forms of lung disease where efficient CO_2 removal devices are desired, Chronic Obstructive Pulmonary Disease (COPD) and Acute Respiratory Distress Syndrome (ARDS), as well as their current treatment strategies. The basic principles of gas exchange in CO_2 removal devices and the role of carbonic anhydrase in carbon dioxide transport are detailed.

1.1 LUNG FAILURE AND CURRENT TREATMENT STRATEGIES

1.1.1 Respiratory Diseases

Approximately 30 million Americans are estimated to be living with some form lung disease [1]. Chronic obstructive pulmonary disease (COPD) results in 400,000 hospitalized patients per year with a rate of incidence that has tripled over the last ten years [10]. Adult respiratory distress syndrome (ARDS) affects 190,000 per year and even more has a mortality rate of 40% [6,11]. Considering these staggering statistics, medical management is still the standard of care for preliminary therapy. This basic approach quickly becomes limited throughout disease progression and as a result the demand for viable therapies and artificial support are ever prominent today.

COPD is the third leading cause of death within the United States and currently affects an estimated 23.6 million adults [12,13]. In total the economic costs of COPD are growing within the United States, from $32 billion in 2002 to $43 billion in 2007 [14,15] Direct medical expenditures are largely related to in-hospital care. The characteristic symptoms of COPD are chronic and progressive dyspnea, cough, and sputum production [16]. Often associated with a history of smoking, COPD is a group of progressive and often interconnected respiratory disease processes: (1) airway thickening and narrowing with expiratory airflow obstruction; (2) chronic mucus hypersecretion, resulting in chronic cough and phlegm production; and (3) emphysema, an abnormal dilation of distal airspaces combined with destruction of alveolar walls [17,18]. An exacerbation of COPD is an acute event characterized by a worsening of the patient's respiratory symptoms that is beyond normal day-to-day variations and leads to a change in medication [16,19]. Acute exacerbations of COPD can onset from bacterial exposure, viral infection, or exposure to pollution [20]. More than 80% of exacerbations can be managed on an outpatient basis with

pharmacologic therapies including bronchodilators, corticosteroids, and antibiotics [16,21]. While these pharmacologic agents are available to control symptoms and reduce the occurrence of COPD exacerbations, they have not been shown to modify the long-term decline of lung function in COPD patients [16,17]. In 15-25% of patients, exacerbations result in moderate-to-severe respiratory acidosis (pH < 7.25 and/or $PaCO_2$ > 45 mmHg) requiring invasive mechanical ventilation (IMV) [22]. Up to 30% of intubated patients with COPD die while on the ventilator [23].

A life-threatening condition of critically-ill patients, acute respiratory distress syndrome (ARDS) has been observed with a mortality rate of 40 to 45% and reported to afflict 190,000 patients each year [6,24,25]. Overall 28-day mortality was recently reported at a controversial 25-30%, in specialized centers with selection criteria of randomized clinical trials [26]. ARDS is characterized by abrupt onset of clinically significant hypoxemia and described by diffuse alveolar damage which leads to inflammation and fluid infiltration of the alveoli, limiting gas exchange and decreasing lung compliance due to fibrosis [27]. Patients usually have varying degrees of pulmonary artery vasoconstriction and may subsequently develop pulmonary hypertension [28]. Diagnosis is made by a history of a predisposing illness, acute onset, bilateral pulmonary infiltrates on chest X-ray, and severe hypoxemia [24]. ARDS can be caused by both direct and indirect lung injury, from pneumonia, gastric aspiration, drowning, smoke or toxic gas inhalation, and pulmonary contusion, to sepsis, transfusions, shock and pancreatitis [29]. Few therapeutic modalities exist to ameliorate this deadly condition. Invasive mechanical ventilation with low tidal volumes has been the most effective strategy to prevent lung injury and improve survival to date [27,28]. For most patients an outcome is determined within 7-10 days, by which time nearly half

of patients will have died from hypoxemia and multi-organ failure, or been weaned from treatment [30].

1.1.2 Current Treatment Strategies

Medical treatment for acute and chronic respiratory failure remains a significant healthcare problem in the US, with over several hundred thousand adult patients each year [31,32]. When pharmacotherapy and non-invasive ventilation fail, patients suffering from ARDS or acute exacerbations of COPD are transitioned to mechanical ventilation. After intubation and sedation, forced respiration through positive pressure can support adequate gas exchange in these patients for days, usually at the risk of ventilator-induced lung injuries (VILI) which may further exacerbate acute respiratory insufficiency [1]. Historically the primary goal was to achieve near normal arterial blood gasses though large plateau pressures (P_{plat} >30 cmH_20) and tidal volumes (V_T = 12 mL/kg), roughly 50-100% greater volume than healthy spontaneously breathing individuals (5-7 mL/kg) [27]. These invasive mechanical ventilation settings are known to be a major contributor to VILI, which can lead to lung damage such as volutrauma (over-distension of the lung), barotrauma (over pressurization of the lung), atelectrauma (shear stress on the epithial cells of the alveoli due to repetitive closing and opening of the alveolar sac), and biotrauma (lung injury due to inflammation) [1,6,27,33]. Advancements in mechanical ventilation have focused on reducing VILI through lung protective ventilation (LPV) strategies.

Patients suffering from acute exacerbations of severe COPD are often associated with hypercapnic respiratory failure requiring hospitalization and respiratory support. IMV has demonstrated no benefit in outcomes for this population as compared to no treatment, has demonstrated a risk of prolonged weaning when compared to other hypercapnic respiratory failure,

and has a mortality rate as high as 39% [23,34]. While the risks of VILI have been alleviated for this patient population through LPV strategies, recent reviews established further benefit by avoiding intubation altogether through use of a facial mask for respiration. This approach termed non-invasive positive pressure ventilation (NPPV) is now the standard of care and has reduced hospital mortality rates by 55%. However NPPV is not successful in all cases of acute or chronic COPD, with failure rates between 9% and 50% [22,35]. Despite the continued advancement in non-invasive ventilation strategies, patient's initial blood pH during admission is a strong predictor and the most important variable in determining their outcome during NPPV [36–38]. A blood pH less than 7.25 has a predicted risk of failure >70% and if this pH persists for more than two hours, the risk of failure significantly increases to >90% [39]. The complications surrounding NPPV failure including hypercapnia, severe acidosis, dyspnea and increased respiratory rate are the result of a limited ability to properly ventilate CO_2 [36]. Patients transitioned to IMV after failing NPPV have demonstrated higher mortality rates than patients who were initially treated with IMV [40,41]. The use of higher ventilation rates through restricted airways exacerbates lung damage and leads to concomitant complications including pneumothorax and pneumomediastinum [36]. Managing IMV settings to reduce pressure or volume and prevent complications leads to CO_2 retention, blood acidosis, and downstream can prevent successful weaning from MV. Further research has estimated up to a 23% increase in metabolic CO_2 production in patients with acute exacerbations of COPD due to the increased work of breathing, and up to 26% of patients require ventilatory support to supplement the removal of CO_2 [42]. The complications around CO_2 management for the COPD patient population highlight a need for adjuvant therapeutic modalities which can regulate blood CO_2 independent of mechanical ventilator settings, enabling LPV and NPPV strategies and facilitating weaning [36].

In patients suffering from ARDS, the mortality rate remains unacceptably high even with the introduction of LPV strategies. The seminal ARDS Network trial demonstrated that delivery of low tidal volume MV at 6mL/kg instead of 12 mL/kg resulted in reduced lung injury and improved survival by 22% [43]. While LPV strategies can sufficiently oxygenate patients, sufficient CO_2 removal remains a challenge and necessitates higher tidal volumes. Clinicians are often unable to apply LPV strategies, reporting hypercapnia and acidosis as significant barriers to implementation, as exhibited in 14% of the ARDS Network trial patients [44,45]. Permissive hypercapnia is an approach shown to positively impact oxygenation and attenuate inflammation, however improvements in mortality were only seen in patients ventilated with high tidal volumes [6,45]. Alveolar over-distention is still seen at 6mL/kg, exposing the ARDS lung to 25- to 30-times the mechanical stress of a normal lung [3,46]. Evidence suggests the observed reduction in mortality is linearly correlated with tidal volume and even more protective MV settings (< 6 mL/kg) are needed. Further investigation into the effectiveness of these ultra-protective MV settings (V_T = 4 mL/kg, $P_{plat} \leq 25$ cmH_2O) necessitates strategies to manage the unavoidable hypercapnia and thereby open the door to ultra-protective MV settings [6,47]. Today mortality rates remain between 40 and 45% for ARDS ICU patients [24]. Extracorporeal carbon dioxide removal is one possible strategy to control blood CO_2 independent of alveolar ventilation, decreasing MV requirements and facilitating lung rest.

The use of extracorporeal gas exchange for support of acute respiratory failure began in 1972 as cardio-pulmonary bypass [48]. Aimed at providing full oxygenation to allow the lungs to rest and heal, extracorporeal membrane oxygenation (ECMO) facilitates gas exchange independent of the lungs. High cost, complexity and incidence of adverse events has relegated this therapy to the sickest of patients as a last ditch lifesaving effort [33,36]. As experience with MV

developed it was appreciated that a significant portion of gas exchange could be realized through native lung tissues under LPV, and extracorporeal gas exchange was needed primarily for CO_2 removal rather than oxygenation [36]. An approach to focus on partial extracorporeal CO_2 removal was first explored by Gattioni in 1986, who was able to maintain NPPV by removing only 33% of basal CO_2 production [49]. Although early studies on partial CO_2 removal relied on the same large gas exchangers and complex circuits typically used in ECMO, the focus towards CO_2 removal enabled their use at much lower blood flow rates compared to the high blood flow rates required for blood oxygenation. This advantage lies in CO_2 and O_2 kinetics, where 1 liter of venous blood hemoglobin will saturate with up to an additional 60 mL of O_2, while conversely 250 mL of CO_2 can be removed from 1 liter of arterial blood [6]. Partial $ECCO_2R$ reduced the risk of typical ECMO by employing lower blood flow rates at 0.4 – 0.6 L/min (with 12 Fr cannula) compared to the 4 - 7 L/min (17 – 23 Fr cannula) typical of ECMO [36,50,51]. Several animal studies have validated improved survival with $ECCO_2R$ compared to conventional mechanical ventilation and low tidal volume ventilation [52,53]. A case report in 1990 highlighted partial $ECCO_2R$ at very low flow rates (<0.5 L/min), proving that minimally invasive approach could enable liberation from MV and even foster spontaneous breathing [54]. More recently, the CESAR study demonstrated enhanced survival benefit for lung-rest ventilation in tandem with ECMO as compared to protective ventilation alone [55]. These studies highlight extracorporeal CO_2 removal is a powerful alternative or adjuvant therapy to MV in patients suffering from acute lung failure. The safety and effectiveness of $ECCO_2R$ systems to facilitate ultraprotective ventilation strategies was recently evaluated in the SUPERNOVA trial (A Strategy of Ultraprotective Lung Ventilation with Extracorporeal CO_2 Removal for New-Onset Moderate to Severe ARDS), sponsored by the European Society of Intensive Care Medicine [11]. While ECMO devices can be employed for

CO_2 removal, a significant and unmet need exists for a highly efficient CO_2 removal device specific to minimally invasive therapy for $ECCO_2R$ [6].

1.2 PRINCIPLES OF GAS EXCHANGE IN CO_2 REMOVAL DEVICES

Current artificial lungs, ECMO or $ECCO_2R$ devices employ the use of microporous polymer tubes, termed hollow fiber membranes (HFMs), that act as the blood gas interface for gas exchange. The typical extracorporeal device consists of a large bundle of hollow fiber membranes contained within a housing, inlets and outlets for blood and oxygen gas, and a heat exchanger to maintain body temperature as the blood returns to the patient (Figure 1.1). Gas exchange occurs as blood flows along the outside of the HFMs while an oxygen sweep gas flows through the fiber lumen, creating a diffusional partial pressure gradient is driving gas exchange across the fiber membrane. Oxygen diffuses from the inside fiber lumen to the outer fiber surface, traveling down its gradient and into the blood. Conversely CO_2 diffuses from the blood and into the fiber lumen while traveling down it's diffusional gradient. As a result blood is oxygenated, and CO_2 is removed as the sweep gas flows out of the device (Figure 1.2). Hollow fibers used in respiratory support are comprised of hydrophobic polypropylene (PP) or polymethylpentene (PMP) polymers, which are designed to facilitate gas exchange by being impermeable to fluids while maintaining the gas filled pores of the membrane wall. Each hollow fiber is approximately 200-400 μm in diameter and has a microporous wall of 20-50 μm [1]. Common oxygenators are designed to maximize gas exchange efficiency while minimizing the blood priming volume, blood flow resistance and membrane surface area.

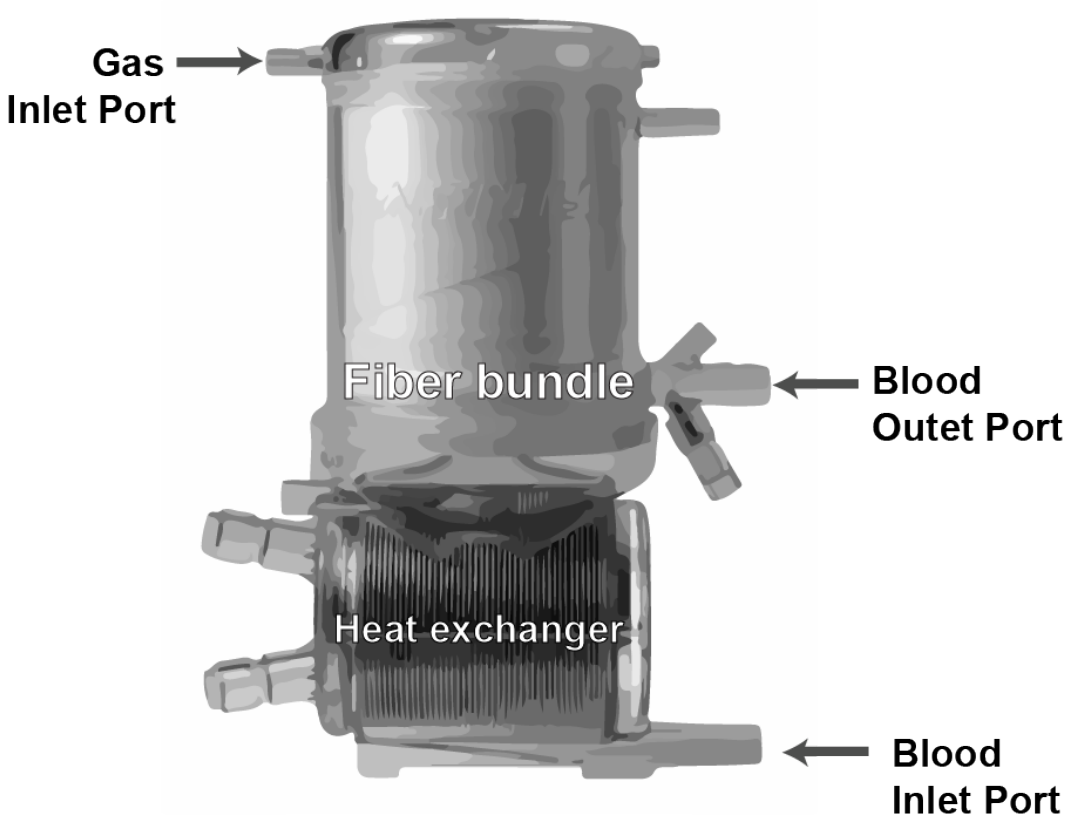

Figure 1.1 Commonly use extracorporeal membrane oxygenator, the Medtronic Affinity® NT.

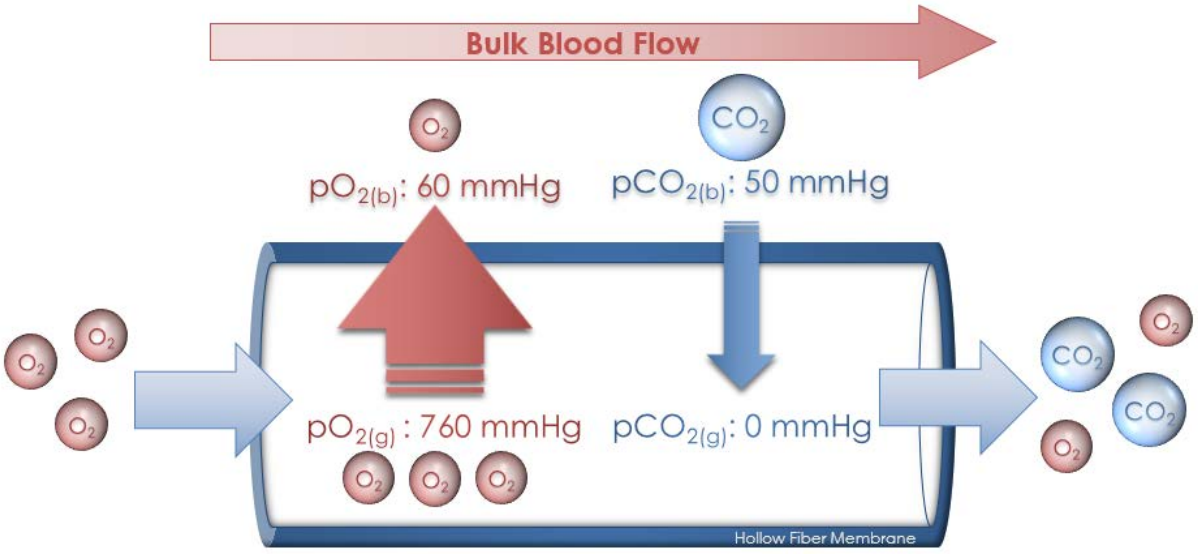

Figure 1.2 Diffusion of oxygen and carbon dioxide across as hollow fiber membrane.

1.2.1 Mass Transport in Hollow Fiber Membranes

The phenomenon governing diffusion of gasses across hollow fiber membranes is well characterized by the following series of mass transport equations. Fick's Law describes diffusional flux as proportional to concentration gradient, where a species will flux from regions of high concentration to regions of low concentration. This equation can be rearranged to yield the following equations describing the gas exchange rates for O_2 and CO_2 [1,56,57].

$$\dot{V}_{O_2} = K_{O_2} A \left(P_{O_2(g)} - P_{O_2(b)} \right) \quad \textbf{Equation 1.1}$$

$$\dot{V}_{CO_2} = K_{CO_2} A \left(P_{CO_2(b)} - P_{CO_2(g)} \right) \quad \textbf{Equation 1.2}$$

In this form $\dot{V}$ represents the overall exchange rate of each gas species, K the gas permeance (commonly known as the mass transfer coefficient), A the total blood contacting area of a hollow fiber bundle, and P the partial pressure of each gas in the blood or gas phases. The above mass transport equations describe an increase gas exchange can be achieved by increasing the fiber membrane surface area, partial pressure gradient or permeance each gas encounters.

The overall diffusional resistance is the sum of diffusional resistances, which can be described as the inverse of gas permeance (K^{-1}) [1,56].

$$K^{-1} = K_g^{-1} + K_m^{-1} + K_b^{-1} \quad \textbf{Equation 1.3}$$

This is characterized by the resistance each gas encounters within the gas pathway (K_g^{-1}), the membrane (K_m^{-1}) and blood (K_b^{-1}). Transfer resistance due to the gas pathway (K_g^{-1}) is negligible and can be eliminated [1]. The overall diffusional resistance is dominated by gas movement through blood side diffusional boundary layer adjacent to the fiber surface, and less importantly the membrane diffusional resistance. This blood side resistance is related to the diffusional boundary layer thickness, which exists due to the no slip condition where a reduction in blood

velocity occurs by drag forces as it flows over the membrane surface reaching zero velocity relative to the HFM surface. The loss of convection near the HFM surface means oxygen and carbon dioxide gas molecules must traverse the entire thickness of the boundary layer via diffusion before reaching the convective blood flowing past the HFM surface or sweep gas within the fiber lumen. The rate of gas exchange is dictated by a serial transport process of the membrane and blood resistance, which add directly to determine overall resistance [1]. Consequently, gas exchange is influenced by both the diffusional resistance and partial pressure gradient when traveling from gas to blood or vice versa. Decreasing the diffusive boundary layer thickness by directly increasing blood velocity via mechanical forces and employing cross flow fiber orientation (rather than parallel) has been the focus of several novel respiratory assist devices to actively increase CO_2 removal [1,36,56,58–60]. The focus of this thesis has been to explore chemical means of accelerating CO_2 removal beyond relatively small partial pressure gradients which naturally exist. The partial pressure diffusional gradient driving carbon dioxide removal is nearly 93% less than partial pressure gradient for blood oxygenation, where P_{CO_2} is approximately 50 mmHg while P_{O_2} is approximately 700 mmHg. Since over 90% of blood CO_2 is transported as bicarbonate (HCO_3^-), CO_2 removal devices are challenged by the small CO_2 partial pressure gradients across HFMs which limit CO_2 removal.

1.2.2 The Role of Carbonic Anhydrase in CO_2 Transport

Within the body CO_2 is transported in three different forms, dissolved CO_2 gas, bicarbonate (HCO_3^-), and carbamate (CO_3^{2-}). Only small portion of arterial CO_2 is present as dissolved gas or carbamate. The majority (>90%) of CO_2 in the body is transported as bicarbonate and at normal pH 7.4, HCO_3^- is 20 fold that of gaseous CO_2 [61]. The contribution of bicarbonate to overall CO_2

transport was first described by Longmuir in 1966 as "facilitated CO_2 diffusion" [62]. As CO_2 is produced within the intracellular space of muscle tissue, it enters convective blood flow and readily diffuses within red blood cells to encounter the enzyme carbonic anhydrase (CA) which catalyzes the interconversion of CO_2 by the following reaction $CO_2 + H_2O \overset{CA}{\Leftrightarrow} HCO_3^- + H^+$. Without CA the hydration / dehydration reaction would require more than 1 min to approach completion, but is accelerated nearly 25,000 fold by CA to completion within 2 ms [61,63]. Upon reaching the lungs, bicarbonate is catalytically dehydrated back to gaseous CO_2 by CA within red blood cells and on the endothelial surfaces of lung capillaries to accelerate CO_2 excretion by the lungs [64]. Hollow fiber membrane devices must overcome the small CO_2 partial pressures (50mmHg) across HFMs limiting CO_2 removal which our tissues face. Therefore, in this work we propose a biomimetic approach to facilitate CO_2 removal by generating diffusional gradients through the immobilized carbonic anhydrase, which converts bicarbonate to CO_2 directly at the HFM surface.

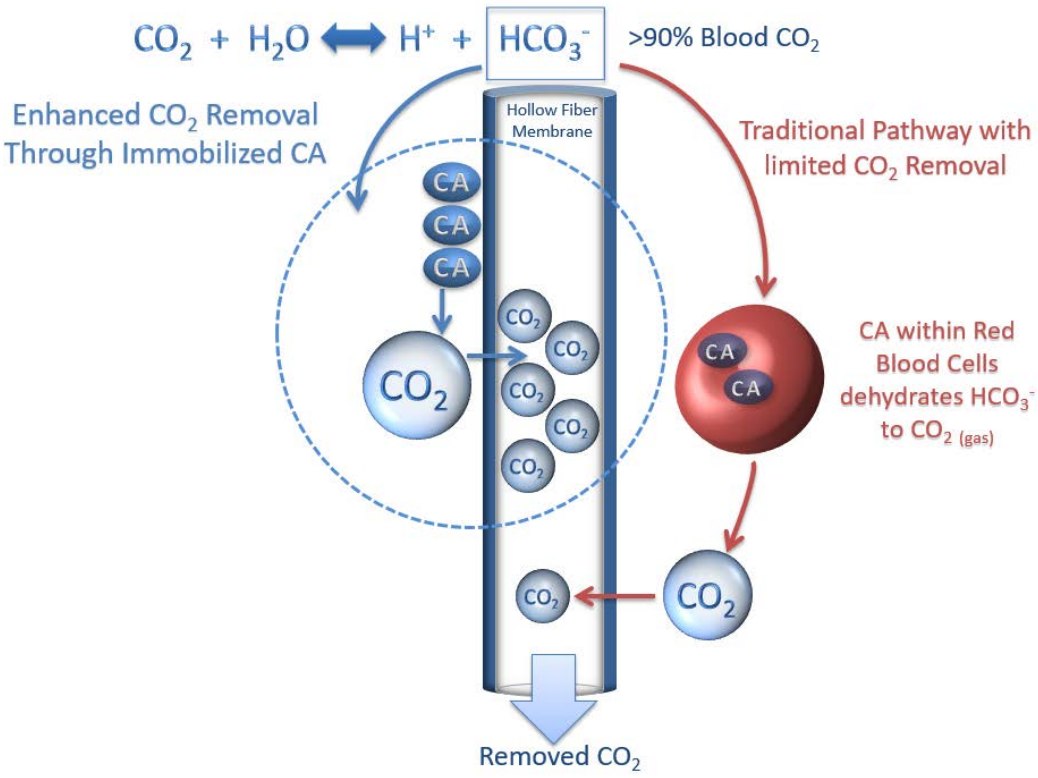

Figure 1.3 Carbonic anhydrase immobilized on HFMs facilities CO_2 removal by converting bicarbonate to CO_2 directly at the HFM surface.

1.3 CURRENT CO_2 REMOVAL DEVICES

A highly efficient, low flow CO_2 removal device offers an adjunct therapy for acute and possibly chronic respiratory insufficiency. $ECCO_2R$ in combination with LPV has not seen widespread application as current devices require surgical placement of cannula 19 Fr or larger to facilitate blood flow rates up to 1 L/minute or higher, in order to remove a significant fraction (50%) of total adult CO_2 production [3,9]. Several novel respiratory assist devices have been developed and/or proposed which mechanically enhance gas exchange by actively mixing the blood flow over the HFM surface. These devices could decrease patient ventilator needs by more than 50% relieving

dyspnea and distress while requiring blood flow rates as small as 300-500 mL/min [3]. Novalung (Baden-Württemberg, Germany) and Hemolung (Alung Technologies, Pittsburgh PA) are a realization of low flow partial CO_2 removal devices, capable of eliminating 20-30% of resting metabolic CO_2 production. Pumpless, percutaneous and arteriovenous, the Novalung device has been recognized for its CO_2 removal capacity in facilitating lung protective MV settings[65]. Despite the promising de-escalation of invasive ventilatory variables, arterial canulation systems have shown complication rates as high as 24% leading to limb ischemia, compartment syndrome, and intracranial hemorrhage, in part due to their demand for approximately 25% of cardiac output [66]. To avoid such difficulties, the Hemolung employs a venovenous system incorporating the pump and hollow fiber membranes (HFMs) as one cartridge and a 15.5 Fr dual-lumen cannula. The central cylindrical core of the device rotates adjacent hollow fiber membrane, generating an active mixing effect within the HFM bundle, reducing the diffusional boundary layers and increasing CO_2 removal by up to 60%. This allows the Hemolung to reduce the fiber surface area (0.59 m^2) required for respiratory support and additionally washes the fiber surface to minimize thrombus formation [67]. While offering the first steps in CO_2 removal these devices' efficiency can be further improved towards increasing overall CO_2 removal, decreasing blood contacting surfaces areas and lowering blood flow rates, thereby expanding their audience for therapeutic potential. An ideal low flow CO_2 removal device would eliminate up to 200 ml/min carbon dioxide to meet the metabolic needs for an adult patient on cardiopulmonary bypass [68]. To achieve this goal the devices must overcome the small CO_2 partial pressures (50mmHg) across HFMs limiting CO_2 removal. Since more than 90% of blood CO_2 is carried as HCO3- (bicarbonate), a chemical means of increasing gas exchange efficiency is needed.

Two unique approaches to chemically increase CO_2 removal through blood acidification or electrodialysis have been explored. Blood acidification was first described by Snider et al. in 1987, in which infusion 2-8 mEq/min of lactic acid infusion was used to chemically increase trans-HFM CO_2 pressure gradients by acidifying the blood entering the $ECCO_2R$ devices, shifting equilibrium from bicarbonate to favor gaseous CO_2 and increasing CO_2 removal by 120-170%, however visible hemolysis was present [69]. More recently, Zanella et al. have refined this approach to mitigate hemolysis concerns[70–73]. In their work, whole blood acidification was performed utilizing lactic acidic (LA) mixed with bulk extracorporeal blood via direct infusion or dialysis, upon which acidified blood flowed into a HFM device for CO_2 removal, with no significant indications of red blood cell or organ damage [70–73]. When directly infusing LA with 500 mL/min extracorporeal blood flow rate, a 70% increase in CO_2 removal (up to 95 mL/min/m^2) was observed, and when using a dialysis membrane to acidify blood with 250 mL/min blood flow rate, a 62-78% increase in CO_2 (up to 160 mL/min/m^2). The pH drop observed in the acidified blood was similar to the pH values measured in human capillaries during heavy exercise [61]. Additionally, blood acidification offsets respiratory alkalosis as the blood leaving $ECCO_2R$ devices without acidification have an increased pH [70]. Clinically, lactate is monitored as a biomarker of organ dysfunction, shock and has been correlated with increased mortality in critically ill patients [74–79]. Consequently, addition of exogenous LA may limit the diagnostic potential of blood lactate levels as a predictor of adverse outcomes. Zanella et al. have additionally explored electrodialysis to augment CO_2 removal by acidifying blood with a transient increase in blood chloride [80,81]. At a blood flow rate of 250 mL/min, a 75% increase in CO_2 removal rate was observed (up to 140 mL/min/m^2). This approach could be used to modulate the balance between anions-cations in blood and therefore help manage acid-base balance in blood, however

it adds significant complexity to the circuit. Further testing is ongoing to determine safety with respect to renal function.

1.4 OBJECTIVES FOR ACCELERATED CO_2 REMOVAL

Augmenting carbon dioxide removal remains a major challenge in the development of highly efficient artificial lungs and respiratory assist devices. This thesis covers work to develop a hollow fiber membrane coating capable of selectively accelerating CO_2 removal from blood through facilitated diffusion of bicarbonate to the membrane surface.

Aim 1: The first goal of this work was to assess and optimize the impact of CA-modified HFMs on both CO_2 removal efficiency from blood and hemocompatibility (Chapter 2: Arazawa DT, Oh H-I, Ye S-H, Johnson Jr. CA, Woolley JR, Wagner WR, Federspiel WJ. Immobilized carbonic anhydrase on hollow fiber membranes accelerates CO_2 removal from blood. J Membr Sci 2012;403–404:25–3). Overall these findings revealed increased CO_2 removal and decreased platelet deposition can be realized through bioactive HFMs, and increasing immobilized CA activity could further improve CO_2 removal efficiency.

Aim 2: Bioconjugation methods to further increase the CA loading on HFMs and subsequently improve the impact of CA on HFM CO_2 removal were examined (Chapter 3). We developed a stable amine based conjugation strategy and interrogated surface amine group density, crosslinker length and necessity of binding site amplification towards maximizing CO_2 removal efficiency. While increasing total immobilized CA, it was appreciated further improvement beyond CA loading would be necessary for the development of next-generation minimally invasive CO_2 removal devices.

Aim 3: We characterized the CO_2 mass transport processes within these biocatalytic devices which impede CA coating efficacy, and developed approaches towards improving bioactive HFM efficiency (Chapter 4: Arazawa DT, Kimmel JD, Federspiel WJ. Kinetics of CO_2 exchange with carbonic anhydrase immobilized on fiber membranes in artificial lungs. J Mater Sci Mater Med 2015;26). Based on our findings, we proposed a bicarbonate/CO_2 disequilibrium hypothesis to describe performance of CA-modified devices in both buffer and blood.

Aim 4: Improvement in CO_2 removal rates using CA-modified devices in blood may be realized by maximizing bicarbonate/CO_2 disequilibrium at the fiber surface via strategies such as blood acidification (Chapter 5: Arazawa DT, Kimmel JD, Finn MC, Federspiel WJ. Acidic sweep gas with carbonic anhydrase coated hollow fiber membranes synergistically accelerates CO_2 removal from blood. Acta Biomater 2015; 25:143–9). Since HFM CO_2 removal is driven by trans-HFM pressure gradients, it should not be necessary to acidify the blood bulk fluid, but instead only the diffusional boundary layer adjacent to the HFM surface via an acidic sweep gas.

This thesis describes the unique approach of a carbonic anhydrase HFM coating capable of significantly accelerating CO_2 removal through facilitated diffusion. Through these technologies the next generation of intravascular and paracorporeal respiratory assist devices can remove more CO_2 with smaller blood contacting surface areas. Bioactive HFMs are a promising step towards the design of more efficient and hemocompatible HFM-based artificial lungs.

2.0 IMMOBILIZED CARBONIC ANHYDRASE ON HFMS IN BLOOD

The following chapter presents work peer-reviewed and published in the Journal of Membrane Science without modification [82]: Arazawa DT, Oh H-I, Ye S-H, Johnson Jr. CA, Woolley JR, Wagner WR, Federspiel WJ. Immobilized carbonic anhydrase on hollow fiber membranes accelerates CO_2 removal from blood. J Membr Sci 2012;403–404:25–3. The abstract of the paper follows:

2.1 SUMMARY

Current artificial lungs and respiratory assist devices designed for carbon dioxide removal (CO_2R) are limited in their efficiency due to the relatively small partial pressure difference across gas exchange membranes. To offset this underlying diffusional challenge, bioactive hollow fiber membranes (HFMs) increase the carbon dioxide diffusional gradient through the immobilized enzyme carbonic anhydrase (CA), which converts bicarbonate to CO_2 directly at the HFM surface. In this study, we tested the impact of CA-immobilization on HFM CO_2 removal efficiency and thromboresistance in blood. Fiber surface modification with radio frequency glow discharge (RFGD) introduced hydroxyl groups, which were activated by 1M CNBr while 1.5M TEA was added drop wise over the activation time course, then incubation with a CA solution covalently linked the enzyme to the surface. The bioactive HFMs were then potted in a model gas exchange device (0.0084 m^2) and tested in a recirculation loop with a CO_2 inlet of 50mmHg under steady blood flow. Using an esterase activity assay, CNBr chemistry with TEA resulted in 0.99U of

enzyme activity, a 3.3 fold increase in immobilized CA activity compared to our previous method. These bioactive HFMs demonstrated 108 ml/min/m^2 CO_2 removal rate, marking a 36% increase compared to unmodified HFMs ($p < 0.001$). Thromboresistance of CA-modified HFMs was assessed in terms of adherent platelets on surfaces by using lactate dehydrogenase (LDH) assay as well as scanning electron microscopy (SEM) analysis. Results indicated HFMs with CA modification had 95% less platelet deposition compared to unmodified HFM ($p < 0.01$). Overall these findings revealed increased CO_2 removal can be realized through bioactive HFMs, enabling a next generation of more efficient CO_2 removal intravascular and paracorporeal respiratory assist devices.

2.2 INTRODUCTION

Over the last 10 years carbon dioxide (CO_2) removal has been emphasized to improve survival outcomes for patients suffering from acute lung failure. Due to significant limitations in its clinical application, the lifesaving efforts of traditional therapy such as mechanical ventilation (MV) are often marred by unfavorable effects which initiate and more often exacerbate lung injury, substantially contributing to patient morbidity and mortality [2]. Consequently, breathing support independent of the lungs through low blood flow CO_2 removal devices are needed as a tool for the management of acute and possibly chronic respiratory insufficiency. Considering current respiratory assist devices designed for extracorporeal carbon dioxide removal can require blood flow rates of 1 L/min for to extract a therapeutic level of carbon dioxide, advances in CO_2 removal membranes with sufficient clinical impact has yet to be realized. Development of a bioactive

hollow fiber membrane (HFMs) which facilitates CO_2 removal may provide the next generation of highly efficient CO_2 removal membranes for respiratory assist devices.

Medical treatment for acute and chronic respiratory failure remains a significant healthcare problem, with over several hundred thousand adult patients in the US [31,32]. High tidal volume ventilation known to be a major contributor to ventilator induced lung injury could be avoided by decreasing ventilatory needs of the patient through extracorporeal carbon dioxide removal. The seminal acute respiratory distress syndrome (ARDS) Network trial demonstrated that delivery of low tidal volume MV at 6mL/kg instead of 12 mL/kg resulted in reduced lung injury and improved survival[43]. Evidence suggests however, that even more protective MV settings are needed as alveolar over-distention is still seen at 6mL/kg exposing the ARDS lung to 25- to 30-times the mechanical stress of a normal lung[3,46]. These patients are susceptible to micro vascular occlusion and alveolar dead space which lead to under perfused respiratory units limited in gas exchange[83,84]. Control of PCO_2 independent of alveolar ventilation is possible through extracorporeal carbon dioxide removal, decreasing MV requirements and facilitating lung rest. For patients suffering from acute exacerbation of chronic obstructive pulmonary disease (COPD), MV could be avoided as CO_2 removal itself maybe adequate. Zwischenberger et al. have shown improved survival with arterio-venous CO_2 removal ($AVCO_2R$) compared to conventional mechanical ventilation, high frequency percussive ventilation and low tidal volume ventilation, observing recovered lung cell proliferation and tissue architecture along with reduced apoptosis through $AVCO_2R$ treatments in model sheep ARDS [52,53]. More recently, the CESAR study demonstrated enhanced survival benefit for lung-rest ventilation in tandem with ECMO as compared to protective ventilation alone [55]. These studies demonstrate CO_2 removal is a powerful alternative to MV in patients suffering from acute lung failure.

A highly efficient, low flow CO_2 removal device offers an adjunct therapy for acute and possibly chronic respiratory insufficiency. Several novel respiratory assist devices have been developed and/or proposed which mechanically enhance gas exchange by actively mixing the blood flow over the HFM surface. These devices could decrease patient ventilator needs by more than 50% relieving dyspnea and distress while requiring blood flow rates as small as 300-500 mL/min[3]. Novalung (Baden-Württemberg, Germany) and Hemolung (Alung Technologies, Pittsburgh PA) are a realization of low flow partial CO_2 removal devices, capable of eliminating 20-30% of resting metabolic CO_2 production. Pumpless, percutaneous and arteriovenous, the Novalung device has been recognized for its CO_2 removal capacity in facilitating lung protective MV settings[65]. Despite the promising de-escalation of invasive ventilatory variables, arterial canulation systems have shown complication rates as high as 24% leading to limb ischemia, compartment syndrome, and intracranial hemorrhage, in part due to their demand for approximately 25% of cardiac output[66]. To avoid such difficulties, the Hemolung employs a venovenous system incorporating the pump and hollow fiber membranes (HFMs) as one cartridge. While offering the first steps in CO_2 removal these devices are limited in their efficiency, and therefore limited in their audience for therapeutic potential. An ideal low flow CO_2 removal device would eliminate up to 200 ml/min carbon dioxide to meet the metabolic needs for an adult patient on cardiopulmonary bypass[68]. To achieve this goal the devices must overcome the small CO_2 partial pressures (50mmHg) across HFMs limiting CO_2 removal. Since more than 90% of blood CO_2 is carried as HCO3- (bicarbonate), a chemical means of increasing gas exchange efficiency is needed.

We propose a bioactive HFM to facilitate CO_2 removal by increasing the diffusional gradient at the HFM surface through immobilization of carbonic anhydrase (CA), an enzyme

which dehydrates bicarbonate to CO_2. Our tissues face the same diffusional challenges as HFM devices; however they employ CA within red blood cells and on the endothelial surfaces of lung capillaries to accelerate diffusion. In a biomimetic approach, we reported the development of a carbonic anhydrase (CA) immobilized bioactive HFM coating[85]. Through radio frequency flow discharge (RFGD) treatment hydroxyl groups were deposited upon the fiber membrane. Scanning electron microscopy (SEM) and gas permeance tests demonstrated an exposure time of 30 sec and 25W did not affect the integrity and gas permeability of the HFMs. After CNBr activation and CA coupling, further gas permeance data indicated CA does not impede gas diffusion across the membrane. These CA HFMs demonstrated the ability to improve CO_2 removal rates by 75% from PBS in small gas exchange devices (0.0074 m^2) compared to unmodified devices [85].

In respiratory assist devices where HFM surface area can be greater than 1 m^2, hemocompatibility is a major concern. A wide variety of surface modification techniques currently exist and have been evaluated to reduce the thrombogenicity of blood-material interaction [86–88]. However, to date there are few reports specifically focused on HFMs utilized in artificial lung applications, especially those employing plasma polymerization and bioconjugation techniques. Platelet adhesion and subsequent protein-based coagulation cascades are well known mechanisms of thrombus formation on the surfaces of polymeric materials [89]. As a result, large blood-contacting surface presents significant challenges in terms of hemocompatibility for HFMs, where clots can reduce performance of respiratory assist devices and even prevent blood flow [90]. Next generation respiratory assist devices will need improved hemocompatibility of HFMs for the successful continued operation. While heparin coated materials are well known for enhanced hemocompatibility [91], a single coating capable of significantly enhancing gas exchange while

simultaneously decreasing thrombogenicity could afford the next generation of low flow CO_2 removal device with minimal complications.

This present study sought to further improve CA immobilization upon HFMs through optimized CNBr chemistry, quantify HFM CO_2 removal performance in blood and assess hemocompatibility of a CA coating. HFMs were plasma RFGD treated to create surface functional groups, to which CNBr activation chemistry was optimized with TEA and finally incubated with CA solution for covalent conjugation to the HFM surface. The improved CA modified HFMs were fabricated into model gas exchange devices to assess CO_2 removal performance from blood under a mass transfer environment similar to those of commercially available oxygenators. Platelet deposition was quantified through lactate dehydrogenase assay and SEM. Our study demonstrates CA immobilized HFMs are a viable means of augmenting CO_2 removal and hemocompatibility for artificial lung devices.

2.3 METHODS

2.3.1 Materials

Carbonic anhydrase (CA) from bovine erythrocytes, cyanogen bromide (CNBr), triethylamine (TEA), paranitrophenol acetate (pNPA), N,N'-dimethylbarbituric acid, Triton X-100, glutaraldehyde and acetone were purchased from Sigma-Aldrich (St. Louis, MO). A commercial polymethyl-pentene (PMP) fiber (Oxyplus^{TM}, OD: 380 μm, ID: 200 μm) was obtained from Membrana GmbH (Wuppertal, Germany). Bovine blood for the gas exchange experiments was

purchased from Lampire Biological Laboratories (Pipersville, PA). All other reagents were purchased from Sigma-Aldrich and were of analytical grade or purer.

2.3.2 CA Immobilization on HFMs

HFMs were modified with water plasma using a RFGD instrument (March Plasma Systems, Concord, CA) under conditions of 25 W and 30 s treatment time. After plasma modification, the HFMs were immersed in 60% acetone solution equlibrated to -15C^{o} through an ice bath, to which a solution of cyanogen bromide (CNBr) in acetone was added to a yield a final 1M CNBr concentration. While vigorously mixed, 1.5 M TEA was added drop wise over 3 minutes to yield a final ratio of 1:1.5 CNBr:TEA. The HFMs were subsequently rinsed 3 times for 3 minutes each with deionized water (DIW). The reaction time was optimized through the cyanate ester assay to maximize cyanate ester production, while the rinse time was optimized to remove any residual CNBr. The activated HFMs were then incubated with 1 mg/mL of CA in 50 mM sodium phosphate buffer (pH 7.5) for 3 h at 25C^{o}. Any loosely bound CA was removed through three 15 minute phosphate buffer wash sessions.

HFMs for hemocompatibility assessment (section 2.6) were modified in similar fashion but without the addition of TEA catalyst. The modifications listed below are the only changes. After plasma treatment, the HFMs were immersed in 2 M of sodium carbonate to which a solution of CNBr in acetonitrile was added to yield a final concentration of 1M. The solution was incubated for 10 min. At the completion of the activation reaction, the HFMs were washed with deionized water. The CNBr activated HFMs were then incubated with 1 mg/mL of CA in 100 mM sodium carbonate buffer (pH 8.0) for 3 h.

2.3.3 Assay for Cyanate Ester Active Groups

A quantitative assessment of CNBr/TEA activation was performed through colormetric quantification of cyanate ester active groups[92]. The assay buffer was created by mixing 0.75 g of N,N'-dimethylbarbituric acid in 45mL analytical grade pyridine. The modified HFMs were cut into 1-2 mm segments, placed in assay buffer (4 mL) and vigorously mixed using a magnetic stirrer for 10 minutes. Reaction of cyanate ester with the assay buffer yields a strong purple color. Activation quality was measured spectrophotometrically using a Genesys 5 UV spectrophotometer (Thermo Spectronic, Somerset, NJ) by monitoring absorbance change at 588nm.

2.3.4 Esterase Assay of CA Activity

The enzyme activity on HFMs was assayed using the substrate p-nitrophenyl acetate (p-NPA) as described previously[85]. Enzyme activity was measured spectrophotometrically by monitoring the hydrolysis of *p*-nitrophenyl acetate (*p*-NPA) to *p*-nitrophenol (*p*-NP) at 412 nm. The modified HFMs were cut into 1-2 mm segments and placed in assay buffer (4 mL; 50 mM phosphate buffer, pH 7.5) to measure the esterase activity. The reaction was initiated by the addition of *p*-NPA (40 μL) and vigorously mixed using a magnetic stirrer. Absorbance measurements were recorded every 3 min over a 9 min period, and plotted as a function of time. One activity unit was defined as the amount of enzyme required to generate 1 μmol pNP per minute.

2.3.5 In Vitro CO_2 Exchange in a Model Oxygenator

A scaled-down model gas exchange module was fabricated by inserting HFMs (70 fibers, 18 cm) into a 1/4 in. ID polycarbonate-tubing (McMaster Carr, Elmhurst, IL) to which single luer locks were UV-glued 1.25 in. from each end in opposing directions (Figure 2.1A). Both ends of the HFMs were secured to the tubing using an epoxy adhesive (Devcon, Danvers, MA) and then trimmed to the length of the tubing to expose the HFM lumens, yielding 10 cm of HFM uncovered within the module for a total active surface area of 0.0074 m^2. An *in vitro* recirculating test loop was used to assess CO_2 exchange rates using CA-immobilized and unmodified HFMs (Figure 2.1B).

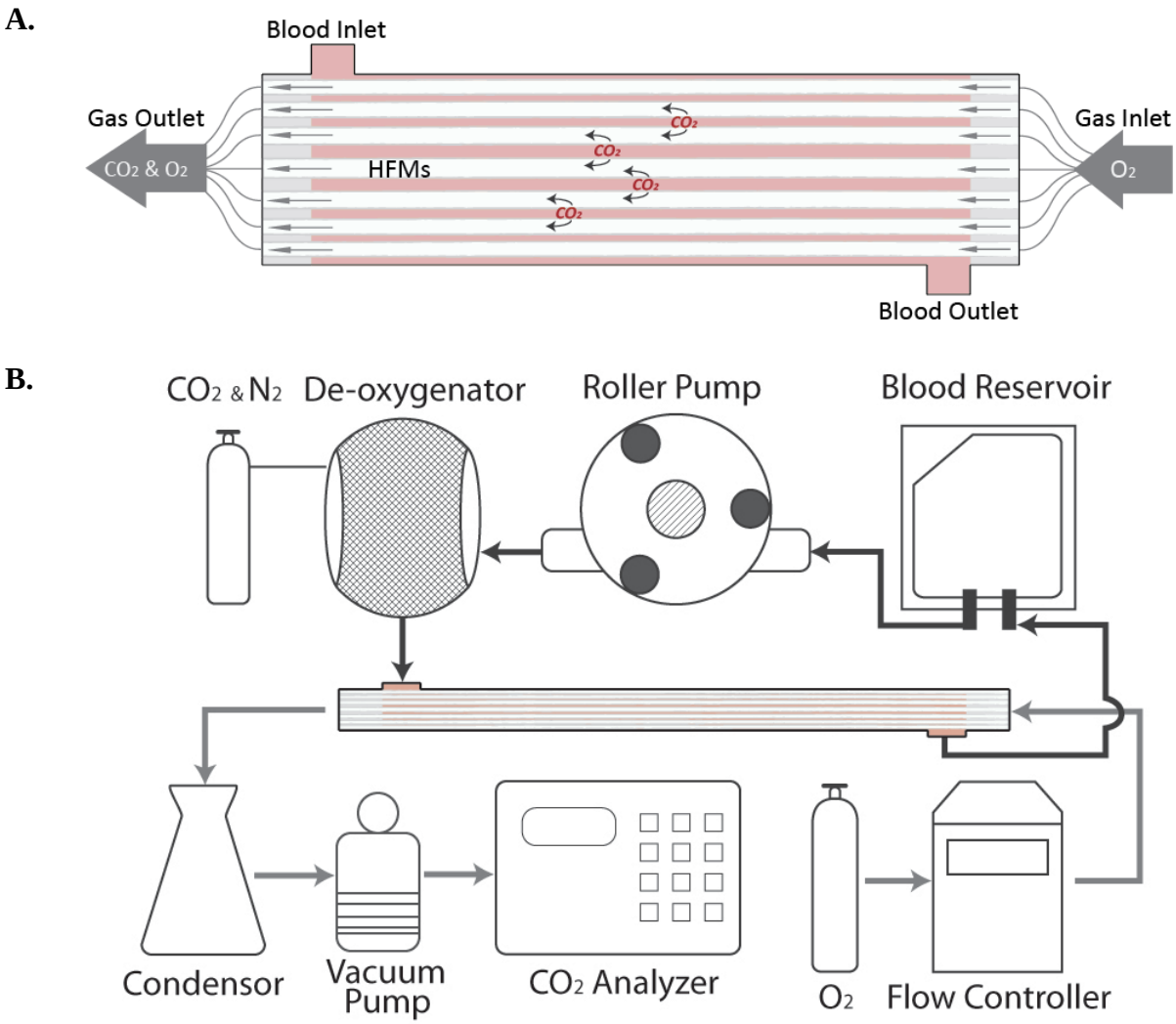

Figure 2.1. Model respiratory assist device and in vitro gas exchange setup. A. Diagram of a model respiratory device employed for measuring CO_2 removal rates of unmodified and modified HFMs. Bovine blood or PBS was perfused over the outside of the fibers while oxygen sweep gas was passed through the fiber lumens in the opposite direction. B. Experimental setup for the in vitro CO_2 gas exchange assessment. Both the blood reservoir and de-oxygenator employed the use of a heat exchanger to maintain blood temperature at 37C°.

2.3.5.1 PBS CO_2 Removal

The loop consisted of a fluid reservoir, peristaltic pump, oxygenator, vacuum pump and the model gas exchange device. The testing fluid (180 mL of PBS), flowed from a MasterFlex L/S peristaltic pump (Vernon Hills, IL) to a Terumo CAPIOX RX05 Baby RX Oxygenator (Ann Arbor, Michigan), then to the model gas exchange testing module and finally back to the reservoir. The inlet partial pressure of CO_2 (PCO_2) was adjusted to 50 mmHg and measured with a RAPIDLAB 248 Blood-Gas analyzer (Siemens, Deerfield, IL). Pure oxygen sweep gas was pulled by vacuum through a GR Series Gas Regulator (Fathom, Round Rock, TX), through the model gas exchange testing module HFM lumens, moisture trap condenser immersed in ice, KNF Lab UN811KV.45P Vacuum Pump (USA) and finally a WMA-4 CO_2 Analyzer (PP Systems, Amesbury, MA). The fluid flow rate through the module was set at 10 mL/min and the sweep gas through the HFM lumens at 50 mL/min. The fluid temperature was maintained at 37C^o by heat bath. The rate of CO_2 removal ($\dot{V}CO_2$) for each model oxygenator device was calculated using the sweep gas flow rate (Q_{OUT}^{STP}) and CO_2 fraction (F_{CO_2}) exiting the model respiratory assist device and then normalized to 50mmHg to correct for small deviations in the inlet PCO_2:

$$\dot{V}CO_2 = Q_{OUT}^{STP} F_{CO_2} \frac{50}{PCO_2} \qquad \textbf{Equation 2.1}$$

For each device the fluid inlet PCO_2 and resulting F_{CO_2} were measured in triplicate. The $\dot{V}CO_2$ for each model gas exchange device is reported as an average of these measurements. The percent enhancement in CO_2 removal from PBS was determined for various levels of immobilized enzyme activity ranging from 0.30 to 0.99 U (Figure 2.3). By modifying the time of enzyme immobilization between 0.5 and 3 hours this spectrum of enzyme activity could be created.

2.3.5.2 Blood CO_2 Removal

To match CO_2 mass transfer environment of commercially available oxygenator devices, the gas exchange module surface area was increased to 0.0084 m^2, the recirculating loop liquid flow rate was set to 60 mL/min and a sweep gas flow rate to 300 mL/min. Under these conditions the HFM CO_2 removal efficiency (ml/min/m2) matches commercially available devices. Prior to testing, blood glucose was equilibrated to 200 mg/dL and allowed to incubate for 1 hour. A solution of PBS was circulated through the testing loop for 15 minutes to remove bubbles. Blood was introduced to the loop through a wet connection (no bubbles between the PBS/blood interface) to limit hemolysis. The PBS/blood mixture was allowed to flow through the loop and drain into a waste container until no signs of blood dilution were present, upon which the loop was reconnected to the blood reservoir filled to 180mL. For each device the fluid inlet PCO_2 and resulting F_{CO_2} were measured in triplicate and averaged. The VCO_2 for modified devices is reported as an average of four separate devices and trials.

2.3.6 Blood collection and assessment of acute thrombotic deposition

The HFM samples (0.6 cm^2) were placed into Vacutainer® blood collection tubes (BD Biosciences, Franklin Lakes, NJ) filled with 5 mL of heparinized ovine blood and incubated for 2 h at 37˚C on a hematology mixer (Fisher Scientific, Pittsburgh, PA). The number of platelets deposited on the samples was determined by a lactate dehydrogenase (LDH)[93] assay with an LDH cytotoxicity detection kit (Takara Bio, Otsu, Shiga, Japan). The samples were rinsed thoroughly with 50 mL of PBS and then immersed in 1 mL of 2% Triton X-100 solution for 20 min to lyse surface deposited platelets. Surface imaging studies were performed after continuous rocking of blood for 2 h, as mentioned above. The HFM sample surfaces were then rinsed with 50

mL PBS and immersed in 2.5% glutaraldehyde solution for 2 h at 4ºC to fix the surface deposited platelets in order to perform scanning electron microscopic (SEM) analysis [86].

2.3.7 Statistical Analyses

All data are presented as a mean with standard deviation. A Student's *t*-test assuming equal sample variance was used to determine *p*-values and assess any statistically significant differences between unmodified and CA-modified HFMs. Differences were considered statistically significant for $p<0.05$.

2.4 RESULTS

CNBr activation of surface hydroxyl groups was optimized to yield the highest level of enzyme immobilization on HFMs. In our previous study, a maximal activity of 0.30 U was reported, producing a 75% enhancement in CO_2 removal from PBS [85]. Using the optimized method described here, an immobilized enzyme activity of .99 U was obtained (Figure 2.2), marking a 3.3 fold increase in maximal immobilized enzyme activity compared to the method in our previous study. It is important to note the in-vitro testing loop employed in these studies differs from the loop of our previous study [85], which limits direct comparison. The percent increase in CO_2 removal from PBS was determined for various levels of immobilized enzyme activity ranging from 0.30 to 0.99 U (Figure 2.3). Within this invitro test loop, immobilized enzyme activity (0.30 U) produced a 40% enhancement in $\dot{V}CO_2$. Increasing immobilized enzyme activity resulted in a

proportional increase in CO_2 removal where maximal enzyme activity (0.99 U) increased $\dot{V}CO_2$ by 95%.

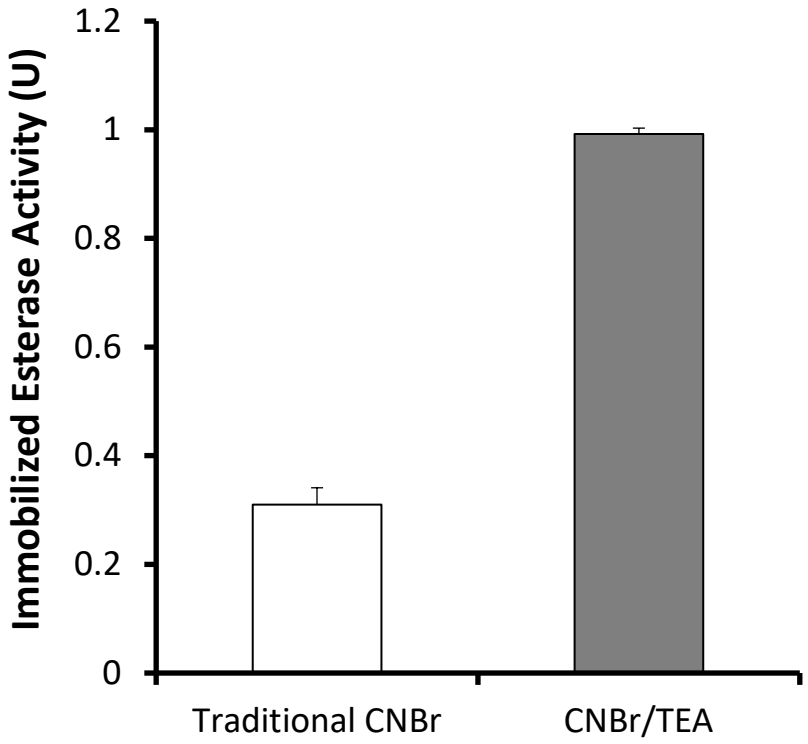

Figure 2.2. Esterase activity units of CA-modified HFMs. Traditional CNBr (Kaar et al.) activation reflects the activity level resulting from our previous work. CNBr/TEA activation demonstrates the enhanced activity of the optimized method. *p < 0.005

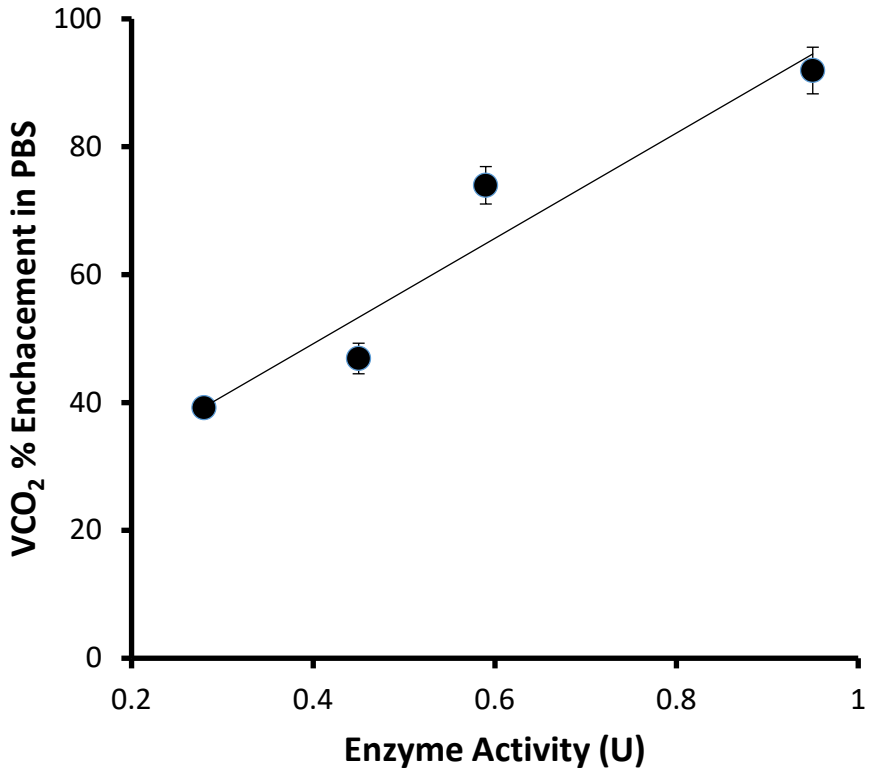

Figure 2.3. Increasing immobilized CA activity results in a proportional increase in CO_2 removal from PBS. (N=2)

The CO_2 removal capacity of the CA-immobilized HFMs was also assessed in bovine blood. To mimic the mass transfer environment of commercially available oxygenators, a few modifications were made to the model oxygenator device used in PBS. As described in section 2.5.2, the surface area was increased to 0.0084 cm^2 to match the void fraction of current commercial oxygenators. Furthermore the liquid flow rate was increased to 60 mL/min and sweep gas flow rate to 300 L/min match the mass transfer coefficient of commercial oxygenators. Figure 2.4 illustrates the impact of CA- immobilized HFMs on CO_2 removal in blood. The unmodified testing module removed 79 ± 4.7 mL/min/m^2 of CO_2 while the bioactive (0.99 U) testing module

removed 108 ± 3.7 mL/min/m^2, marking a 36% increase compared to unmodified HFMs ($p < 0.001$).

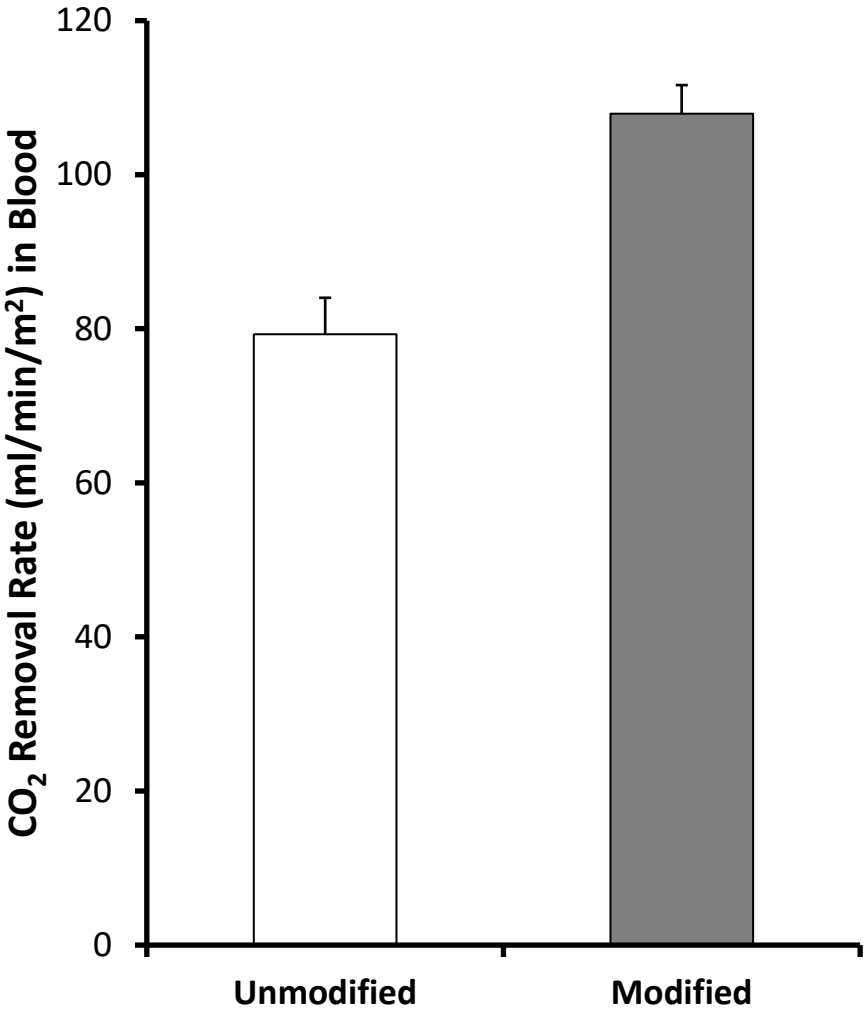

Figure 2.4. CO_2 removal by unmodified (control) and modified (CA immobilized) HFMs in bovine blood in a model respiratory assist device (N=4). The modified fibers demonstrated a 36% increase in CO_2 removal capacity. *p <0.005

Thromboresistance of CA-modified HFMs was assessed in terms of adherent platelets on surfaces by using LDH assay as well as SEM analysis. Figure 2.5 illustrates the impact of surface modification on thromboresistance by measuring platelet adhesion to the HFMs. Quantification

through LDH assay indicated the CA fiber surface reduced platelet deposition by 95% relative to unmodified fiber. The SEM micrographs support the results from the indirect platelet deposition assay, with CA-modified HFM surfaces showing less platelet deposition compared to unmodified HFM (Figure 2.6).

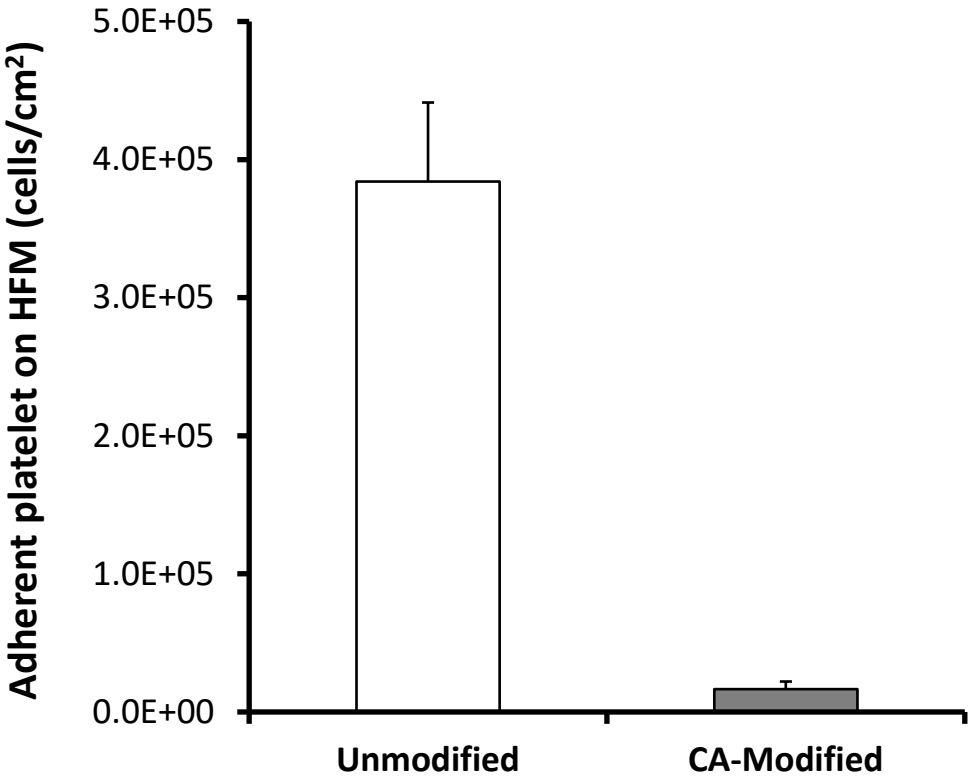

Figure 2.5. Platelet deposition onto surfaces after contact with ovine blood for 2 h as determined by a lactate dehydrogenase (LDH) assay (N=3).

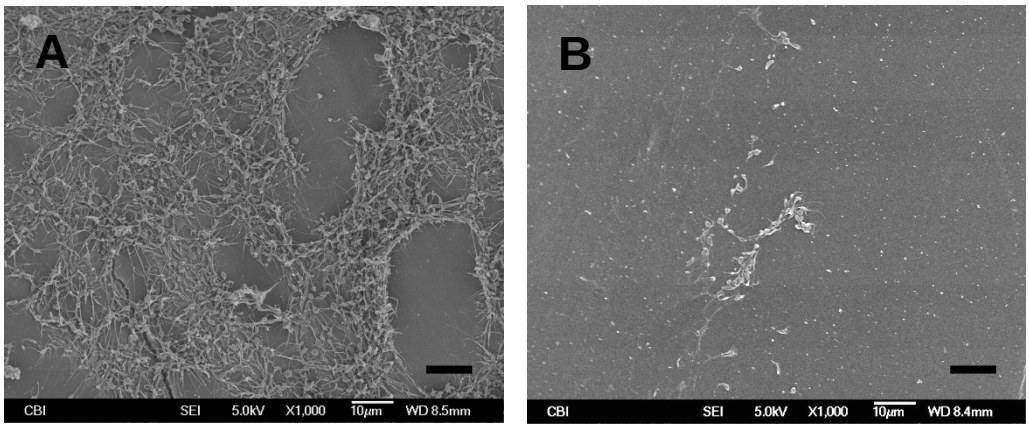

Figure 2.6. SEM images of HFM surfaces after contact with heparinized ovine blood for 2 h at 37˚C. (A) Unmodified PMP; (B) CA-modified PMP. Images were recorded using an accelerating voltage of 5 kV at a magnification of 1,000× (scale bar = 10 µm).

2.5 DISCUSSION

The present study sought to demonstrate the increased CO_2 removal capacity of CA modified HFMs could be further developed as a viable technology for HFM respiratory assist devices. By activating the hydroxyl groups introduced to the HFM surface using CNBr/TEA, free amine groups on the enzyme surface are able react with the HFM, covalently linking the enzyme to the surface. Improvements in CNBr activation chemistry were made to enhance enzyme loading and consequently increase CO_2 removal efficiency. A proportional increase between immobilized enzyme activity and percent enhancement of CO_2 removal was demonstrated in PBS. Once fully optimized, the CO_2 removal performance of the CA-HFMs was quantified in bovine blood under a CO_2 mass transfer environment similar to those of commercially available oxygenators. Furthermore hemocompatibility of the CA-modified fibers was explored. To our knowledge, this

is the first report assessing the potential enhancement of CO_2 removal from blood using CA-immobilized HFMs.

We hypothesized through immobilization of CA on HFMs, HCO_3^- in the bulk fluid could be converted directly to gaseous dissolved CO_2 at the membrane surface (Eq. 2), creating a gradient in which HCO_3^- diffuses to the fiber surface.

$$\boldsymbol{CO_2 + H_2O \overset{CA}{\Leftrightarrow} HCO_3^- + H^+} \qquad \textbf{Equation 2.2}$$

Consequently, a "facilitated diffusion" of CO_2 is created in the form of HCO_3^- diffusion, increasing the rate of CO_2 removal. Our results here demonstrate the viability of CA immobilized HFMs as a means of enhancing the CO_2 removal capacity of commercially available oxygenators. The linear increase in $\dot{V}CO_2$ with immobilized enzyme activity suggests even greater improvements in CO_2 removal performance could be realized through enhanced immobilization techniques.

The CNBr activation of hydroxyl groups employed here was first described in 1967 by means of a basic pH where highly amine reactive cyanate ester and less reactive imidocarbonate functional groups were generated with limited efficiency [94]. While at the time popular, this technique also formed inert carbamates which only contaminated the surface. TEA has since emerged as a reaction catalyst to enhance the efficiency of CNBr activation chemistry at a neutral pH [95,96]. This works by the formation of N-cyanotriethylammonium (CTEA) boride, which by the von Braun reaction is unstable and will decay at temperatures above -10^0C [97]. We employed the CNBr/TEA method to increase the level of cyanate esters generated in our activation, as a means of increasing immobilized enzyme activity on the HFM surface. To avoid the decay of reactive groups, an ice bath of propanol and dry ice was used to maintain a reaction temperature of -15C. Subsequent reaction with CA under mild conditions yielded primarily N-substituted

imidocarbonate linkages between lysines and the fiber membrane [98,99]. In our previous study, an average 0.30 U enzyme activity, as determined by the esterase assay was observed. After employing the CNBr/TEA activation technique, an average of 0.99 U was observed, marking a 330% increase in overall immobilized enzyme activity. When comparing the 0.99 U activity level to previous work [85], we cannot accurately predict the percent surface coverage based upon monolayer CA immobilization through the esterase activity assay without first determining the Km for the immobilized enzyme state. Since enzyme attachment to cyanogen bromide-activated substrates is only stable in solution over a period of days to weeks [100], the immobilization chemistry is a suitable model for proof of principle of CA-facilitated diffusion. However, alternate methods of attaching CA may need to be explored to extend the operational stability of CA-modified HFMs in respiratory assist devices. This would also include study of enzyme loading versus enzyme activity, as a means to understand the efficiency of the various bioconjugation chemistries.

This work demonstrated bioactive CA-HFMs are capable of accelerating CO_2 removal efficiency by 36% from blood. While this level of CA enhancement does not afford low flow CO_2 removal devices capable of fully supporting adult resting metabolic CO_2 production, it can potentiate more efficient and even smaller CO_2 removal devices. Comparison of the mass transfer environment for the scaled-down control testing module with surface area (0.0084 m^2) and CO_2 removal efficiency of 79 ml/min/m^2, to the Novalung with surface area (1.3 m^2) and a mean CO_2 removal rate of 119.3 ml/min, would yield a comparable 102.7 ml/min CO_2 removal rate for the scaled-down module [101]. The equivalent CO_2 removal rates between the Novalung and the scaled-down control testing module demonstrate the clinical relevance of the mass transfer environment for the scaled-down module in this work. By increasing the immobilized CA activity

upon HFMs a proportional enhancement in CO_2 removal efficiency was observed (Figure 2.3). This behavior suggests continued optimization in CA immobilized activity could offer even greater increases in HFM CO_2 removal efficiency. Based upon our previous study, immobilizing CA on the HFM has negligible effect on HFM permeance and therefore does not increase diffusional resistance of carbon dioxide [85]. Further work will assess strategies to improve CA immobilization activity with more efficient bioconjugation chemistries, spacer molecules [102], and site specific immobilization [103,104].

The percent enhancement in CO_2 removal rate by 0.99U HFMs diverged from PBS to blood as a result of differences in mass transfer environment. Since CA-modified HFMs demonstrated improved thromboresistance, platelet deposition is not likely the cause. Instead, competition with native CA in blood may lower the impact of CA-modified HFMs. Our current gas exchange modules have relatively low CO_2 mass transfer and removal rates (~100 mL/min/m^2) which may diminish the impact of CA on CO_2 removal..

Several types of biomolecules have been immobilized onto HFMs in an effort to improve their surface hemocompatibility, including chitosan, heparin and albumin. Liu *et al*. [105] and Sperling *et al*. [106] demonstrated that albumin-coated surfaces exhibited significant inhibition of platelet adhesion. The albumin mechanism acts similar to an inactive protein, lacking cell adhesion, but also occupying potential sites of protein deposition. A passivating protein layer might serve as an ideal non-thrombogenic surface if adhesive plasma proteins, such as fibrinogen, are minimally adsorbed. Several studies observed that reused hemodialyzers have better thromboresistance compared to new ones, due to such a bland protein layer acting to discourage thrombogenic activity [107]. In the present study, commercial PMP HFMs (Oxyplus) modified with CA reduced platelet adhesion by 95% (Figure 2.5 & Figure 2.6). As platelets may become

activated without adhering to the HFMs, previous work has demonstrated a reduction in activated platelets within the bulk phase of blood with CA-HFMs [108]. Our findings indicate that surface attached CA is associated with reduced acute platelet deposition, which may be caused by a similar effect related to albumin attachment. CA occupies deposition sites that otherwise might be bound with adhesive plasma proteins. However new work suggests CA may play a role in nitric oxide (NO) generation [109], which is a well-known inhibitor of platelet adhesion and activation on normal blood vessel walls [110].

3.0 DEVELOPMENT OF PLASMA MODIFIED AND CARBONIC ANHYDRASE IMMOBILIZED HOLLOW FIBER MEMBRANES FOR ARTIFICIAL LUNG APPLICATIONS

3.1 INTRODUCTION

Extracorporeal CO_2 removal ($ECCO_2R$) devices provide breathing support independent of lung tissues, allowing the lungs to rest and recover during acute respiratory failure [3–9]. These devices are a viable alternative or adjuvant therapy to invasive mechanical ventilation, which can initiate and exacerbate lung injury, substantially contributing to patient mortality [2,9,47,111,112]. Sufficient CO_2 removal from the blood is often a primary obstacle in the treatment of acute respiratory failure, rather than O_2 delivery [3,113]. Current CO_2 removal devices are limited in their efficiency, due to the small trans-membrane pressure gradient (50 mmHg), which can require blood flow rates of 1 L/min and surface areas greater than 1.8 m^2 to extract a therapeutic 50% of metabolic CO_2 production (100 mL/min) [3]. Advances in CO_2 gas exchange membranes with sufficient clinical impact could afford devices with smaller surface areas and low blood flow rates (250 -500 mL/min), alleviating the need for invasive cannulation (≥ 20 Fr) which currently limits common practice [3,9].

We recently demonstrated a bioactive HFM which chemically accelerates CO_2 removal through the immobilized enzyme carbonic anhydrase (CA) [82,85,114]. Since more than 90% of blood CO_2 is hydrated in the bicarbonate ion form (HCO_3^-), endogenous CA within our red blood cells (RBCs) and endothelial lung tissue plays a critical role to facilitate CO_2 removal during respiration, catalyzing the reversible dehydration of bicarbonate: $CO_2 + H_2O \overset{CA}{\Leftrightarrow} HCO_3^- + H^+$.

HFMs used in $ECCO_2R$ devices cannot remove bicarbonate from the blood, consequently CO_2 removal rates are partly limited by endogenous bicarbonate to CO_2 conversion. Previous work demonstrated covalent immobilization of CA onto poly (methyl pentene) (PMP) HFMs increases CO_2 removal rates up to 95% in PBS and 36% in blood, compared to unmodified HFMs [82]. This proof of principle conjugation approach utilized oxygen plasma treatment and CNBr activation chemistry to form an isourea linkage that is labile and susceptible to leaching [100,115]. Compared to our current 30 – 40% increase in blood CO_2 removal, we anticipate at least 100% increase will be necessary for next-generation minimally invasive devices. Development of stable covalent CA immobilization strategies were continued with amine functional groups on siloxane aminated polypropylene (PP) HFMs where amplification of HFM reactive amine binding groups through tethering of chitosan polymers was required to increase CO_2 removal by 115% in PBS and 37% in blood [114]. Strategies which adequately functionalize PMP HFMs for covalent CA immobilization will be important steps towards creating stable CA coatings capable of improving CO_2 removal efficiency.

Due to the inert nature of most commercial polymers, plasma polymerization is a widely used surface modification technology, enabling modification of polymer surface properties for the biomaterial field [116–118]. Amine polymer films are among the most chemically reactive and demonstrated strong adherence and stability on a variety of surfaces [119,120]. While original plasma polymerization focused on highly cross-linked films with minimal intact primary amines, the advent of pulsed plasma polymerization has afforded depositions with controllable, stable and reactive primary amines [121,122]. Previous work by our group demonstrated HFMs with thin films can adversely impact gas permeance and limit CO_2 removal efficiency [123]. Additionally an overabundance of surface functional group density can instigate multi-point attachment of

enzymes, promoting steric hindrance and limiting protein activity [115]. Plasma deposition on HFMs must balance surface functional group density with membrane permeance.

An effective carbonic anhydrase coating for HFMs should immobilize a sufficient number of CA molecules to maximize CO_2 removal rate and sustains catalytic activity of the immobilized CA. Binding of proteins to polymer surfaces through adsorption or covalent attachment can lead to their partial or complete denaturation, rendering them inactive [124–126]. Tethering of proteins to a surface via a spacer molecules such as polyethylene glycol (PEG) is well established promote protein mobility and activity [125,127–129]. Additionally, multifunctional polymer molecules such as chitosan can amplify the density of reactive functional groups and shield proteins from hydrophobic surface interactions that can initiate surface induced enzyme denaturation [88,114,130,131]. These strategies have yet to be explored on PMP HFMs for CA immobilization.

This present study sought to develop an optimal stable CA immobilization strategy for PMP HFMs. We hypothesized increasing amine density on HFMs would increase immobilized monolayer CA, and spacing CA from the surface would improve CA activity. The PECVD process parameters which maximize amine deposition were characterized through a design of experiments (DOE) approach to statistically model the effect of each parameter and their interactions within the PECVD process. Once optimized we varied HFM surface amine density for monolayer CA immobilization using short and long chain amine crosslinkers and then assessed the need for amplification of available binding groups through chitosan polymers. The impact of HFM surface amine density, crosslinker length and binding sight amplification on carbonic anhydrase immobilized HFM CO_2 removal rates were evaluated. CA modified HFMs were fabricated into model gas exchange devices to characterize CO_2 removal performance from PBS under a mass transfer environment similar to those of commercially available oxygenators. The results of this

study are an important addition to the development of a bioactive CA coating for PMP HFMs capable of accelerating CO_2 removal from blood.

3.2 METHODS

3.2.1 Materials

Allylamine, glutaraldehyde (GA), O,O′-Bis[2-(N-Succinimidyl-succinylamino)ethyl] polyethylene glycol (NHS-PEG-NHS) (MW = 3000 Da), chitosan (MW= 50-190kDa, based on viscosity), N,N′-disuccinimidyl carbonate (DSC), acetonitrile, dimethylformamide (DMF), glacial acetic acid and carbonic anhydrase II from bovine erythrocytes were purchased from Sigma-Aldrich (St. Louis, MO). Commercial poly (methyl pentene) (PMP) hollow fiber membranes (HFMs) (Oxyplus^{TM}; OD: 380 µm, ID: 200 µm) were obtained from Membrana GmbH (Wuppertal, Germany). Sulfosuccinimidyl-4-0-(4,4′-dimethoxytrityl) butyrate (sulfo-SDTB) was purchased from Prochem, Inc. (Rockford, IL). All other reagents were purchased from Sigma-Aldrich and were of analytical grade or purer.

3.2.2 Design of Experiments Characterization of Allylamine PECVD

PECVD process parameters were optimized for maximal amine deposition through a 2^5 fractional factorial design of experiments approach. Five process parameters consisting of allylamine monomer gas flow rate, final chamber pressure, generator power, generator duty cycle and generator frequency were chosen and set at a high or low value within the operational limits of the

PECVD system suggested by the manufacturer. Minitab (version 16.1.1) was used to design and analyze the trials summarized in Table 3.1. A total of 20 experimental runs were conducted, comprised of 16 combinations at the highs and lows of each process variable and 4 center points replicated to independently assess error within the process. After identification of the significant PECVD variables and interactions, optimization of the inputs was assessed by modifying the fractional factorial design into a central composite response surface design. An additional 13 trials, comprised of 10 axial points and 3 replicated center points were performed to model the nonlinear behavior of the system and predictively to optimize the input variables to maximize amine deposition rate Table 3.2. After performing the 13 additional trials, a regression model of the main effects, second order terms and interactions were assessed for statistical significance ($P < 0.05$). Terms which did not meet significance were removed one term at a time and a stepwise regression was performed to reduce all non-significant terms from the model. The final model was used to predictively optimize process parameters which maximize amine deposition, which were then confirmed experimentally. All depositions were performed for 5 minutes during the DOE optimization.

Table 3.1 Experimental trials for 2^5 fractional factorial design of experiments. All depositions were performed for 5 minutes.

Trial	*Pressure*	*Flow Rate*	*Duty Cycle*	*Frequency*	*Power*
	[mTorr]	*[sccm]*	*[%]*	*[Hz]*	*[Watts]*
1	300	60	10	150	150
2	500	180	20	150	300
3	400	120	15	100	225
4	300	60	20	50	150
5	500	180	10	50	300
6	300	180	20	50	300
7	400	120	15	100	225
8	500	60	20	150	150
9	300	180	10	150	300
10	500	60	10	50	150
11	300	60	20	150	300
12	500	180	20	50	150
13	400	120	15	100	225
14	500	180	10	150	150
15	300	60	10	50	300
16	500	60	20	50	300
17	300	180	10	50	150
18	400	120	15	100	225
19	500	60	10	150	300
20	300	180	20	150	150

Table 3.2 Additional experimental trials for the central composite response surface design.

Trial	*Pressure*	*Flow Rate*	*Duty Cycle*	*Frequency*	*Power*
	[mTorr]	*[sccm]*	*[%]*	*[Hz]*	*[Watts]*
21	300	120	15	100	225
22	500	120	15	100	225
23	400	60	15	100	225
24	400	180	15	100	225
25	400	120	15	100	150
26	400	120	15	100	300
27	400	120	10	100	225
28	400	120	20	100	225
29	400	120	15	50	225
30	400	120	15	150	225
31	400	120	15	100	225
32	400	120	15	100	225
33	400	120	15	100	225

3.2.3 Plasma Enhanced Chemical Vapor Deposition onto HFMs

Allylamine was polymerized onto unmodified PMP HFMs through plasma enhanced chemical vapor deposition (PECVD) with the PVA TePla Ion 40 system to create amine functional groups for covalent CA immobilization. PMP HFMs samples (114 fibers, 18cm, 238 cm^2) were placed on the second shelf from the top. PECVD optimization through design of experiments was carried out first to identify process inputs which maximize amine deposition rate. The chamber was evacuated to a pressure of 50 mTorr and then allylamine was continuously introduced to the chamber through a mass flow controller at 60 - 180 mL/min for a final chamber pressure of 300 - 500 mTorr. Pulsed power was applied at 150 - 300 watts, with a 10 - 20% duty cycle and 50 - 150 Hz frequency. Treatment time was constant at 5 minutes. After DOE identification of optimal process inputs which maximize amine deposition rate were selected. Allylamine monomer flow rate was 180 mL/min, final chamber pressure of 350 mTorr, pulsed power was applied at 300 watts, with a 20%

duty cycle and 150 Hz frequency. HFM coatings with varied amine density and permeance were then created by using the optimized PECVD process inputs while treatment time ranged from 2 - 15 minutes. After deposition the samples were immediately rinsed with 100mM Phosphate Buffer (PB) at pH 8.5, 3 times for 15 minutes each.

3.2.3.1 Quantification of HFM surface amine groups

Amine functional group density for unmodified and PECVD allylamine treated HFMs was quantified using a colorimetric assay [114,132]. Briefly, 25mg sulfo-SDTB was dissolved in 2mL DMF and diluted to 1 mM sulfo-SDTB with 100 mM PB at pH 8.5. Aminated PMP (40 fibers, 18 cm, 83.6 cm^2 surface area) was folded into a 15 mL test tube and incubated under constant inversion by orbital mixer with 10 mL of 1 mM sulfo-SDTB for 30 minutes, covalently linking sulfo-SDTB colorimetric moiety to HFM amine groups. Unreacted sulfo-SDTB was removed with three 20 minute rinses under constant inversion by orbital mixer, twice with 1 M NaCl + 0.5 % Tween-20 in DI water and once with pure DI water. The bound sulfo-SDTB colorimetric moiety was cleaved with 10 mL of a 35% perchloric acid under constant inversion by orbital mixer for 10 minutes, and was quantified in the supernatant at 498 nm with a UV–Vis spectrophotometer (Thermo Fisher Scientific, Waltham, MA).

3.2.3.2 XPS Analysis of HFM

Unmodified and PECVD allylamine modified (5 minute treatment) HFM samples surface chemistry were characterized using XPS. Fibers were analyzed using a Surface Science Instruments S-probe spectrometer at the University of Washington National ESCA and Surface Analysis Center for Biomedical Problems (Seattle, WA). Three 800 μm spots were analyzed for each sample, using 150 eV pass energy and take off angle of 55°. Service Physics ESCA2000A

Analysis Software was used to determine peak areas and to calculate elemental compositions from peak areas above a linear background.

3.2.3.3 HFM CO_2 Gas Permeance

Gas permeance of HFMs was measured using the method of Eash et al [123]. Briefly, an individual fiber membrane was placed in nylon tubing, with the fiber end at the tubing inlet sealed with glue. CO_2 flowed from a tank through a pressure regulator, into the nylon tubing, through the fiber membrane, and out the lumen to a bubble flow meter (Supelco, Bellefonte, PA). The differential pressure between the inlet and outlet of the nylon tubing was subsequently measured using a pressure transducer (SenSym Inc., Milpitas, CA), and a bubble flow meter was employed to record the flow of gas at the outlet. All measurements were conducted at room temperature. Gas permeance was calculated as a function of the measured differential pressure (ΔP in cmHg) and gas flow rate (Q in mL/s) as well as the theoretical surface area of exposed membrane (S in cm^2): $K = Q / (S \times \Delta P)$.

3.2.4 Carbonic Anhydrase Immobilization onto HFMs

Covalent CA immobilization onto HFMs was optimized through conjugation strategies employing DSC, GA, PEG and chitosan with GA. Aminated HFMs (238 cm^2 surface area) were folded into a 60 mL test tube and incubated under constant inversion by orbital mixer with 40mL of DSC cross-linker (5 mM in acetonitrile) or GA cross-linker (5% (v/v) in 100mM PB at pH 8.5) for 1 hour at 25^oC. Subsequently the fibers were rinsed with pure acetonitrile (after DSC conjugation) or 100mM PB at pH 8.5 (after GA conjugation), 3 times for 10 minutes each under constant inversion by orbital mixer to remove residual unreacted cross-linker. Bovine CA II was immobilized to the

HFMs by incubating 40mL of 1mg/mL in 100 mM PB at pH 8.5 for 15 hours at 25ºC under constant inversion by orbital mixer, for a monolayer immobilization. Any non-covalently bound CA was removed through 3, 15 minute PB wash sessions. Immobilizing CA by physical adsorption yielded fibers with no detectable activity after 3+ rinses (data not shown). PEG-NHS crosslinkers were employed as spacer molecules under the same methods of DSC crosslinkers.

Chitosan spacers were employed with GA crosslinkers for amplification of amine binding sites [114]. Aminated HFMs were incubated under constant inversion by orbital mixer with 40mL of 5% GA in 100mM PB at pH 8.5 for 1 hour at 25ºC. Fibers were subsequently rinsed with 100mM PB at pH 8.5, 3 times for 10 minutes each, to remove residual unreacted GA. Chitosan was immobilized by reacting HFMs with 40mL of 1% (w/v) chitosan suspended in 1% (v/v) acetic acid in DI water for 1 hour at 25ºC under constant mixing, and rinsed with PB as previously described. A second GA incubation and rinse was performed again to activate chitosan amine groups for enzyme immobilization. Finally bovine CA II was immobilized to the HFMs by incubating 40mL of 1mg/mL in 100mM PB at pH 8.5 for 15 hours under constant inversion by orbital mixer. HFM amine density was 3 – 18.5 nmol/cm^2 for immobilization with DSC and GA crosslinkers, and 6.5 nmol/cm^2 for PEG and chitosan strategies.

3.2.5 Total Immobilized Protein µBCA Assay

CA-HFMs with 6.5 nmol/cm^2 amine density were assessed for total immobilized protein with the Pierce Micro BCA Protein Assay Kit (Rockford, IL). The method utilizes bicinchoninic acid (BCA) as the detection reagent for Cu^{+1}, which is formed when Cu^{+2} is reduced by protein in an alkaline environment. CA-HFMs (107.8 cm^2) were cut into 1-2 mm segments and placed in 50 mM PB pH 8.5 and mixed 1:1 with BCA assay buffer, incubated at 60ºC for 60 minutes, and

measured spectrophotometrically at 562 nm. Absorbance signal of aminated-HFMs was subtracted from the CA protein measurements reported.

3.2.6 SEM Imaging of HFMs

Unmodified and CA immobilized HFMs were imaged by SEM (JSM-6330F, JEOL, Peabody, MA) to characterize the surface of the fiber membranes. Prior to analysis, the specimens were coated with a conductive 3.5 nm gold–palladium composite layer using a sputter coater (Auto 108, Cressington, Watford, UK).

3.2.7 In-vitro CO_2 Removal in a Model Oxygenator

A scaled-down gas exchange module was fabricated by inserting HFMs (114 fibers, 18 cm, 0.0238 m^2) into a 1/4 in. ID polycarbonate-tubing (McMaster Carr, Elmhurst, IL) to which single luer locks were UV-glued 0.75 in. from each end in opposing directions. Both ends of the HFMs were secured to the tubing using a 5 minute epoxy adhesive (Devcon, Danvers, MA) and then trimmed to the length of the module to expose the HFM lumens, yielding 11 cm of HFM uncovered within the module for a total active surface area of 0.0151 m^2.

In vitro gas exchange was performed as previously detailed by our group [114]. Briefly, model oxygenator CO_2 removal rate was examined under steady fluid and sweep gas flow. A phosphate buffered saline (PBS) solution flowed from a reservoir, through a peristaltic pump, into a Medtronic Minimax Plus Pediatric Oxygenator (Minneapolis, MN) to balance the fluid gasses, then to the model oxygenator testing module and finally back to the reservoir. PBS solution was created with physiologic pH, Na+ ionic strength and PCO_2 by diluting PBS to 0.78X with

deionized water and then adding 30mMoles sodium hydroxide. The basic PBS solution was introduced to the gas exchange loop and upon solvation of CO_2 gas, carbonic acid is formed, decreasing PBS pH back to physiologic 7.4 and increasing PCO_2 to 50mmHg. The pCO_2 at the model oxygenator inlet was measured with a RAPIDLAB 248 Blood-Gas analyzer (Siemens, Deerfield, IL). Pure oxygen sweep gas was pulled by vacuum and regulated with a GR Series mass flow controller (Fathom Technologies, Georgetown, TX) through the model oxygenator HFM lumens, moisture trap condenser and finally into an infrared CO_2 analyzer (WMA-4 CO_2 Analyzer ,PP Systems, Amesbury, MA). For all experiments, the system was maintained at 37°C, ~50mmHg pCO_2, and liquid flow rate was 115 mL/min, unless otherwise indicated. In order to compare gas exchange modules with different CO_2 removal efficiencies, the sweep gas flow rate was adjusted to maintain a constant CO_2 concentration in the sweep gas exiting the model oxygenator at approximately 3000 ppm. This approach reduced buildup of CO_2 within the HFM sweep gas exiting the device which adversely affects trans-HFM CO_2 partial pressure gradient [114]. Under these conditions the HFM CO_2 removal efficiency (ml/min/m^2) matches commercially available devices. The rate of CO_2 removal ($\dot{V}CO_2$) for each model oxygenator device was calculated using the sweep gas flow rate (Q_{OUT}^{STP}) and CO_2 fraction (F_{CO_2}) exiting the scaled-down gas exchange module and then normalized to 50mmHg to correct for small deviations in the inlet PCO_2: $\dot{V}CO_2 = Q_{OUT}^{STP} F_{CO_2} \frac{50}{PCO_2}$. For each device the fluid inlet / outlet PCO_2 and resulting F_{CO_2} were measured in triplicate. The $\dot{V}CO_2$ for each model gas exchange device is reported as an average of these measurements.

3.2.8 Statistical Analyses

All data beyond the design of experiments analysis are presented as a mean with standard deviation. Statistical significance between more than two sample groups was determined using ANOVA followed by post hoc Tukey testing of specific differences. All other data was compared using a Student's *t*-test assuming equal sample variance. Differences were considered statistically significant for $P < 0.05$.

3.3 RESULTS

3.3.1 Optimization of PECVD Process for Amine Deposition

PECVD process parameters were characterized for their impact on HFM amine density. Five process parameters consisting of allylamine monomer gas flow rate, final chamber pressure, generator power, generator duty cycle and generator frequency were tested at combinations of high, low and center point settings as described in Table 3.1. Minitab (version 16.1.1) was used to calculate the main effect of each process variable, their interactions, along with the standard errors and P-values. Mean amine density ranged from 1.8 to 3.8 nmol/cm^2 for the corner points, and was 4.0 nmol/cm^2 for the center points. The PECVD power, pressure, duty cycle and flow rate were found to have statistically significant effects on HFM amine density ($P < 0.05$). High chamber pressure conditions (500mTorr) decreased amine density, while high power (300 watts), high flow rate (180 sccm) and high duty cycle (20%) increased amine density (Figure 3.1). Frequency was not found to have a statistically significant effect on amine density within the tested range (P >

0.50). The center point of each process variable plotted in Figure 3.1 resulted in the greatest HFM amine density, indicating the strong nonlinear relationship between each process input and HFM amine density ($P < 0.05$).

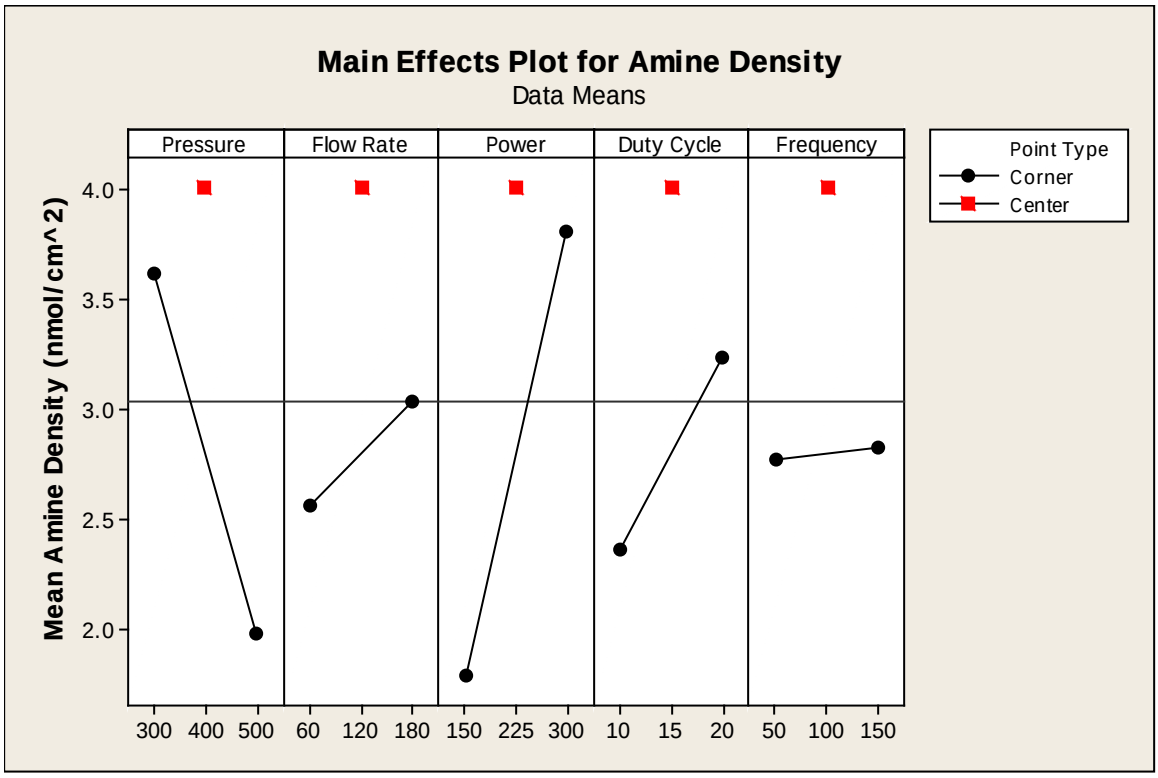

Figure 3.1. Main effects plot for amine density by pressure, flow rate, power, duty cycle and frequency.

A central composite design was required to obtain the second order nonlinear response surface and predictively optimize input variables which maximize HFM amine deposition. In addition to the process variables previously found to be significant, second order terms and interactions of power^2, pressure^2, pressure*power, pressure*duty cycle and power*frequency reached statistical significance ($P < 0.05$) (Figure 3.2). The R^2 value demonstrates the final reduced model fits the data well and describes 97.4% of the variation in HFM amine density. The model was checked to ensure residuals are normally distributed, have constant variance, and are

independent of trends or patterns (Figure 3.3). The fractional factorial design experimentally demonstrated a maximum amine density of 4.0 nmol/cm^2 could be achieved with a deposition at the central point of each process parameter (Figure 3.1). The central composite regression model predicted an optimal amine density of 5.6 nmol/cm^2 was attainable with the following process parameter settings: allylamine monomer flow of 180 mL/min, final chamber pressure of 350 mTorr, pulsed power applied at 300 watts, with a 20% duty cycle and 150 Hz frequency. Experimental test of the optimal process settings confirmed predicted amine density, yielding HFMs with an amine density of 5.7 ± 0.1 nmol/cm^2 (N=3).

Response Surface Regression: Amine Density

The analysis was done using coded units.

Estimated Regression Coefficients for Amine Density

Term	Coef	SE Coef	T	P
Constant	3.86351	0.06357	60.776	0.000
Pressure	-0.83093	0.05595	-14.853	0.000
Flow Rate	0.25424	0.05595	4.545	0.000
Power	1.03779	0.05595	18.550	0.000
Duty Cycle	0.46969	0.05595	8.396	0.000
Frequency	0.03378	0.05595	0.604	0.552
Pressure*Pressure	-0.74823	0.12667	-5.907	0.000
Power*Power	-0.34002	0.12667	-2.684	0.014
Pressure*Power	0.25103	0.05934	4.231	0.000
Pressure*Duty Cycle	-0.12656	0.05934	-2.133	0.044
Power*Frequency	0.14187	0.05934	2.391	0.026

S = 0.237355 PRESS = 3.33113
R-Sq = 97.44% R-Sq(pred) = 93.13% R-Sq(adj) = 96.28%

Analysis of Variance for Amine Density

Source	DF	Seq SS	Adj SS	Adj MS	F	P
Regression	10	47.2277	47.2277	4.7228	83.83	0.000
Linear	5	36.9691	36.9691	7.3938	131.24	0.000
Pressure	1	12.4280	12.4280	12.4280	220.60	0.000
Flow Rate	1	1.1635	1.1635	1.1635	20.65	0.000
Power	1	19.3861	19.3861	19.3861	344.11	0.000
Duty Cycle	1	3.9710	3.9710	3.9710	70.49	0.000
Frequency	1	0.0205	0.0205	0.0205	0.36	0.552
Square	2	8.6719	8.6719	4.3360	76.96	0.000
Pressure*Pressure	1	8.2660	1.9657	1.9657	34.89	0.000
Power*Power	1	0.4059	0.4059	0.4059	7.21	0.014
Interaction	3	1.5866	1.5866	0.5289	9.39	0.000
Pressure*Power	1	1.0083	1.0083	1.0083	17.90	0.000
Pressure*Duty Cycle	1	0.2563	0.2563	0.2563	4.55	0.044
Power*Frequency	1	0.3220	0.3220	0.3220	5.72	0.026
Residual Error	22	1.2394	1.2394	0.0563		
Lack-of-Fit	16	1.0553	1.0553	0.0660	2.15	0.176
Pure Error	6	0.1841	0.1841	0.0307		
Total	32	48.4671				

Figure 3.2. Response surface regression analysis of the reduced model.

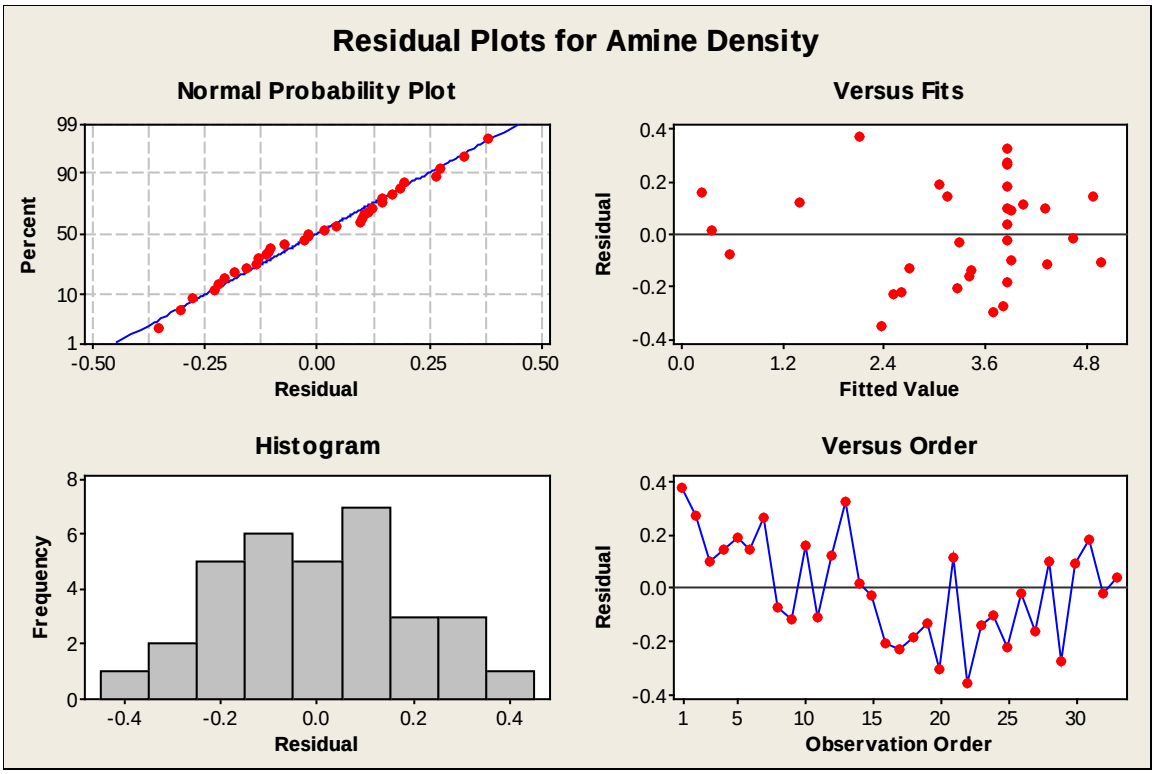

Figure 3.3. Residual plots for central composite surface regression.

3.3.2 Characterization of PECVD on HFM Amine Density and Permeance

Aminated-HFMs were characterized for their amine density after PECVD allylamine treatments from 0 to 15 minutes. Amine group density increased from 0 nmol/cm^2 for unmodified fibers to 3.0, 6.5, 14.6 and 18.5 nmol/cm^2 for PMP HFMs after PECVD deposition times of 2, 5, 10 and 15 minutes. Secondary confirmation of allylamine HFM surface modification was observed through XPS chemical surface analysis (Table 3.3). Unmodified HFMs predominantly contained carbon (93.6%) and oxygen (6.4%). After 5 minutes of plasma treatment, aminated-HFMs demonstrated reduced carbon contend (69.9%), and increased nitrogen content (11.0%), due to allylamine deposition. These findings demonstrate PECVD treatment introduces allylamine to the

HFM surface, and affords control of functional amine density from 3.0 – 18.5 nmol/cm^2 by varying plasma treatment times.

Table 3.3. XPS elemental analysis for unmodified and allylamine HFMs.

XPS	***C 1s***	***N 1s***	***O 1s***	***F 1s***	***Si 2p***
Unmodified HFM	93.6 ± 0.5	-	6.4 ± 0.5	-	-
Allylamine HFM	69.9 ± 0.1	11.0 ± 0.1	13.4 ± 0.2	3.3 ± 0.7	2.4 ± 0.5

Aminated-HFMs were characterized for their permeance after PECVD allylamine treatments from 0 to 15 minutes. The CO_2 permeance decreased from 1.35E-3 (mL/s.cm^2.cmHg) for unmodified HFMs to 1.06E-3, 6.97E-4, 2.26E-4 and 6.36E-5 mL/s.cm^2.cmHg for PMP HFMs, after PECVD deposition times of 2, 5, 10 and 15 minutes. The time varying decrease in permeance is consistent with a time varying increase in amine density. Increasing PECVD treatment time decreases HFM permeance, while increasing functional amine density (Figure 3.4)

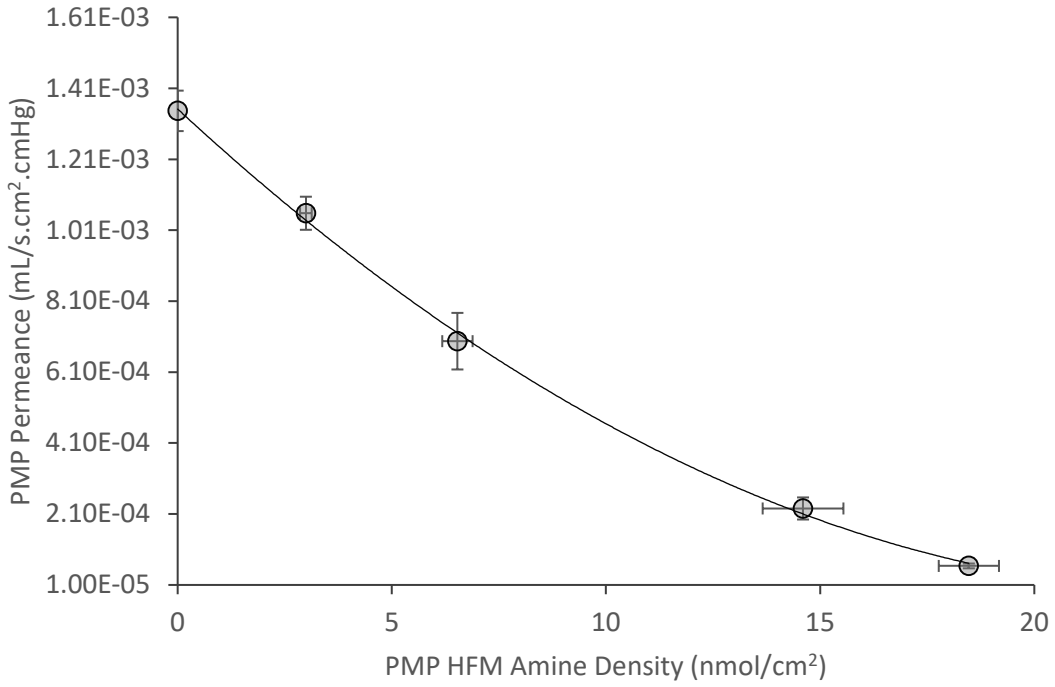

Figure 3.4. HFM permeance is inversely related with HFM functional amine density.

3.3.3 Effect of Aminated-HFM Permeance on CO_2 Removal

In-vitro CO_2 gas exchange was assessed on unmodified and aminated HFMs by varying fluid flow rates from 115 to 800 mL/min. We observed an increase in CO_2 removal rate from 108 to 311 mL/min/m^2 for unmodified HFMs, indicative of a reduction in liquid boundary layer diffusive resistance with increasing flow rate. Aminated fibers with the lowest permeance (15 minute plasma treatment) at 6.36E-5 mL/s.cm^2.cmHg demonstrated no statistical difference in CO_2 removal rate compared to unmodified HFMs ($P < 0.01$), for all fluid flow rates (Figure 3.2). The decrease in HFM permeance measurements as a result of allylamine deposition does not have a detrimental impact on HFM CO_2 removal under clinically relevant rates.

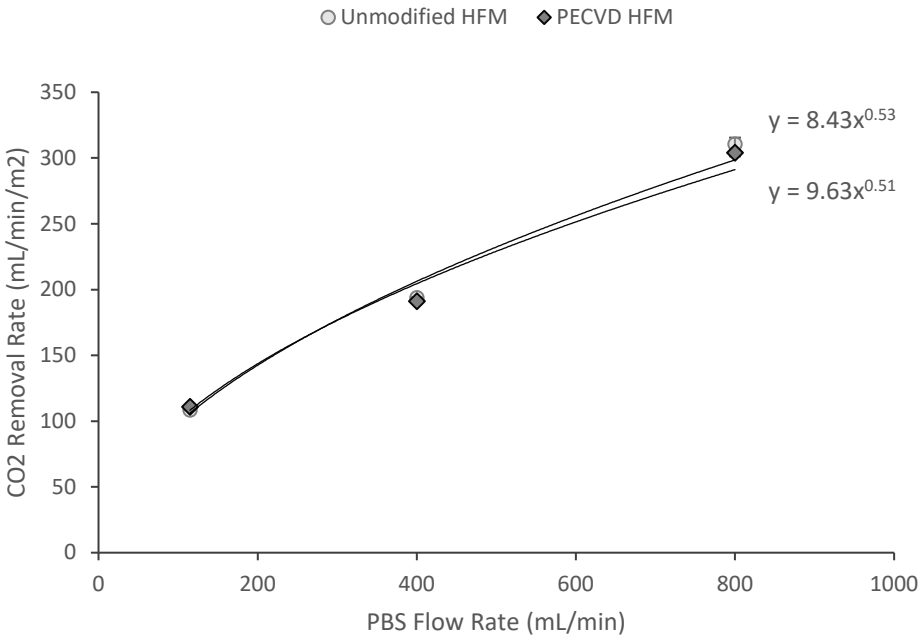

Figure 3.5. CO_2 removal rate for allylamine coated HFM does not differ from unmodified HFM.

3.3.4 CA Immobilization Strategy on CO_2 Removal

HFM amine density, crosslinker length, and chitosan polymers were examined to optimize immobilized CA activity. By varying amine density from 3.0 – 18.5 nmol/cm^2 we observed an increase in CO_2 removal by CA-HFMs as compared to unmodified HFMs (Figure 3.3). Using zero length DSC crosslinker, increasing amine density demonstrated parabolic increase in CO_2 removal, with a maximum 31% increase (159 mL/min/m^2) at amine density 14.6 nmol/cm^2, compared to 121 mL/min/m^2 for unmodified HFMs. Similar behavior was observed employing GA crosslinker, with a maximum 36% increase (167 mL/min/m^2) with amine density 14.6 nmol/cm^2. For both GA and DSC crosslinkers, there was no statistical difference in CO_2 removal rate with amine density at 6.5 or 14.6 nmol/cm^2. Increasing amine density to 18.5 nmol/cm^2 had a detrimental effect on

CA-HFM CO_2 removal rate. These observations indicate monolayer CA immobilization with short chain DSC and GA crosslinkers increases CO_2 removal rate by up to 36%, and HFM amination beyond 6.5 nmol/cm^2 does not significantly improve CA-HFM CO_2 removal activity.

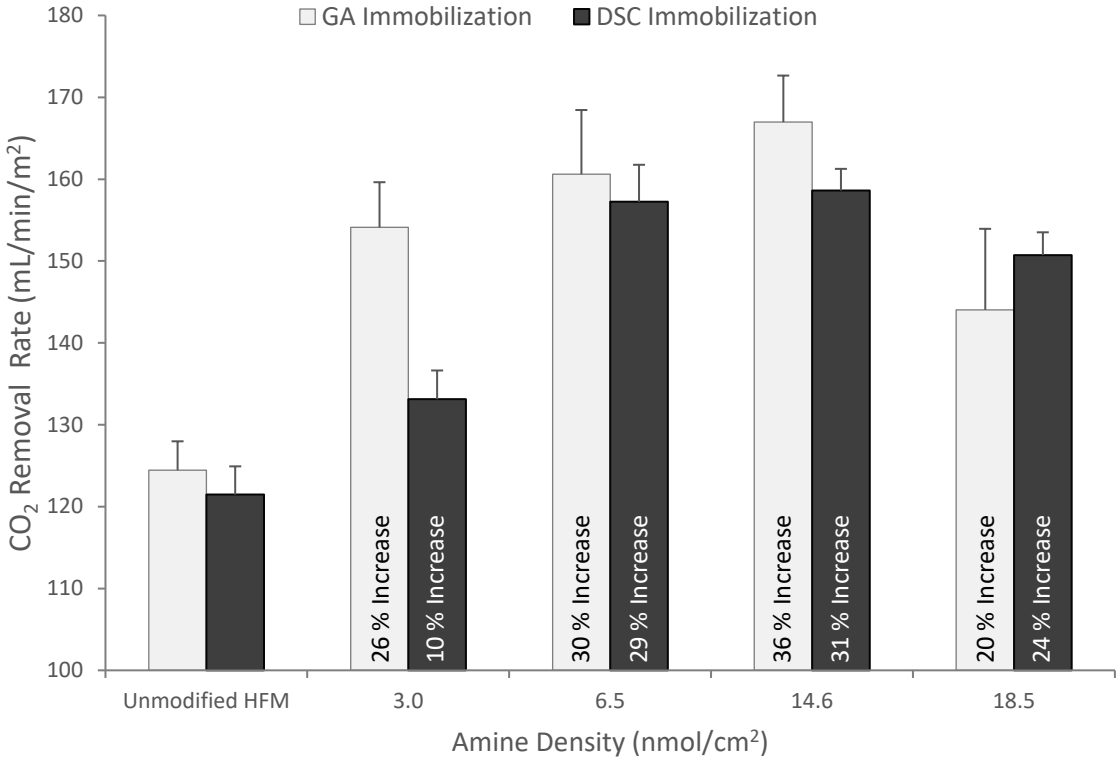

Figure 3.6. Amine density versus CO_2 removal rate for monolayer immobilization with GA or DSC crosslinkers.

PEG-NHS was employed to investigate the effect of spacing immobilized CA from the HFM surface. Using aminated-HFMs at 6.5 nmol/cm^2, PEG-NHS crosslinker increased CO_2 removal rate by 13% (142 mL/min/m^2), compared to unmodified HFMs (Figure 3.4). PEG spacing does not improve CA-HFM CO_2 removal rate over short chain DSC or GA crosslinkers. Chitosan polymers were employed to investigate the effect of binding site amplification. Immobilized CA

through chitosan polymers with GA crosslinkers on aminated-HFMs at 6.5 nmol/cm^2, increased CO_2 removal rate by 62% (204 mL/min/m^2) compared to unmodified HFMs (Figure 3.4). Chitosan spacers offer the highest performance of all bioconjugation techniques employed in this study.

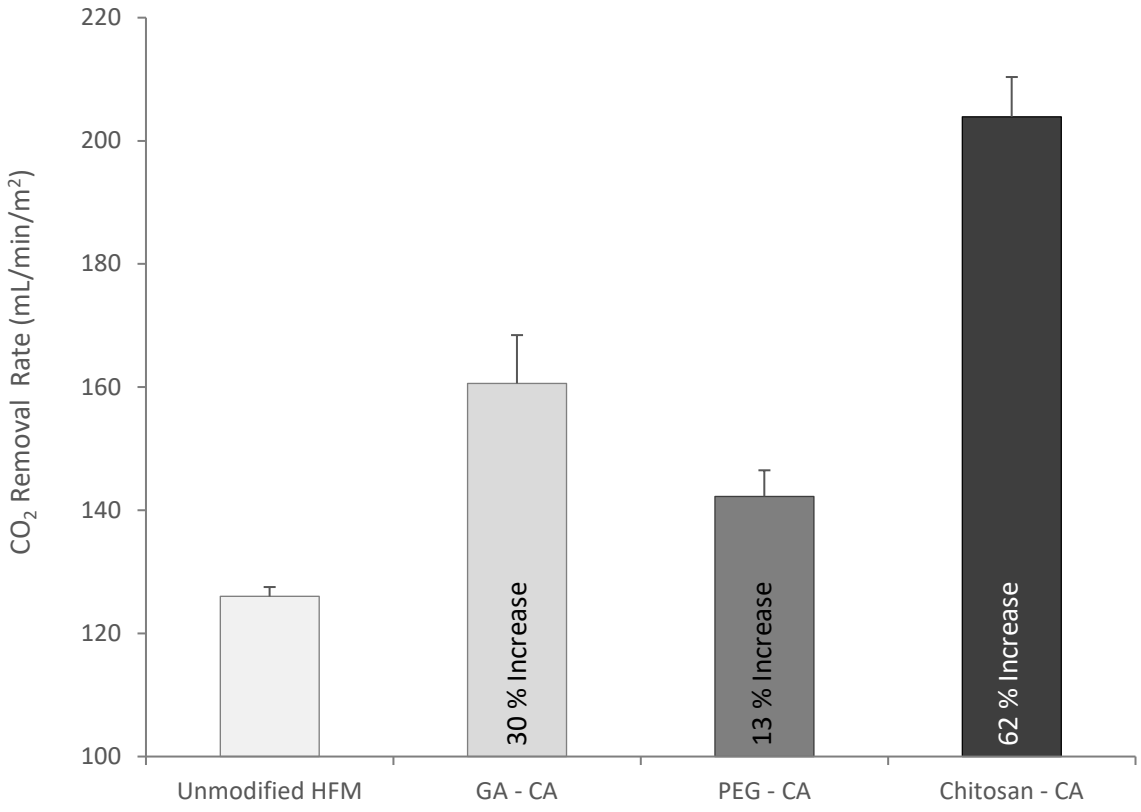

Figure 3.7. CO_2 removal rate for various CA immobilization strategies, monolayer-GA, monolayer-PEG, and chitosan amplification.

3.3.5 CA Immobilization Strategy on Enzyme Loading

Total immobilized CA protein was quantified using the µBCA assay on fibers with 6.5 nmol/cm^2 amine density. The chitosan immobilization strategy increased CA loading onto HFMs by 561% compared to monolayer immobilization with GA crosslinkers, with 3.10 µg/cm^2 and 0.47 µg/cm^2

respectively (Figure 3.5). Chitosan polymers amplified the available binding groups for CA, increasing the immobilized protein density.

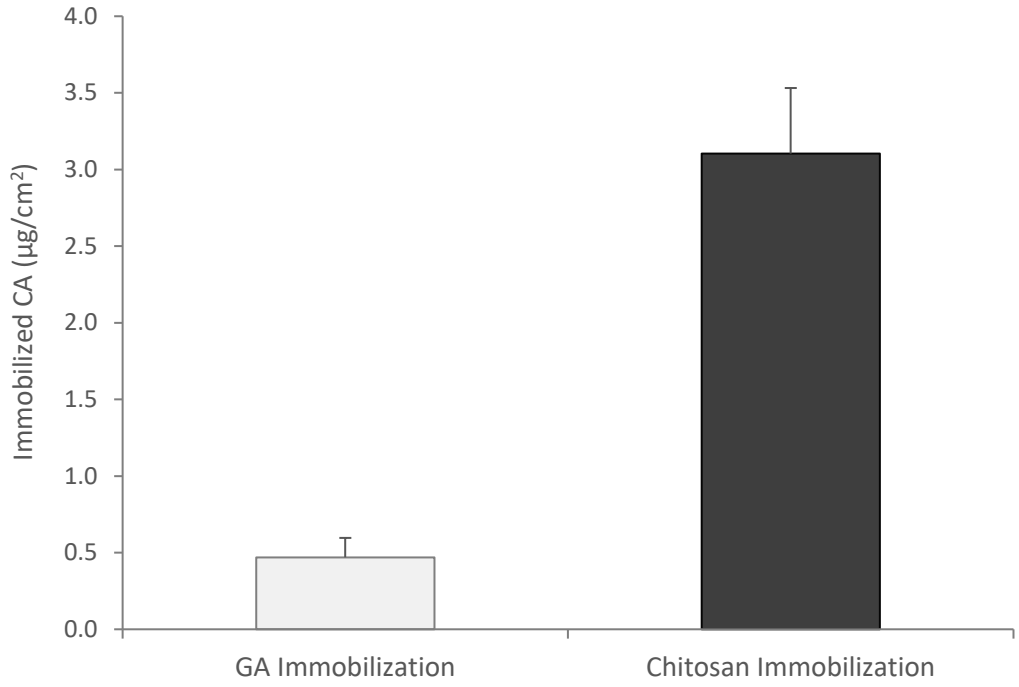

Figure 3.8. Total protein assay for GA monolayer and chitosan immobilization strategies.

3.3.6 SEM Analysis of Chitosan CA-HFMs

SEM images illustrated in Figure 3.6 show the fiber surface before and after chitosan-CA immobilization. In the unmodified HFM sample, the surface appears clean with marks from the manufacturing process. After chitosan-CA immobilization, small aggregates are observed throughout the fiber surface. The coating appears to be comprised of local deposits of chitosan and CA, rather than a continuous coating evenly dispersed on the membrane.

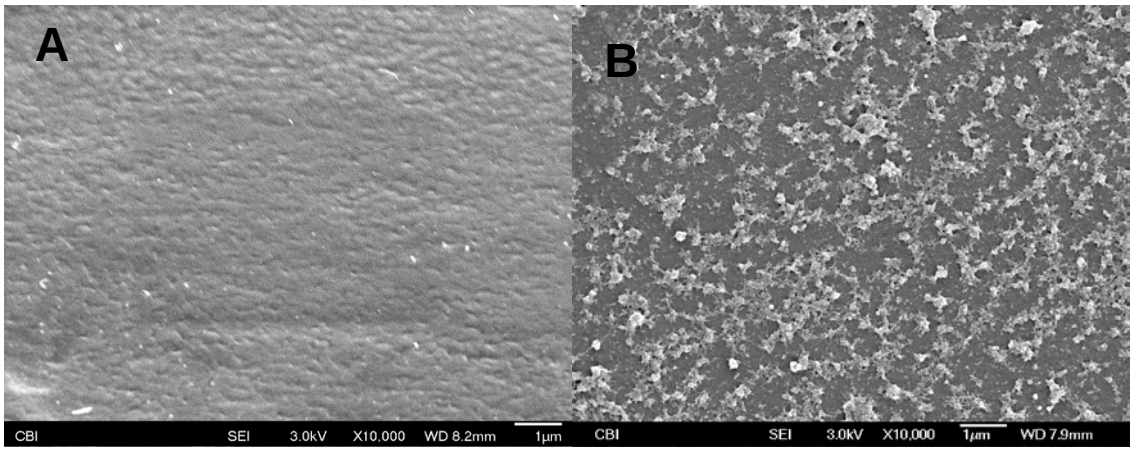

Figure 3.9. SEM of (A) Unmodified PMP and (b) Chitosan-CA PMP HFMs.

3.4 DISCUSSION

The goal of this study was to develop a stable CA conjugation strategy for PMP HFMs which maximizes CO_2 removal efficiency. Previous work by our group demonstrated the efficacy of a CA coating for PMP HFMs with oxygen plasma surface modification and CNBr based chemical attachment, resulting in a CA coating susceptible to leaching due to an isourea linkage [100,115]. In this work we optimize a stable immobilization strategy for PMP HFMs using amine based conjugation chemistries and interrogate surface amine group density (with PECVD design of experiments), crosslinker length (with DSC, GA and NHS-PEG) and necessity of binding site amplification (with chitosan). Our results indicate PMP amination beyond 6.5 nmol/cm^2 did not improve immobilized CA HFM CO_2 removal activity, and while PEG spacing was ineffective, chitosan polymers amplified the available binding groups for CA, increasing the immobilized protein density and HFM CO_2 removal by up to 62%.

A carbonic anhydrase coating for gas permeable membranes should aim to maximize immobilized enzyme activity with a stable conjugation chemistry. The immobilization strategy in our previous work was only stable in solution over a period of days, limiting the practical clinical utility of the coating [100]. Kimmel et al. developed a stable amine based conjugation strategy to immobilize CA onto aminated polypropylene (PP) HFMs through glutaraldehyde crosslinkers, and found the use of polymeric chitosan was necessary to amplify surface amine groups for CA attachment [114]. We employed PECVD to precisely and repeatable aminate the surface of chemically inert PMP HFMs through the polymerization of allylamine. While PECVD has gained traction in the device world for its uniform coatings, many studies have focused on one or a few process conditions at a time, ultimately failing to provide a comprehensive description of the process [133–138]. Through a design of experiments approach we modeled the significance of

each process variable, second order nonlinear behavior and resolved interactions between process variables to describe their impact on HFM amine density. Compared with the amine density of chitosan coated PP HFMs (3.3 nmol/cm^2), allylamine PECVD enabled amination of PMP HFMs with an amine density ranging from 3.0 to 18.5 nmol/cm^2, as measured by the sulfo-STDB amine assay. Monolayer CA immobilization onto PECVD aminated PMP HFMs with GA crosslinkers increased CO_2 removal rate by up to 36%, an improvement over the negligible monolayer activity observed prior studies with PP HFMs, suggesting the efficacy in this allylamine amination approach [114]. In comparison to the previously reported 115% increase in CO_2 removal with CA immobilized onto chitosan PP HFMs, allylamine aminated PMP HFMs with a similar 3.0 nmol/cm^2 increased CO_2 removal by 26%, and when employing chitosan improved to 62%. The hydroxyl plasma surface modification in prior work increased CO_2 removal by up to 95%, an improvement not yet replicated by monolayer conjugation to aminated surfaces, signifying aminated surfaces may impact immobilized enzyme efficiency [82]. These results in whole suggest beyond amine amplification, the hydrophilic properties of a chitosan or hydroxyl modified surface may have also provided a more favorable microenvironment for stable CA enzymatic function. The use of PEG in this application was not effective towards increasing immobilized CA activity, likely due to use of a homobifunctinoal crosslinker which has the capacity to conjugate both ends to the support, limiting the available binding sites for CA [127]. The benefits of hydrophilic surfaces for immobilized proteins are documented in the literature, and considering the catalytic mechanism of CA is dependent upon available water, further investigation into the specific impact of hydrophilic environments is warranted [139–141].

The impact of allylamine deposition on PMP HFM permeance was assessed. Coatings for gas permeable membranes should balance loading of CA and membrane gas permeance. Although

allylamine decreased HFM permeance with increasing treatment time, aminated fibers with the lowest permeance (15 minute plasma treatment) at 6.36E-5 mL/s.cm^2.cmHg demonstrated no statistical difference in CO_2 removal rate compared to unmodified HFMs (Figure 3.2). In contrast, previous work with chitosan coated PP HFMs was measured with a permeance an order of magnitude greater at 8.4E-4 mL/s.cm^2.cmHg, and observed decreases in CO_2 removal compared to control fibers [114]. Overall mass transport in the system is governed by the individual resistances of each process in series. Previous work demonstrated the rate limiting step in CO_2 removal for unmodified HFMs is diffusion of CO_2 through the liquid-side diffusional boundary layer, not diffusion through the HFM itself [1,123,142]. Additionally, increasing the blood flow rate past the fiber surface decreases the boundary layer thickness, favorably varying gas exchange permeance as the square root of flow velocity, as demonstrated in Figure 3.5. Surprisingly allylamine deposition did not impact HFM CO_2 removal (at clinically relevant rates), even with a permeance measured 92% less than the previously reported chitosan PP HFMs. The disconnect in gas-gas permeance versus liquid CO_2 removal may be attributed to the porous nature of allylamine when hydrated, which may improve the observed permeability of in an aqueous environment [133,143]. Additionally, we measured CA monolayer loading at 0.47 mg/cm^2, nearly 1.9x the theoretical mass for a monolayer coverage of CA [144]. The observed CA loading beyond monolayer coating may further suggest an irregular and porous allylamine network for CA to bind.

Development of improved and more efficient respiratory assist devices will enable next generation, minimally invasive extracorporeal support of failing lungs at low blood flows. Carbonic anhydrase immobilized on HFMs is a novel approach to increase CO_2 removal rates, but the factors limiting the enhancement of CO_2 removal by CA-HFMs are not well understood. We optimized an approach to amplify CA loading onto PMP HFMs with chitosan and GA crosslinkers,

with a maximum 62% increase in CO_2 removal. We expect this level of enhancement to be less when tested in blood. The difference in CA HFM catalyzed CO_2 removal between PBS and blood is not well understood. Compared to our current 30 – 40% increase in blood CO_2 removal, we anticipate at least 100% increase will be necessary for the development of next-generation minimally invasive devices. Future work will examine the kinetics of CO_2 transport within CA-modified gas exchange devices in PBS and blood, to elucidate strategies for further improving blood CO_2 removal using CA-HFM devices.

4.0 KINETICS OF CO_2 EXCHANGE WITH CARBONIC ANHYDRASE IMMOBILIZED ON FIBER MEMBRANES IN ARTIFICIAL LUNGS

The following chapter presents work peer-reviewed and published as the Editor's Choice Article in the Journal of Materials Science: Materials in Medicine without modification [145]: Arazawa DT, Kimmel JD, Federspiel WJ. Kinetics of CO_2 exchange with carbonic anhydrase immobilized on fiber membranes in artificial lungs. J Mater Sci Mater Med 2015;26. Editorial commentary published with the article and abstract follows:

"Acute Respiratory Failure: Design Innovations in Respiratory Assist Devices"

by Gabriela Voskerician, PhD

"Patients admitted to the Intensive Care Unit (ICU) with acute respiratory failure require the use of a respiratory assist device. The primary specification of such a device is its extracorporeal blood flow rate of ~1 L/min. This flow rate is needed to extract 50% of the metabolic CO2 production (~100 mL/min), which is accepted as a physiological requirement for survival. Immediate treatment is dependent on the availability of a trained surgeon responsible for inserting the assist device access cannula. Dr. Federspiel and his colleagues at the McGowan Institute of Regenerative Medicine and the University of Pittsburgh Medical Center intend to overcome this limitation in the immediate application of assist devices for patients with acute respiratory failure. Their article can be found at http://link.springer.com/article/10.1007/s10856-015-5525-0.

The group proposes that accelerating the CO_2 extraction per unit of blood passing through the assist device would allow for a reduction in the flow rate. In turn, this method would enable the use of a smaller gauge cannula, easily inserted, without the support of a trained surgeon. Current technologies rely on large gauge cannulae (>15 Fr) and large exchange surface area (> 1.3 m^2). Some technologies have taken steps to lower the flow rate, but maintaining a clinically therapeutic CO_2 removal rate remains a challenge. Dr. Federspiel and his colleagues derive their solution from the fundamental chemical mechanism of physiologic CO_2 removal: $CO_2 + H_2O \Leftrightarrow HCO_3^- + H^+$, reaction catalyzed physiologically by carbonic anhydrase (CA). This is attractive because most of the CO2 in blood is carried as bicarbonate ion (HCO_3^-).

The group tested the performance of immobilized calcium anhydrase (CA) on the surface of the gas exchange membranes in accelerating the CO_2 removal rate. The expected finding of the study validated CA's role in enhancing CO_2 removal. The unexpected finding, however, showed that the immobilized CA was adversely affected as the blood flow rate increased. Using these experimental outcomes, the most efficient CA immobilization density to CO_2 removal ratio was determined. An additional design parameter considered by Dr. Federspiel and his colleagues for improving CO_2 removal targeted the effective role of dilute sulfur dioxide in the oxygen sweep gas for increasing CO_2 removal, especially in the presence of immobilized CA.

In this work, Dr. Federspiel and his colleagues demonstrated the power of understanding the problem before designing a solution. Intervening at the right step of the process, and evaluating the results of a well-designed experiment, settles (for now) the importance of chemical manipulation to effectively improve CO_2 exchange.

While analyzing the experimental design, I became interested in learning more about the potential of platelet adhesion and/or damage at the exchange surface. Such a phenomenon would

certainly cascade into the formation of a thrombus, thereby limiting the efficiency of CO_2 removal. Dr. Federspiel kindly elaborated on some of the previous findings published by the group that compared CA coating to predicate exchange surfaces in their response to platelet adhesion. CA coating demonstrated "a significant reduction in both platelet deposition and activation compared with all other fiber types". While the exact mechanism of action had not been elucidated, Dr. Federspiel suggested that "the hydrophilic chitosan coating in conjunction with the bound enzyme molecule [CA] may help prevent initial protein adsorption on the fiber surface, a known initiator of platelet adhesion and activation".

Considering the significant clinical impact of redesigning such an assist device, it was important to further clarify the validity of the outcomes outside the experimental setting of this work. Specifically, I wondered how the recirculating test loop reflected the reality of CO_2 removal in the case of a patient. The group explained that the recirculating test loop recreated a physiologically relevant environment on two levels: blood parameters and mass transfer characteristics. The experimental design ensured that the temperature, pH, partial pressure of CO_2 were all controlled to replicate the in-situ environment. A tight control over the blood solutions guaranteed that they were maintained at the appropriate glucose concentration; while the circulating hematocrits were examined before and after testing. To manage a relevant comparison, the authors matched the mass transfer coefficient to that of commercial oxygenators. With any experimental design, there were study limitations. Dr. Federspiel believes that while the CA coating performance was demonstrated at prototype level, additional evaluations must be performed to validate its efficacy in clinically sized oxygenators. Further, the sweep gas flow rate (diluted acidic gas discussed above) was regulated to meet the needs of the prototype oxygenator.

The working sweep gas flow rate, however, might have to be adjusted to ensure effective performance when used with real-life clinical oxygenators.

This work highlights two fundamental components of medical device development: (a) understand the problem, and (b) understand the experimental design limitations. I would like to thank Dr. Federspiel and his colleagues for kindly agreeing to offer their team's findings beyond the confines of the published scientific work.

To our readers: I am looking forward to your comments that can be sent to gabriela.voskerician@case.edu using the heading "Editors' Choice". We hope to develop this feature into a dynamic forum think-tank."

4.1 SUMMARY

Artificial lung devices comprised of hollow fiber membranes (HFMs) coated with the enzyme carbonic anhydrase (CA), accelerate removal of carbon dioxide (CO_2) from blood for the treatment of acute respiratory failure. While previous work demonstrated CA coatings increase HFM CO_2 removal by 115% in phosphate buffered saline (PBS), testing in blood revealed a 36% increase compared to unmodified HFMs. In this work, we sought to characterize the CO_2 mass transport processes within these biocatalytic devices which impede CA coating efficacy and develop approaches towards improving bioactive HFM efficiency. Aminated HFMs were sequentially reacted with glutaraldehyde (GA), chitosan, GA and afterwards incubated with a CA solution, covalently linking CA to the surface. Bioactive CA-HFMs were potted in model gas exchange devices ($0.0119 m^2$) and tested for esterase activity and CO_2 removal under various flow rates with PBS, whole blood, and solutions containing individual blood components (plasma albumin, red

blood cells or free carbonic anhydrase). Results demonstrated that increasing the immobilized enzyme activity did not significantly impact CO_2 removal rate, as the diffusional resistance from the liquid boundary layer is the primary impediment to CO_2 transport by both unmodified and bioactive HFMs under clinically relevant conditions. Furthermore, endogenous CA within red blood cells competes with HFM immobilized CA to increase CO_2 removal. Based on our findings, we propose a bicarbonate/CO_2 disequilibrium hypothesis to describe performance of CA-modified devices in both buffer and blood. Improvement in CO_2 removal rates using CA-modified devices in blood may be realized by maximizing bicarbonate/CO_2 disequilibrium at the fiber surface via strategies such as blood acidification and active mixing within the device.

4.2 INTRODUCTION

Removal of CO_2 from circulating blood using extracorporeal gas exchange devices is a promising treatment for acute respiratory failure [3–9]. Current respiratory assist devices used for extracorporeal carbon dioxide removal ($ECCO_2R$) can require blood flow rates in excess of 1 L/min to extract a clinically therapeutic 50% of metabolic CO_2 production (~100 mL/min), necessitating larger cannula inserted by surgeons, rather than the intensivists typically treating these patients. This has been one reason $ECCO_2R$ has seen limited widespread use in ICUs [3,9]. New technologies that facilitate accelerated CO_2 removal may lead to the development of smaller, more efficient respiratory assist devices that can be implemented by intensivists and other nonsurgical clinicians. We recently developed strategies to covalently immobilize the enzyme carbonic anhydrase (CA) to the surface of hollow fiber membranes (HFMs), as a means to increase CO_2 removal efficiency in respiratory assist devices. CA plays a critical role in blood carbon

dioxide transport by catalyzing the reaction $CO_2 + H_2O \overset{CA}{\Leftrightarrow} HCO_3^- + H^+$. Most of blood CO_2 (>90%) is carried as bicarbonate (HCO_3^-), which is dehydrated during respiration to gaseous CO_2 by CA within red blood cells (RBCs). Immobilizing CA on the surface of HFMs locally catalyzes dehydration of HCO_3^- to CO_2, increasing the CO_2 partial pressure (PCO_2) at the fiber surface and increasing CO_2 flux through the membrane. Previous studies demonstrated bioactive CA-HFMs increase CO_2 removal by 115% in phosphate buffered saline (PBS) and 37% in blood, compared to unmodified fibers[82,114].

The difference in CA-HFM catalyzed CO_2 removal between PBS and blood is not well understood. Compared to our current 30 – 40% increase in blood CO_2 removal, we anticipate at least 100% increase will be necessary for the development of next-generation minimally invasive devices. Since both fluid systems operate under the same PCO_2 of 50 mmHg, other predominant blood factors, such as RBCs or plasma proteins, must limit the CA coating performance in whole blood. The presence of endogenous CA within RBCs may compete with immobilized CA, reducing the coating efficacy [61]. Additionally, adsorption of plasma proteins and platelets are well known contributors to thrombus formation on the surfaces of polymeric materials, decreasing transport across the fibers and performance of respiratory assist devices [90]. Our use of immobilized CA on the surface of blood contacting gas exchange membranes is a new development in the field. Examining the kinetics of CO_2 transport within CA-modified gas exchange devices in both PBS and blood is an important step towards elucidating strategies for improved CO_2 removal efficiency.

In this study we examined the mass transport phenomena governing CO_2 removal using bioactive CA-HFMs in gas exchange modules. The roles of immobilized CA activity, liquid flow rate and blood cells and proteins were clarified. Using either high activity human or low activity

bovine enzyme sources, CA II was immobilized onto HFMs. The CA modified HFMs were fabricated into model gas exchange devices to assess CO_2 removal performance from fluids containing individual blood components, PBS, PBS + 5% Albumin, PBS + CA, PBS + RBC and whole blood under a mass transfer environment similar to those of commercially available oxygenators. The results of this study will be used to develop respiratory assist devices in which bioactive CA-HFMs can be employed and more substantially increase CO_2 exchange in blood.

4.3 METHODS

4.3.1 Materials

Carbonic anhydrase II from bovine erythrocytes, glutaraldehyde (GA), chitosan (MW= 50-190kD, based on viscosity) and glacial acetic acid were purchased from Sigma-Aldrich (St. Louis, MO). Purified recombinant human carbonic anhydrase II was provided by Dr. Silverman and Dr. McKenna from University of Florida (Gainesville, Fl) [146]. Commercial microporous polypropylene HFMs (Celgard^{TM}; OD: 300 μm, ID: 240 μm, Membrana GmbH, Wuppertal, Germany) were obtained from ALung Technologies, Inc. (Pittsburgh, PA) with an aminated-siloxane coating. Bovine blood with Na-heparin anticoagulation (1:100 dilution of 1000U/mL) was purchased from Lampire Biological Laboratories (Pipersville, PA). All other reagents were purchased from Sigma-Aldrich and were of analytical grade or purer.

4.3.2 In Vitro CO_2 Exchange in Scaled Down Modules of CA-HFM

CA immobilization onto HFMs was performed as previously detailed [114]. A scaled-down gas exchange module was fabricated and an in vitro recirculating test loop was used to assess CO_2 gas exchange rates using unmodified HFMs and CA-immobilized HFMs (Figure 4.1) [114]. CO_2 removal was assessed with PBS, PBS + 5% Albumin, PBS + CA, PBS + RBC and whole blood. For all testing fluids, the system was maintained at 37°C, ~50mmHg PCO_2, and liquid flow rate was 45, 90, or 200mL/min. Under these conditions the HFM CO_2 removal efficiency (ml/min/m^2) matches commercially available devices. The rate of CO_2 removal ($\dot{V}CO_2$) for each model oxygenator device was calculated using the sweep gas flow rate (Q_{OUT}^{STP}) and CO_2 fraction (F_{CO_2}) exiting the scaled-down gas exchange module and then normalized to 50mmHg to correct for small deviations in the inlet PCO_2: $\dot{V}CO_2 = Q_{OUT}^{STP} F_{CO_2} \frac{50}{PCO_2}$. For each device the fluid inlet / outlet PCO_2 and resulting F_{CO_2} were measured in triplicate. The $\dot{V}CO_2$ for each model gas exchange device is reported as an average of these measurements. The difference in PCO_2 from the device inlet to the outlet (PCO_2 inlet – PCO_2 outlet) is reported as PCO_2 drop.

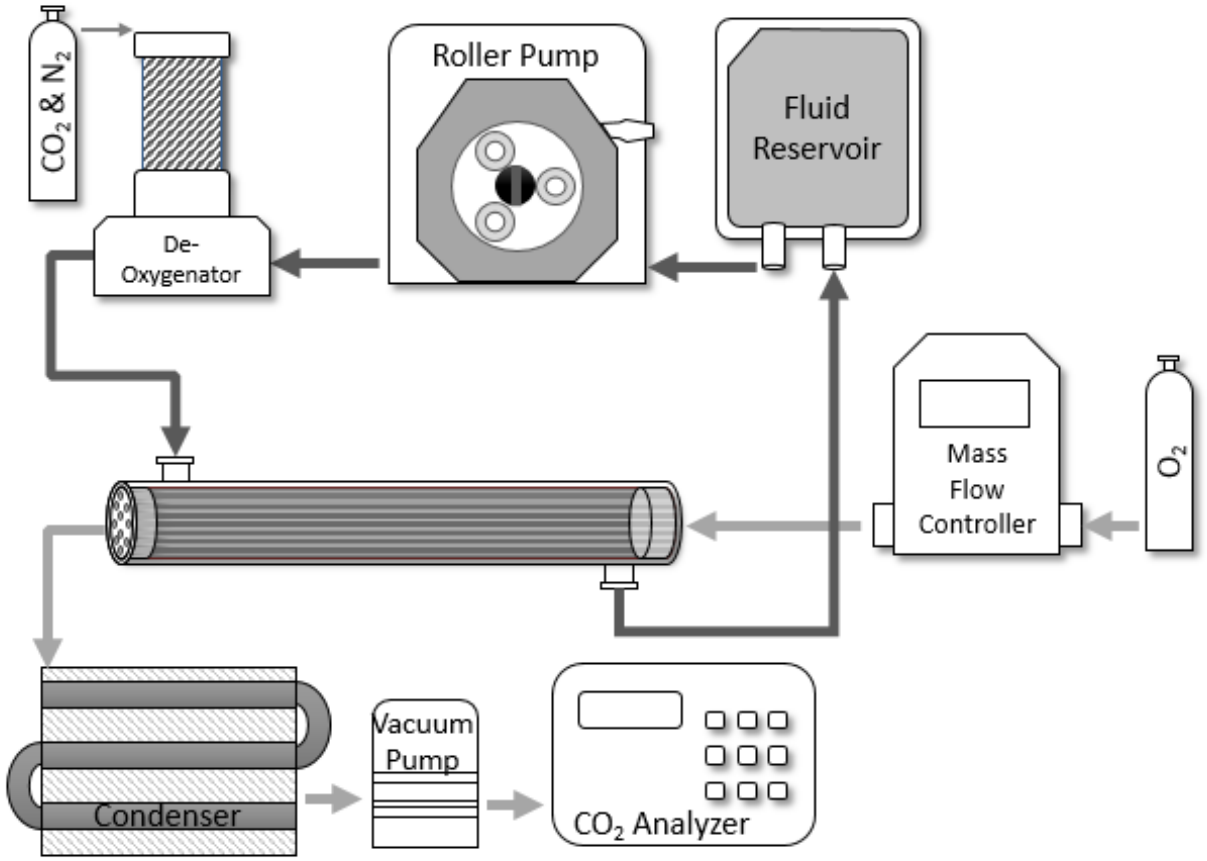

Figure 4.1. Diagram of a model respiratory device and experimental setup for measuring CO_2 removal rates of unmodified and modified HFMs. Bovine blood or PBS solutions were perfused over the outside of the fibers while oxygen sweep gas was passed through the fiber lumens in the opposite direction. De-oxygenator employed the use of a heat exchanger to maintain blood temperature at 37ºC.

The testing fluids were created as described. PBS: A phosphate buffered saline (PBS) solution was prepared with a final pH 7.4 and PCO_2 of 50 mmHg by diluting 780 mL PBS to 1 L with deionized water and adding 30mMoles sodium hydroxide. The basic PBS solution was introduced to the gas exchange loop and upon solvation of CO_2 gas, carbonic acid is formed, decreasing PBS pH to physiologic 7.4. PBS + 5% Albumin: PBS was prepared as described, and once PCO_2 equilibrated to 50mmHg, lyophilized bovine serum albumin was dissolved to 5% (w/v).

PBS + Carbonic Anhydrase: PBS was prepared as described, and once PCO_2 equilibrated to 50 mmHg lyophilized bovine carbonic anhydrase II was added to 16µM. This concentration was selected to mimic physiologic RBC CAII concentration [147]. PBS + RBC: RBCs were isolated from heparinized whole bovine blood and suspended in PBS. Whole bovine blood was centrifuged at 2500 RCFs for 10 minutes and the buffy coat discarded. Packed RBCs were rinsed in PBS under gentle shaking for 10 minutes, centrifuged again and repeated, for a total of 3 wash steps. Packed RBCs were suspended in PBS to 35% hematocrit, glucose was adjusted to 100-300 mg/dL prior to use by the addition of 5% dextrose solution and allowed to incubate for 1 hour [148]. Bovine Blood: Heparinized bovine blood was purchased from Lampire Biological Labs (Pipersville, PA), glucose was adjusted to 100-300 mg/dL by the addition of 5% dextrose solution and hematocrit to 35%, and allowed to incubate for 1 hour [148].

4.3.3 Carbonic Anhydrase Esterase Activity Assay

Immobilized CA enzyme activity was measured spectrophotometrically by monitoring the hydrolysis of *p*-nitrophenyl acetate (*p*-NPA) to *p*-nitrophenol (*p*-NP) at 412 nm. CA-modified fibers were fabricated into model oxygenators as described in section 2.2 and a recirculating loop of 15 mL, 100 mM phosphate buffer pH 7.5, 80 µM *p*-NPA was setup to measure the esterase activity under 45, 90 and 200mL/min flow rate. Absorbance measurements at 412nm were recorded every minute over a 5 minute period, and plotted as a function of time. One activity unit was defined as the amount of enzyme required to generate 1 µmol pNP per minute.

4.3.4 Statistical Analyses

All data are presented as a mean with standard deviation. Statistical significance between more than two sample groups was determined using ANOVA followed by post hoc Tukey testing of specific differences. All other data was compared using a Student's *t*-test assuming equal sample variance. Differences were considered statistically significant for $P < 0.05$.

4.4 RESULTS

4.4.1 Immobilized CA-HFM Activity: Bovine vs Human

Human and bovine CAII HFMs were characterized for both immobilized esterase activity (µmol/min) and CO_2 removal rate (mL/min/m^2) in PBS buffer. Human CA-HFMs demonstrated a 5 fold increase in immobilized esterase activity compared to bovine CA-HFMs, 8.7 U and 1.7 U respectively (Figure 4.2). Flow induced shear under clinically relevant mass transport conditions did not affect immobilized CA esterase activity, as increasing fluid flow rate between 45 and 200 mL/min had negligible effects on immobilized CA activity. In contrast to the esterase activity assay, bovine and human CA devices demonstrated similar CO_2 removal rates. At 45mL/min PBS flow rate, unmodified HFMs removed 85 mL/min/m^2 while bovine and human CA-HFMs removed 135 and 143 mL/min/m^2 respectively (Figure 4.3). Human CA devices attained marginally higher (< 10%) removal rates over bovine CA devices with increasing PBS flow rate. This result indicates that the current level of immobilized bovine CA activity is not a limiting factor in the CO_2 removal

rate of bioactive CA-HFMs. Increasing *p*-NPA activity from 1.8 U (bovine) to 8.8 U (human) did not dramatically increase gas exchange.

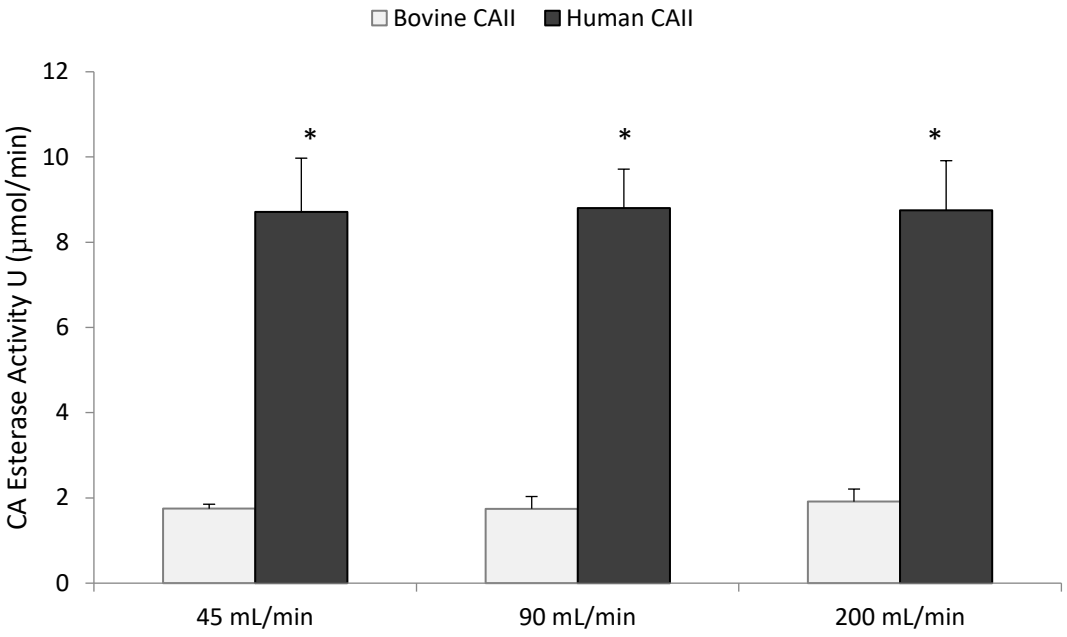

Figure 4.2. Immobilized enzyme *p*-NPA activity is independent of flowrate at 45, 90 and 200 mL/min.

**** P > 0.90***

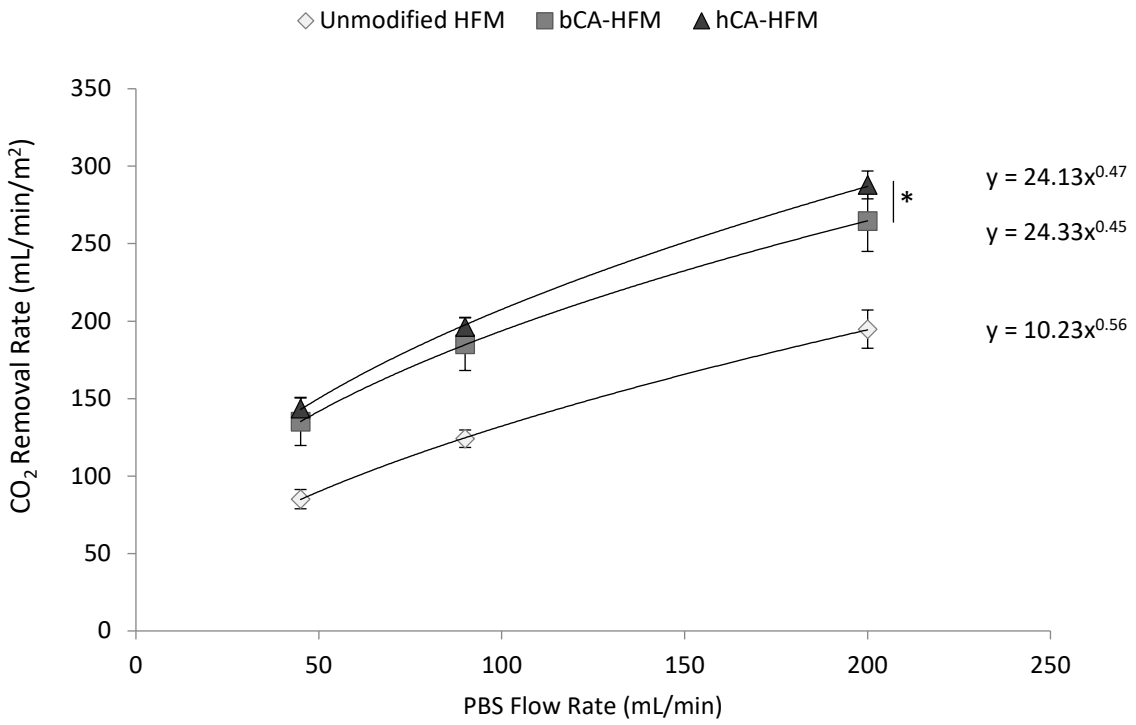

Figure 4.3. CO_2 removal rates for gas exchanges devices in PBS modified with human or bovine CA, compared to unmodified HFMs. Human CA modified HFMs with 4x activity of bovine CA does not significantly increase CO_2 removal. **P > 0.10*

4.4.2 Blood Component Effects on CA-HFM CO_2 Removal Rates

CO_2 removal rates were assessed for unmodified and human CA-HFMs in PBS, PBS + 5% Albumin, PBS + CA, PBS + RBC, and whole blood under a mass transfer environment similar to those of commercially available oxygenators. Albumin solution had no negative effects on CO_2 removal performance by unmodified or CA-HFMs. In PBS and PBS + 5% albumin, unmodified HFMs removed 75 mL/min/m^2 and 88 mL/min/m^2 respectively, while CA-HFMs removed 154 mL/min/m^2 and 187 mL/min/m^2 respectively, for a 106% (PBS) or 112% (PBS + 5% Albumin) increase in CO_2 removal rate (Figure 4.4). Albumin adsorbing onto HFMs did not impede CA coating performance. Conversely, solutions containing CA significantly decreased the enhancement of CA coatings over unmodified HFMs. Unmodified HFMs CO_2 removal increased from 75 mL/min/m^2 in PBS to 172 mL/min/m^2 with PBS + CA, 236 mL/min/m^2 with PBS + RBC and 222 mL/min/m^2 with whole blood. Free CA increased unmodified HFM CO_2 removal rate, which limited immobilized CA contribution to CO_2 removal. CA-HFMs increased CO_2 removal over unmodified fibers by 7% (PBS + CA), 27% (PBS + RBC) and 37% (whole blood). This substantial decrease in CA coating performance as compared to 106% in PBS is attributed to competition between immobilized and free solution CA to catalyze bicarbonate dehydration to CO_2.

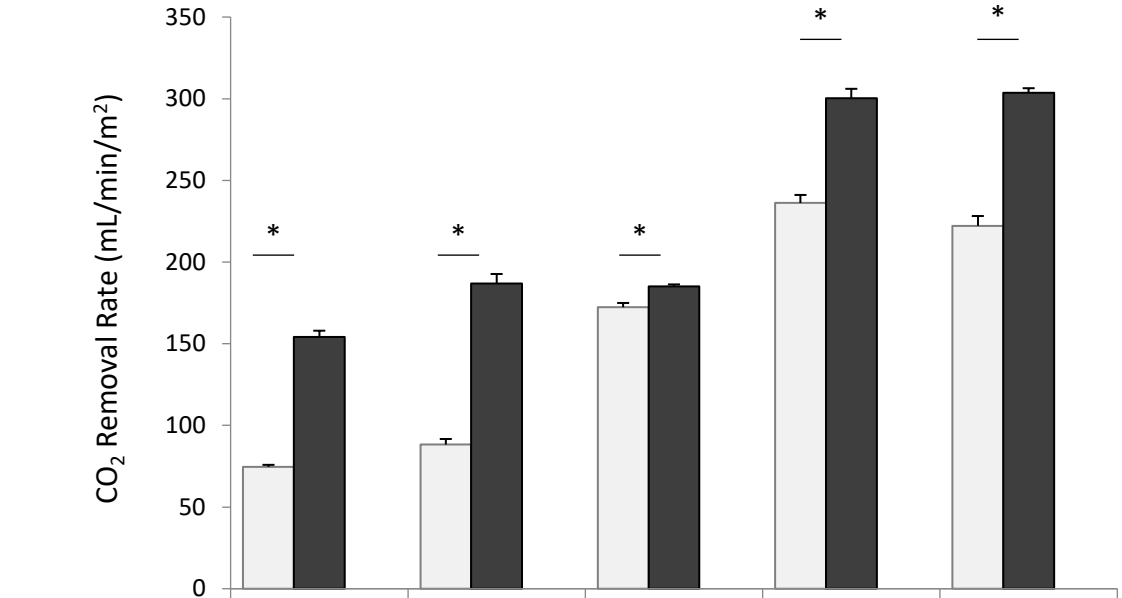

	PBS	PBS+Albumin	PBS+CA	PBS+RBC	Blood
Unmodified-HFM	75	88	172	236	222
hCA-HFM	154	187	185	300	304
% Increase	106	112	7	27	37

Figure 4.4. CO_2 removal by unmodified and human CA immobilized HFMs in PBS, PBS + Albumin, PBS + CA, PBS + RBC and bovine blood in a model respiratory assist device. In PBS and PBS + Albumin, the modified fibers demonstrated a 106% and 112% increase in CO_2 removal rate. In solutions containing carbonic anhydrase, PBS + CA, PBS + RBC and bovine blood, % increase in CO_2 removal rate decreases to 7, 27 and 37%. *$P < 0.05$*

4.4.3 Mass Transport Limitations by CA-HFMs in Blood CO_2 Removal

Bioactive CA-HFM CO_2 removal rate and fluid PCO_2 were assessed in whole bovine blood with varying flow rates. Increasing fluid flow rate adversely affects CA-HFM performance, with a 37%, 22% and 13% increase in CO_2 removal at 45, 90 and 200 mL/min, respectively (Figure 4.5). The difference in PCO_2 from device inlet to outlet (PCO_2 drop) decreased from 13.9 mmHg at 45 mL/min to 11.0 mmHg at 90 mL/min and 5.0 mmHg at 200 mL/min (Figure 4.6) ($p<0.01$). This PCO_2 drop behavior was similar between unmodified and CA-HFMs within each flow rate. Increasing fluid flow decreased CO_2 removal per unit volume passing through the scaled-down gas exchange module, and adversely affected CA coating contribution to total CO_2 removal rate. Increasing PCO_2 drop improves bioactive CA-HFMs performance.

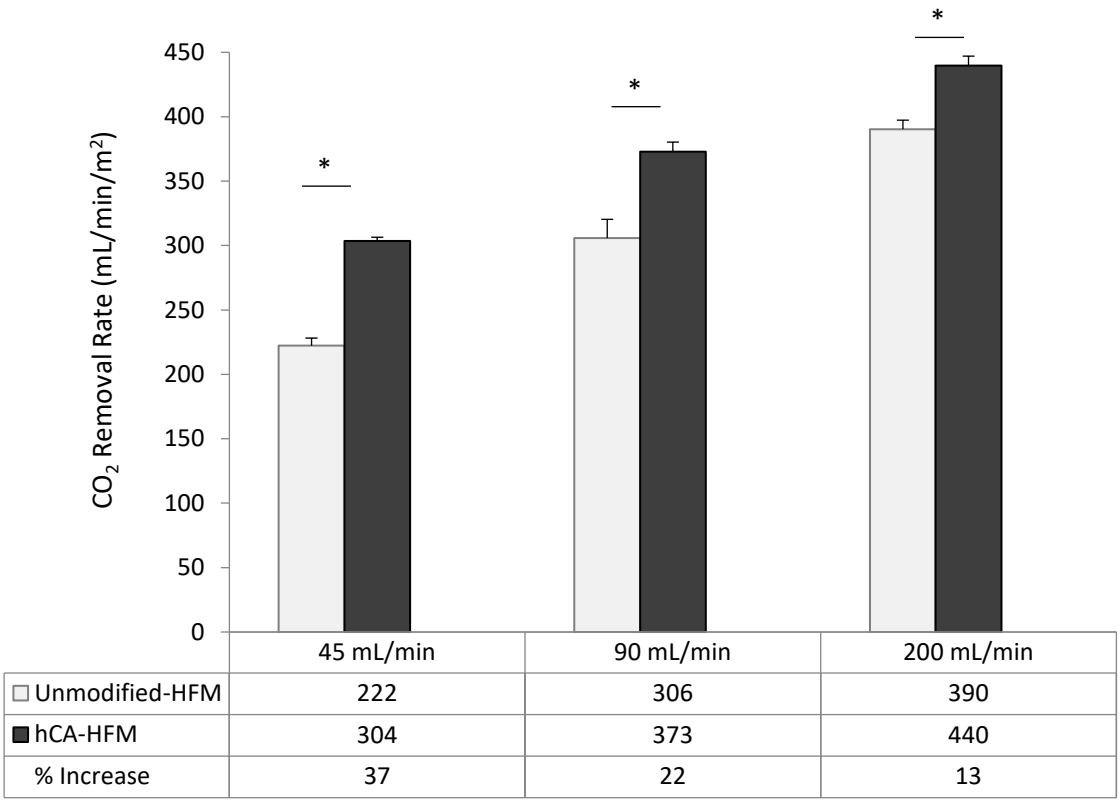

	45 mL/min	90 mL/min	200 mL/min
Unmodified-HFM	222	306	390
hCA-HFM	304	373	440
% Increase	37	22	13

Figure 4.5. CO_2 removal by unmodified and human CA immobilized HFMs in bovine blood at 45, 90 and 200 mL/min. Increasing blood flow rate adversely affects the % increase by carbonic anhydrase coatings on HFMs. *$P < 0.05$*

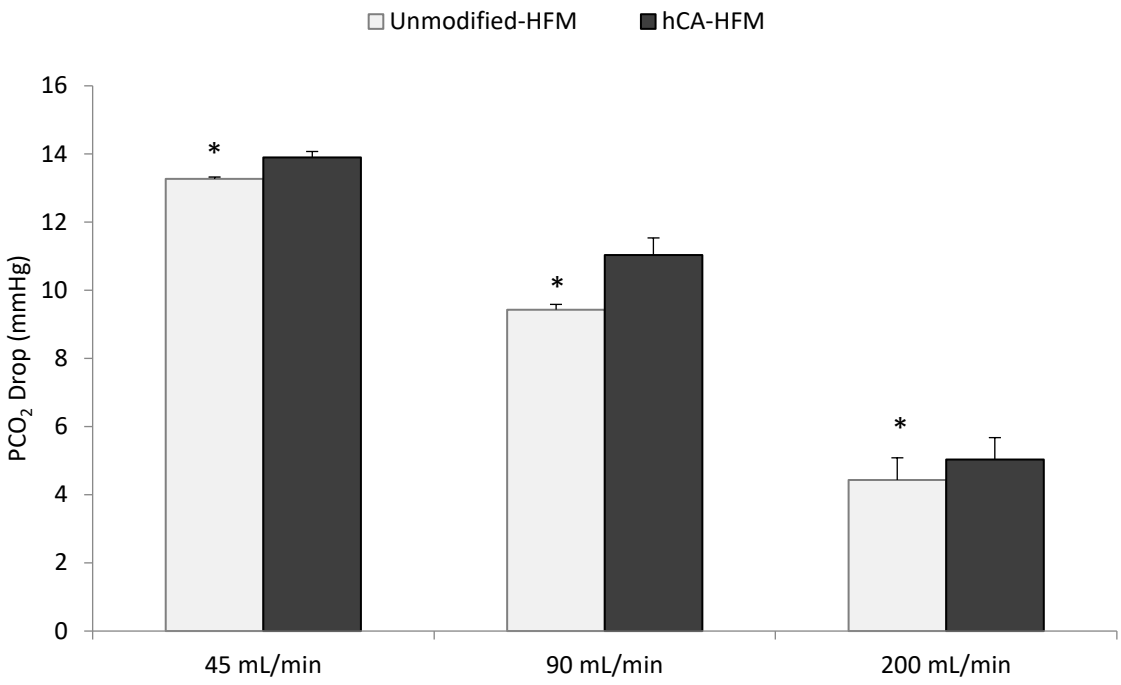

Figure 4.6. Drop in blood PCO_2 across testing module oxygenator, calculated from difference between inlet and outlet, decreases with increasing blood flow rate. *$P < 0.05$*

4.5 DISCUSSION

The goal of this study was to examine the kinetics of CO_2 transport within CA-modified gas exchange devices in PBS and blood, as a means to elucidate strategies for improved blood CO_2 removal using CA-HFM devices. We employed two forms of CA to empirically evaluate the kinetics and mass transport processes limiting HFM CO_2 removal in prototype gas exchange devices. The CO_2 removal performance by CA-HFMs is not influenced by immobilized CA activity or adsorption of blood plasma proteins (albumin). In blood, endogenous CA within RBCs participate along with surface immobilized CA to catalyze bicarbonate/CO_2 equilibrium, in effect throttling immobilized CA.

The mass transport processes for CO_2 removal by CA-modified gas exchange devices is comprised of four distinct physicochemical processes. Overall mass transport in the system is governed by the individual resistances of each process in series. The first resistance in HFM CO_2 removal is interconversion between bicarbonate and CO_2 within the bulk fluid, catalyzed by endogenous CA in blood or uncatalyzed in PBS. Second is diffusion of bicarbonate and CO_2 from the bulk fluid into the liquid diffusional boundary layer adjacent to the HFM surface. Third is the catalyzed dehydration of bicarbonate to CO_2 by immobilized CA on the HFM surface. Last is the diffusion of gaseous CO_2 through the membrane and into the HFM sweep gas stream. Previous work demonstrated the rate limiting step in CO_2 removal for unmodified HFMs is diffusion of CO_2 through the liquid-side diffusional boundary layer, not diffusion through the HFM itself [1,68]. In this application we must additionally consider the impact of immobilized CA catalytic rates, and equilibrium between bicarbonate/CO_2 on system-wide CO_2 transport.

The importance of immobilized CA activity on CO_2 removal was studied through human and bovine CA. Immobilized human CA has 5 fold increase in *p*-NPA activity over bovine CA,

likely due to greater purity of the recombinant human CA solution as compared to the lyophilized bovine CA containing contaminants and denatured proteins. In previous studies, increasing immobilized CA activity through more efficient conjugation strategies increased CO_2 removal rates [114]. We hypothesized higher activity human CA-HFMs would increase CO_2 removal over bovine CA-HFMs. In contrast to the *p*-NPA assay, CO_2 removal rates were comparable between human and bovine CA-HFMs (Figure 4.3). Gas exchange was performed in PBS to avoid effects from protein adsorption on the fiber surface or endogenous CA. Chitosan immobilized CA resulted in sufficient activity such that increasing immobilized CA activity with human CA no longer increased CO_2 removal rate. This suggests diffusive resistance within the liquid boundary layer, as with unmodified HFMs, is the rate limiting step for CO_2 transport rather than immobilized enzyme activity. CA catalyzes bicarbonate/CO_2 and *p*-NPA/*p*-NP using the same active site, however the rate constant (k) is 1 million times greater for CO_2, $1x10^6$ sec^{-1} for CO_2 versus 1 sec^{-1} for *p*-NPA [149,150]. CA catalyzed conversion of bicarbonate/CO_2 is fast enough such that diffusion through the boundary layer dominates transport resistance [151,152]. Decreasing boundary layer resistance by increasing fluid flow rate, increases delivery of *p*-NPA to the fiber surface, but does not increase *p*-NPA catalysis by immobilized CA (Figure 4.2). Differences in immobilized CA activity are measurable with the *p*-NPA assay because CA *p*-NPA catalysis is the rate limiting resistance compared to the fluid boundary layer diffusional resistance. Conversely for bicarbonate or CO_2 as the enzyme substrate, the boundary layer resistance dominates as the rate limiting step over the CA CO_2 catalytic rate. Divergence in the human and bovine CA curves with increasing flow rate in Figure 4.3 is interpreted as reduction in boundary layer thickness (resistance) with increasing flow rate. This hypothesis is supported by regression fits to the data resulting in exponents approaching 0.5, which is the theoretical relationship between boundary

layer thickness and liquid flow rate [1]. Due to the extremely fast catalytic rate of CA (among the highest known) [149], strategies to improve CO_2 removal efficacy through increased CA loading or activity on the fiber surface are not productive avenues unless a corresponding decrease in diffusional boundary layer resistance can be achieved.

The performance of CA-HFMs were examined in whole blood at 45, 90 and 200 mL/min and compared with unmodified HFMs. Increasing blood flow rate increased CO_2 removal rate for unmodified and CA-HFMs, by decreasing the fluid boundary layer resistance. A decrease in CA coating enhancement from 37% to 13% was observed with increasing blood flow rate from 45 to 200 mL/min (Figure 4.5). Shear-induced enzyme activity loss as a consequence of increased liquid flow rate is a potential hypothesis. Data from *p*-NPA activity assay suggest fluid induced shear did not negatively impact CA under these flow rates (Figure 4.2). Additionally, CO_2 removal at 45 mL/min is repeatable after exposure to 200 mL/min flow rate (data not shown), indicating permanent shear-induced effects are unlikely, although transient shear effects under clinically relevant conditions still need to be explored. While increasing blood flow rate increases total CO_2 removal, fluid residence time within the device decreases and consequently the CO_2 removal per fluid volume declines (Figure 4.6). In PBS, HFMs remove CO_2 faster than bicarbonate can dehydrate to CO_2 (uncatalyzed), resulting in a pool of bicarbonate as PBS is depleted of gaseous CO_2. As a drop in bulk PCO_2 is observed, disequilibrium between bicarbonate/CO_2 is created. Approximately 10^3 CO_2 molecules are removed per second by CA-HFMs at a liquid flow rate of 45mL/min, while the uncatalyzed bicarbonate to CO_2 conversion rate is ~1 sec^{-1}. Bioactive CA-HFMs facilitate the dehydration reaction to restore CO_2 pressure in the fluid boundary layer. In blood, endogenous CA within RBCs catalyzes bicarbonate/CO_2 conversion in the bulk fluid, but cannot maintain equilibrium within the fluid boundary layer, evidenced by the impact of CA

coatings on HFM CO_2 removal. The fluid PCO_2 drop can be considered a metric of disequilibrium between bicarbonate and CO_2 where the higher the fluid flow rate, the smaller the PCO_2 drop, and the smaller the impact of bioactive CA coatings on HFM CO_2 removal.

We consistently observed a significant reduction in CA coating efficacy in blood compared to PBS. CO_2 removal by bioactive CA-HFMs was assessed in solutions containing individual blood components: plasma protein albumin, free CA and RBCs. Protein adsorption onto CA-HFMs did not decrease CO_2 removal by unmodified or CA-HFMs. In contrast, endogenous CA within circulating RBCs reduced enhancement of the immobilized CA coating on CO_2 removal. Blood maintains bicarbonate/CO_2 equilibrium more effectively than PBS and directly limits the CA-HFM CO_2 removal enhancement, evident by the 106% increase in CO_2 removal (PBS) versus 37% increase (blood). RBC CA solutions increased CO_2 removal rates for both unmodified and CA-immobilized devices compared to PBS solution (Figure 4.4). Free CA spiked in PBS decreased CA coating efficacy to only 7% improvement over non CA-HFM devices. Since CA-HFM performance increases when CA is localized to RBCs (7% free CA vs 27% RBC CA), diffusion of bicarbonate/CO_2 across the RBC membrane potentially contributes to the resistance limiting bulk fluid equilibrium from restoring gaseous CO_2 as it is depleted by HFMs. Free CA spiked in PBS may localize closer to the HFM surface similar to immobilized CA, whereas RBCs tend to migrate away from stationary surfaces due to hydrodynamic forces, a phenomenon known as the Fahraeus effect for blood flow in small tubes [153].

Development of improved and more efficient respiratory assist devices will enable next generation, minimally invasive extracorporeal support of failing lungs at low blood flows. Carbonic anhydrase immobilized on HFMs is a novel approach to increase CO_2 removal rates, but the factors limiting the enhancement of CO_2 removal by CA-HFMs were not well understood. Our

results demonstrate bioactive CA-HFMs operate under Le Chatelier's principle, catalyzing conversion of bicarbonate/CO_2 to preserve chemical equilibrium within the fluid boundary layer. In blood, endogenous CA within RBCs also catalyzes bicarbonate/CO_2 equilibrium, in effect throttling immobilized CA's contribution towards CO_2 removal. Mechanisms which reduce the diffusional boundary layer resistance and conditions which promote local bicarbonate/CO_2 disequilibrium, such as fluid longer transit times, will result in the largest contribution from the CA coating. Development is underway on CO_2 removal devices which reduce the boundary layer resistance by increasing fluid velocity past HFMs through mechanical mixing independent of fluid flow rate through the device [56,59,154]. This approach increases delivery of bicarbonate/CO_2 to the HFM surface without decreasing blood transit time, which may take advantage of CA's rapid catalysis and boost CO_2 removal performance from increased substrate delivery. Active mixing and CA-HFMs can only restore equilibrium within the fluid boundary layer, but cannot augment fluid PCO_2 above the device inlet condition (around 50 mmHg). Since bicarbonate/CO_2 equilibrium is described by $CO_2 + H_2O \overset{CA}{\Leftrightarrow} HCO_3^- + H^+$, increasing the H^+ concentration in the fluid boundary layer will create disequilibrium, forcing CA to catalyze dehydration of bicarbonate, increasing fluid PCO_2 beyond the inlet 50 mmHg, and driving further improvement in HFM CO_2 removal. By using an acidic gas within the oxygen sweep gas passed through the HFM lumens, an acid product can be introduced to the fluid boundary layer, creating local disequilibrium while minimizing acidification of the whole bulk fluid. In subsequent work we demonstrate dilute sulfur dioxide in oxygen sweep gas increases CO_2 removal, and when used in combination with bioactive CA-HFMs has a synergistic effect to more than double CO_2 removal while maintaining physiologic pH [155].

5.0 ACIDIC SWEEP GAS WITH CARBONIC ANHYDRASE COATED HOLLOW FIBER MEMBRANES SYNERGISTICALLY ACCELERATES CO_2 REMOVAL FROM BLOOD.

The following chapter presents work peer-reviewed and published in Acta Biomaterialia without modification [155]: Arazawa DT, Kimmel JD, Finn MC, Federspiel WJ. Acidic sweep gas with carbonic anhydrase coated hollow fiber membranes synergistically accelerates CO_2 removal from blood. Acta Biomater 2015; 25:143–9. The abstract of the paper follows:

5.1 SUMMARY

The use of extracorporeal carbon dioxide removal ($ECCO_2R$) is well established as a therapy for patients suffering from acute respiratory failure. Development of next generation low blood flow (< 500 mL/min) $ECCO_2R$ devices necessitates more efficient gas exchange devices. Since over 90% of blood CO_2 is transported as bicarbonate (HCO_3^-), we previously reported development of a carbonic anhydrase (CA) immobilized bioactive hollow fiber membrane (HFM) which significantly accelerates CO_2 removal from blood in model gas exchange devices by converting bicarbonate to CO_2 directly at the HFM surface. This present study tested the hypothesis that dilute sulfur dioxide (SO_2) in oxygen sweep gas could further increase CO_2 removal by creating an acidic microenvironment within the diffusional boundary layer adjacent to the HFM surface, facilitating dehydration of bicarbonate to CO_2. CA was covalently immobilized onto poly (methyl pentene)

(PMP) HFMs through glutaraldehyde activated chitosan spacers, potted in model gas exchange devices (0.0151m^2) and tested for CO_2 removal rate with oxygen (O_2) sweep gas and a 2.2% SO_2 in oxygen sweep gas mixture. Using pure O_2 sweep gas, CA-PMP increased CO_2 removal by 31% (258 mL/min/m^2) compared to PMP (197 mL/min/m^2) ($P < 0.05$). Using 2.2% SO_2 acidic sweep gas increased PMP CO_2 removal by 17% (230 mL/min/m^2) compared to pure oxygen sweep gas control ($P < 0.05$); device outlet blood pH was 7.38 units. When employing both CA-PMP and 2.2% SO_2 sweep gas, CO_2 removal increased by 109% (411 mL/min/m^2) ($P < 0.05$); device outlet blood pH was 7.35 units. Dilute acidic sweep gas increases CO_2 removal, and when used in combination with bioactive CA-HFMs has a synergistic effect to more than double CO_2 removal while maintaining physiologic pH. Through these technologies the next generation of intravascular and paracorporeal respiratory assist devices can remove more CO_2 with smaller blood contacting surface areas.

5.2 INTRODUCTION

In patients suffering from acute respiratory failure, extracorporeal carbon dioxide removal ($ECCO_2R$) is a powerful alternative or adjuvant therapy to avoid mechanical ventilation (MV) induced lung injury. High tidal volume MV can initiate and often exacerbate lung injury, increasing patient morbidity and mortality [1,2,156]. Delivery of low tidal volumes and airway pressures mitigates these deleterious effects, as demonstrated by the acute respiratory distress syndrome (ARDS) Network trial where low tidal volume MV at 6 mL/kg vs 12 mL/kg reduced lung injury and improved survival [43]. Recent data suggests even more ultra-protective MV settings may further improve outcomes, as alveolar over-distention is still observed at 6 mL/kg

[3,46,47]. Clinicians are often unable to apply lung protective ventilation (LPV) strategies, reporting hypercapnia and acidosis as significant barriers to implementation [45]. In consequence, mortality rates remain between 40 and 45% for ARDS ICU patients [24]. For the chronic obstructive pulmonary disease (COPD) population, concerns over hypercapnia and severe acidosis can be mitigated through $ECCO_2R$, enabling LPV, weaning of patients off MV, or avoiding intubation altogether [36,157–159]. $ECCO_2R$ in combination with LPV has not seen widespread application as current devices require surgical placement of cannula 19 Fr or larger to facilitate blood flow rates up to 1 L/minute or higher, in order to remove a significant fraction (50%) of total adult CO_2 production [3,9]. Large diameter arterial cannulation systems have shown complication rates as high as 24% comprising of vein tearing, limb ischemia, compartment syndrome and intracranial hemorrhage, in part due to their demand for approximately 25% of cardiac output [66,160]. A clinical need exists for low blood flow $ECCO_2R$ devices (< 500 ml/min) that require less invasive cannulation and can regulate blood CO_2 independent of alveolar ventilation in patients suffering from acute lung failure [7,8,156].

Blood acidification was first described by Snider et al. in 1987, in which infusion 2-8 mEq/min of lactic acid infusion was used to chemically increase trans-HFM CO_2 pressure gradients by acidifying the blood entering the $ECCO_2R$ devices, shifting equilibrium from bicarbonate to favor gaseous CO_2 and increasing CO_2 removal by 120-170%, however visible hemolysis was present [69]. More recently, Zanella et al. have refined this approach to mitigate hemolysis concerns [70–73]. The resulting acidified blood increased PCO_2 from 56 to 136 mmHg, decreased pH from 7.39 to 6.91, and increased CO_2 removal up to 70% [70]. The pH drop is similar to the pH values measured in human capillaries during heavy exercise [61]. Additionally, blood

acidification offsets respiratory alkalosis as the blood leaving $ECCO_2R$ devices without acidification have an increased pH [70].

In this study we hypothesized local blood acidification at the HFM surface would increase CO_2 removal while minimizing perturbations in whole blood pH. Since HFM CO_2 removal is driven by trans-HFM pressure gradients, it should not be necessary to acidify the bulk fluid, but instead only the diffusional boundary layer adjacent to the HFM surface. While lactic acid infusions increase blood PCO_2, this approach acidifies the entire blood volume passing through the device. By mixing dilute concentrations of acidic sulfur dioxide (SO_2) gas into the oxygen (O_2) sweep gas, we created an acidic HFM boundary layer, synergistically working with CA-HFMs to increase trans-HFM CO_2 gradients and accelerate CO_2 blood removal while preserving whole blood pH. The acidic byproduct sulfite naturally occurs in mammalian systems, and has been shown safe in animal models at doses similar to those which would be seen in clinical use of an acidic sweep gas device [161].

5.3 METHODS

5.3.1 Materials

Allylamine, Glutaraldehyde, chitosan (MW= 50-190kD, based on viscosity) and glacial acetic acid were purchased from Sigma-Aldrich (St. Louis, MO). Commercial poly (methyl pentene) (PMP) hollow fiber membranes (HFMs) (Oxyplus^{TM}; OD: 380 µm, ID: 200 µm) were obtained from Membrana GmbH (Wuppertal, Germany). Bovine blood with Na-heparin anticoagulation (1:100 dilution of 1000U/mL) for gas exchange was purchased from Lampire Biological Laboratories

(Pipersville, PA). Purified recombinant human carbonic anhydrase II was provided by Dr. Silverman and Dr. McKenna from University of Florida (Gainesville, Fl) [146]. Sulfur dioxide was purchased from Matheson Gas (Pittsburgh, PA). Sulfite assay kit was obtained from R-Biopharm (Darmstadt, Germany). All other reagents were purchased from Sigma-Aldrich and were of analytical grade or purer.

5.3.2 PMP amination

Allylamine was polymerized onto unmodified PMP through plasma enhanced chemical vapor deposition (PECVD) with the PVA TePla Ion 40 system to create amine functional groups for covalent CA immobilization. PMP HFMs samples (238 cm^2 surface area) were placed on the second shelf from the top. The chamber was evacuated to a pressure of 50 mTorr and then allylamine was continuously introduced to the chamber through a mass flow controller at 180 mL/min for a final chamber pressure of 350 mTorr. Pulsed power was applied for 5 minutes at 300 watts, with a 20% duty cycle and a 150 Hz frequency. After deposition the samples were immediately rinsed with 100mM Phosphate Buffer (PB) at pH 8.5, 3 times for 15 minutes each. This treatment results in a 5.6 $nmol/cm^2$ amine density as quantified through colorimetric technique [132].

5.3.3 Carbonic anhydrase immobilization

Carbonic anhydrase (CA) was immobilized onto PMP HFMs (CA-PMP) by secondary amine linkage through reaction of surface amine and glutaraldehyde crosslinkers, as follows. Aminated PMP (238 cm^2 surface area) was folded into a 60mL test tube and incubated under constant

inversion by orbital mixer with 50mL of 5% GA + 120mM Sodium Cyanoborohydride in PB at pH 8.5 for 15 minutes at 25C^{o}. The fibers were rinsed under constant inversion by orbital mixer with 100mM PB pH 8.5, 3 times for 15 minutes each to remove residual unreacted GA. Then chitosan spacers were immobilized by reacting HFMs with 50mL of 1% (w/v) chitosan + 120mM Sodium Cyanoborohydride suspended in 1% (v/v) acetic acid in DI water for 15 minutes at 25C^{o}, and rinsed with PB as previously described. A second GA reaction and rinse was performed to activate chitosan amine groups for enzyme immobilization. Finally CA was immobilized to the HFMs under constant inversion by orbital mixer with 50mL of 1mg/mL hCAII in 100mM PB at pH 8.5 for 12 hours, followed by 15 minute 120mM Sodium Cyanoborohydride incubation in PB at pH 8.5. Any non-covalently bound CA was removed through three, 15 minute PB rinse sessions. Immobilizing CA by physical adsorption yielded fibers with no detectable activity after 3+ rinses (data not shown).

5.3.4 CO_2 Removal with SO_2 Sweep Gas

A scaled-down gas exchange module was fabricated by inserting HFMs (114 fibers, 18 cm, 0.0238 m^2) into a 1/4 in. ID polycarbonate-tubing (McMaster Carr, Elmhurst, IL) to which single luer locks were UV-glued 0.75 in. from each end in opposing directions. Both ends of the HFMs were secured to the tubing using a 5 minute epoxy adhesive (Devcon, Danvers, MA) and then trimmed to the length of the module to expose the HFM lumens, yielding 11 cm of HFM uncovered within the module for a total active surface area of 0.0151 m^2.

An in-vitro gas exchange test loop (Figure 5.1) was setup under a fume hood and used to assess CO_2 removal rates of PMP and CA-PMP HFMs with and without SO_2 acidic sweep gas (N = 3 for each group). Blood flowed in a single pass loop from a 3 L reservoir, through a peristaltic

pump, into a Medtronic Minimax Plus Pediatric Oxygenator (Minneapolis, MN) to balance the fluid gasses, then into the model oxygenator testing module and finally into a waste container. The partial pressure of CO_2 at the model oxygenator blood inlet was adjusted to 50 mmHg. PCO_2 and pH were measured with a RAPIDLAB 248 Blood-Gas analyzer (Siemens, Deerfield, IL). Custom mixtures of acidic sweep gas up to 2.2% SO_2 balanced in oxygen were created and pulled under vacuum from independent O_2 and SO_2 gas tanks and regulated through two separate GR Series mass flow controllers (Fathom Technologies, Georgetown, TX). The gasses were then mixed into a single line which flowed through the scaled-down oxygenator HFM lumens, moisture trap condenser and finally into an infrared CO_2 analyzer WMA-4 CO_2 Analyzer (PP Systems, Amesbury, MA). The following testing conditions were controlled ensured that the HFM CO_2 removal efficiency (ml/min/m^2) matches the commercially available Hemolung device. The fluid flow rate through the model oxygenator was set to 45 mL/min. The sweep gas flow rate was adjusted to maintain a constant CO_2 concentration in the sweep gas exiting the model oxygenator at approximately 3000 ppm to avoid sweep gas flow limitation of gas exchange [114]. The sweep gas flow rate for PMP HFMs ranged from 0.90 L/min (O_2) to 1.02 L/min (O_2 + 2.2% SO_2), while CA-PMP ranged from 1.35 L/min (O_2) to 2.20 L/min (O_2 + 2.2% SO_2). The fluid temperature was maintained at 37C^o by heat bath. The rate of CO_2 removal ($\dot{V}CO_2$) for each model oxygenator device was calculated using the sweep gas flow rate (Q_{OUT}^{STP}) and CO_2 fraction (F_{CO_2}) exiting the scaled-down gas exchange module and then normalized to 50mmHg to correct for small deviations in the inlet PCO_2: $\dot{V}CO_2 = Q_{OUT}^{STP} F_{CO_2} \frac{50}{PCO_2}$. The $\dot{V}CO_2$ for each model gas exchange group is reported as an average of three individual devices.

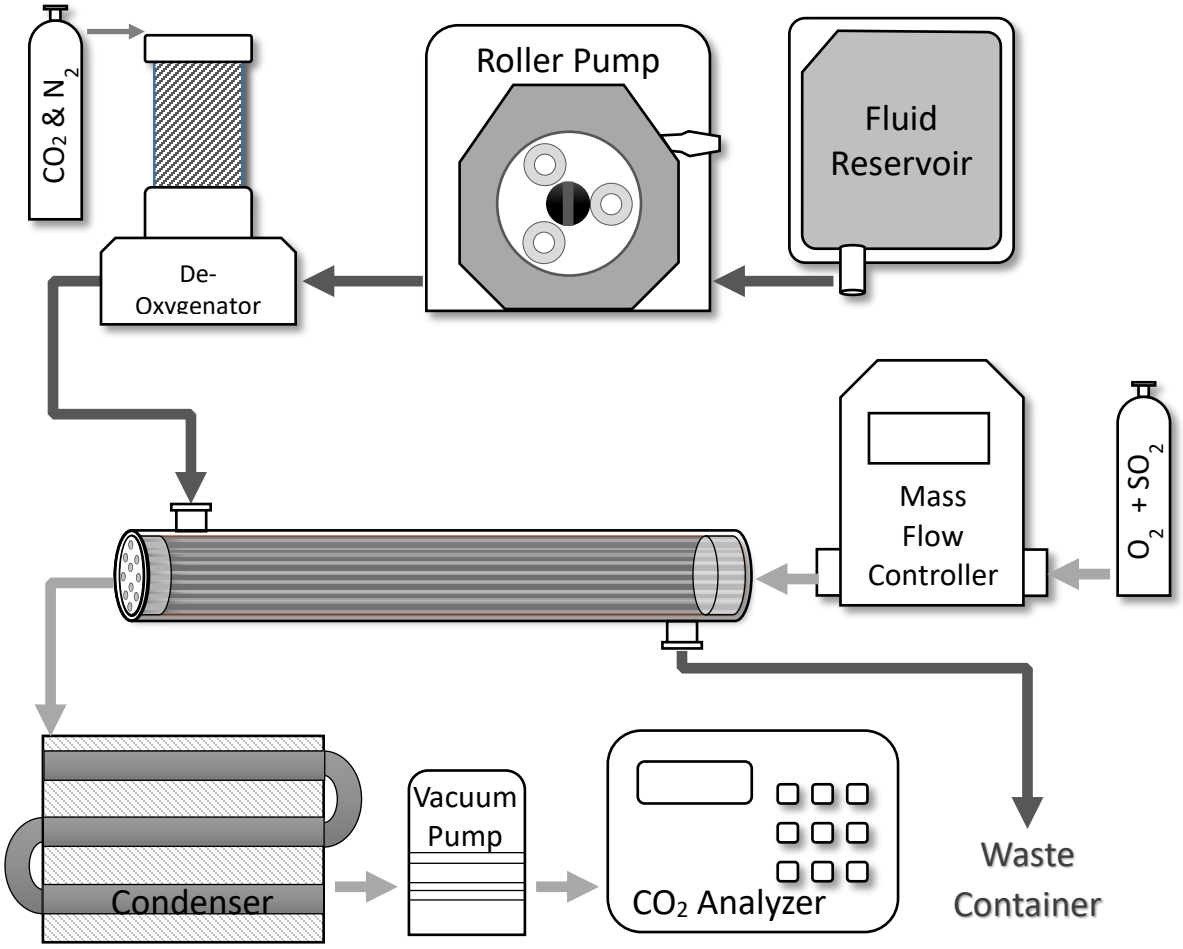

Figure 5.1. Experimental setup for the *in vitro* CO_2 gas exchange assessment. Heparinized bovine blood was deoxygenated to a physiological inlet of 50 mmHg and perfused over the HFMs of a mini respiratory device while SO_2 + O_2 sweep gas was passed through the fiber lumens in the opposite direction. Both the blood reservoir and de-oxygenator employed the use of a heat exchanger to maintain blood temperature at 37C°.

5.3.5 Carbonic Anhydrase Esterase Activity Assay

The CA enzyme activity on HFMs was assayed using the substrate p-nitrophenyl acetate (p-NPA) before and after exposure to SO_2 [162]. CA-PMP fibers were fabricated into model oxygenators as described in section 2.3, assayed for activity, exposed to 2.2% SO_2 acidic sweep gas for 30

minutes as described in section 2.4, and then assayed for activity again. Enzyme activity was measured spectrophotometrically by monitoring the hydrolysis of *p*-nitrophenyl acetate (*p*-NPA) to *p*-nitrophenol (*p*-NP) at 412 nm. A recirculating loop of 15 mL, 100 mM phosphate buffer pH 7.5, 80 µM *p*-NPA was setup to measure the esterase activity. Absorbance measurements at 412nm were recorded every minute over a 5 minute period, and plotted as a function of time. One activity unit was defined as the amount of enzyme required to generate 1 µmol pNP per minute.

5.3.6 Sulfite Assay

The total fluid SO_2 content was assessed using PBS in place of bovine blood, removing potential for interaction between sulfites and plasma proteins. An enzymatic sulfite assay kit (r-Biopharm) was used according to manufacturer's instructions. Briefly, sulfite is oxidized to sulfate by sulfite oxidase, yielding hydrogen peroxide which is reduced by NADH-peroxidase in the presence of NADH. The amount of sulfite is equivalent to the amount of NADH oxidized, which is determined by spectrophotometric absorbance at 340 nm.

5.3.7 Statistical Analyses

All data are presented as a mean with standard deviation. Statistical significance between more than two sample groups was determined using ANOVA followed by post hoc Tukey testing of specific differences. All other data was compared using a Student's *t*-test assuming equal sample variance. Differences were considered statistically significant for $P < 0.05$.

5.4 RESULTS

5.4.1 CO_2 Removal with SO_2 Sweep Gas

PMP and CA-PMP blood CO_2 removal rates were measured using oxygen sweep gas with up to 2.2% SO_2 (Figure 5.2). With pure O_2 sweep gas, bioactive CA-PMP HFMs increased CO_2 removal by 31% (258 ± 10 mL/min/m^2) compared to control PMP (197 ± 3 mL/min/m^2) ($P < 0.05$). Using SO_2 acidic sweep gas through PMP fibers, CO_2 removal increased by 17% (230 ± 5 mL/min/m^2), compared to pure oxygen sweep gas through the same fibers ($P < 0.05$). When employing both CA-PMP and SO_2 acidic sweep gas, CO_2 removal increased by 109% (411 ± 4 mL/min/m^2), compared to unmodified HFMs with pure oxygen sweep gas ($P < 0.05$).

The blood pH and PCO_2 exiting the device were measured to establish the effects of SO_2 acidic sweep gas on the bulk blood. For PMP and CA-PMP devices using pure O_2 sweep gas, blood pH exiting the device increased from 7.37 ± 0.006 at the inlet to 7.44 ± 0.004 and 7.43 ± 0.006 respectively. However when using 2.2% SO_2 acidic sweep gas, blood pH exiting the device was nearly unchanged from the inlet, with an outlet pH of 7.38 ± 0.009 for PMP and 7.35 ± 0.006 for CA-PMP (Figure 5.3). For blood PCO_2 exiting the device, pressure decreased from 50mmHg inlet to 37 ± 0.5 mmHg outlet for PMP and 35 ± 0.4 mmHg for CA-PMP with pure O_2 sweep gas. When using 2.2% acidic sweep gas, PCO_2 exiting the device was 40 ± 0.3 mmHg for PMP and 38 ± 0.5 mmHg for CA-PMP. The addition of dilute SO_2 to O_2 sweep gas maintained near physiologic pH and PCO_2 for blood exiting the device.

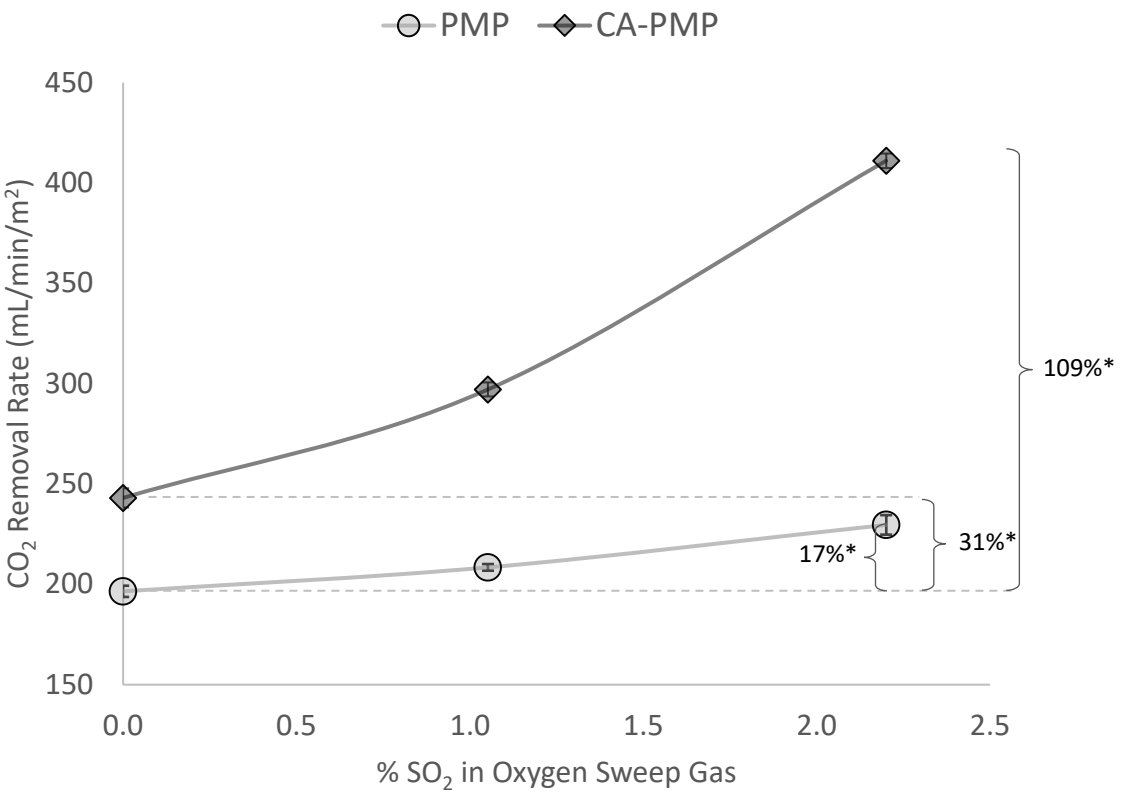

Figure 5.2. CO_2 removal by PMP and CA-PMP HFMs from bovine blood using pure O_2 and 2.2% SO_2 acidic sweep gas. (N=3) *$P < 0.05$*

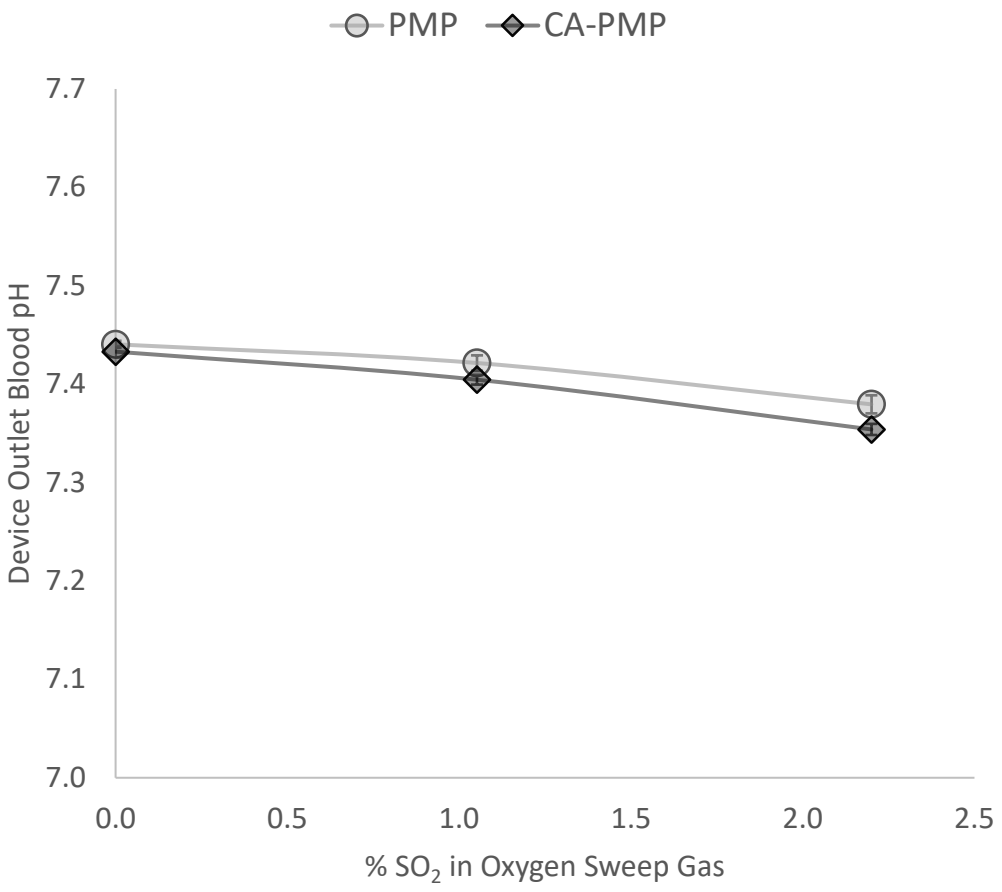

Figure 5.3. Increasing the % SO_2 within oxygen sweep gas decreases blood pH exiting the device. (N=3)

5.4.2 Carbonic Anhydrase Esterase Activity Assay

Immobilized carbonic anhydrase activity was measured before and after exposure to SO_2. Activity remained unchanged with 9.3 ± 0.8 U before and 9.5 ± 0.9 U after exposure to 2.2% SO_2 acidic sweep gas, indicating CA coating stability to the acidic microenvironment over this time course.

5.4.3 Blood Sulfite Assay

Total sulfite was measured in PBS fluid exiting the scaled-down gas exchange module with 2.2% SO_2 sweep gas. The sulfite concentration leaving the device was 0.08 ± 0.001 mMol/L for PMP and 0.28 ± 0.002 mMol/L, or 3.5 times more, for bioactive CA-PMP HFMs ($P < 0.05$) (Figure 5.4).

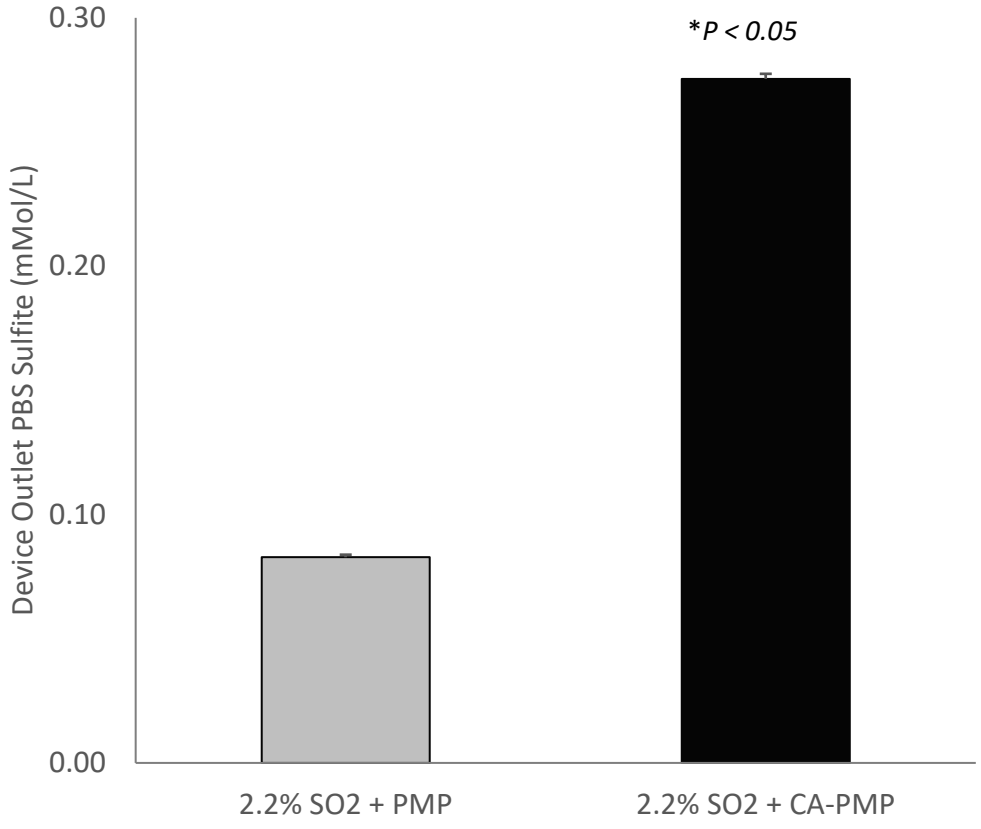

Figure 5.4. Total PBS sulfite concentration of fluid exiting the device with 2.2% SO_2 acidic sweep gas. (N = 3)

Table 5.1. Comparison of blood acidification approaches by pH, CO_2 removal % increase, and total lactate or sulfite anion infused.

Blood Acidification Method	*Blood pH*	*CO_2 Removal % Increase*	*Lactate or Sulfite Infused (mMol/L)*
LA Blood Infusion [70]	7.51	70%	15.1
LA Dialysis: Blood CO_2 Removal [72]	7.41	78%	12.3
LA Dialysis: Dialysate CO_2 Removal [73]	7.43	157%	14.1
Present Study: 2.2% SO_2 + CA-PMP	7.35	109%	0.28

Table 5.2. CO_2 removal rate (mL/min) by PMP and CA-PMP HFMs from bovine blood using pure O_2 and up to 2.2% SO_2 acidic sweep gas.

HFM Type	Average CO_2 Removal Rate (mL/min)		
	O_2	*O_2 + 1.1% SO_2*	*O_2 + 2.2% SO_2*
PMP	2.78	2.95	3.24
CA-PMP	3.65	4.29	5.87

Table 5.3. Acid-Base parameters of the blood at the inlet and outlet of the model oxygenator.

Device	pH	PCO_2 *(mmHg)*	HCO_3^- *(mMol/L)*	B.E. *(mEq/L)*
Inlet Blood	7.37	47.5	26.5	1.57
Outlet Blood				
PMP	7.44	36.6	24.0	0.20
CA-PMP	7.43	34.8	22.5	-1.33
PMP (2.2% SO_2)	7.38	39.7	22.7	-1.89
CA-PMP (2.2% SO_2)	7.35	38.2	20.6	-4.18

5.5 DISCUSSION

The goal of this study was to quantify how local blood acidification using acidified sweep gas could increase CO_2 removal in HFM devices while minimizing effects on whole blood pH. Previous work by our group to chemically increase trans-HFM CO_2 pressure utilized bioactive CA-HFMs for a 31-37% improvement in blood CO_2 removal efficiency [82,114]. In this work, the addition of SO_2 to an oxygen sweep gas increased CO_2 removal of unmodified PMP HFMs up to 17%, and for bioactive CA-PMP HFMs up to 109% (Figure 5.4). Synergy between CA coatings and SO_2 acidic sweep gas dramatically increases CO_2 removal efficiency of HFMs. To our knowledge, this is the first report assessing the potential of an acidic sweep gas to increase CO_2 removal from blood using HFM devices like blood oxygenators.

Zanella et al. have utilized lactic acidic (LA) infusions for increasing HFM CO_2 removal [70–72]. In their work, LA was mixed with bulk extracorporeal blood via direct infusion or dialysis, upon which acidified blood flowed into a HFM device for CO_2 removal. When directly infusing LA with 500 mL/min extracorporeal blood flow rate, pH dropped to 6.91 while lactate concentration increased from 1.2 to 15.1 mM, for a 70% increase in CO_2 removal from 58 mL/min/m^2 to 95 mL/min/m^2 [70]. When using a dialysis membrane to acidify blood with 250 mL/min blood flow rate, pH dropped to 6.99 while lactate concentration increased from 0.7 to 12.3 mM, for a 62-78% increase in CO_2 removal from 99 mL/min/m^2 to 160 mL/min/m^2 [72]. In contrast to bulk LA acidification, we demonstrated HFM CO_2 removal efficiency can be significantly increased through localized blood acidification with SO_2 acidic sweep gas, consequently introducing 50 times less acidic anions to blood, while mitigating transient acidosis (Table 5.1). Recently Zanella et al. described a unique approach utilizing acidified dialysis to transport bicarbonate and CO_2 from blood into a dialysate using a commercial dialysis filter. The

dialysate was then acidified with LA and flowed into a HFM commercial oxygenator device for dialysate CO_2 removal [73]. Using blood flow rates of 250 mL/min, blood pH remained nearly unchanged at 7.43, blood lactate concentration increased from 0.6 to 14.1 mM, and dialysate CO_2 removal increased 157 % from 18 mL/min/m^2 to 48 mL/min/m^2. A drawback of this approach is the requirement of two devices for CO_2 removal from blood, a membrane oxygenator and a dialysis filter to remove bicarbonate/CO_2 from blood. In contrast, our approach suggests that 100 mL/min of CO_2 removal could be accomplished with one HFM based device, with a surface area of 0.25 to 0.5 m^2. In all approaches used by Zanella et. al, blood hyperlactatemia (2-5mM lactate) persists (see Table 5.1). Clinically, lactate is monitored as a biomarker of organ dysfunction, shock and has been correlated with increased mortality in critically ill patients [74–79]. Consequently addition of exogenous LA may limit the diagnostic potential of blood lactate levels as a predictor of adverse outcomes.

We hypothesize SO_2 sweep gas acidifies blood in or near the diffusional boundary layer, which provides the main resistance to CO_2 removal in HFM devices [1]. By reacting with water SO_2 creates sulfurous acid, which rapidly dissociates into bisulfite and sulfite ions: $SO_2 + H_2O \Leftrightarrow HSO_3^- + H^+ \Leftrightarrow SO_3^{2-} + H^+$. SO_2 was selected for its high solubility and acid dissociation constant in water, enabling dilute concentrations (1-2%) within the oxygen sweep gas [163]. The synergistic activity of CA-PMP with SO_2 sweep gas indicates acidification of blood hydrating the immobilized CA layer, adjacent to the HFM surface. Additionally the minimal impact of acidic sweep gas on bulk blood pH demonstrates a majority of acidic protons are consumed in bicarbonate dehydration. By consuming acidic protons during catalysis, immobilized CA facilitates diffusion of SO_2 from the sweep gas into the fluid boundary layer. Consequently, 3.5 times more sulfite was measured in the bulk fluid for CA-PMP compared to PMP, 0.28 mMol/L versus 0.08 mMol/L respectively

(Figure 5.4). Despite the sulfite infusion, blood pH remained near physiologic from inlet of 7.37 to outlet 7.38 for PMP and 7.35 for CA-PMP. Calculation of base excess (BE) demonstrates metabolic acidosis of the blood occurred which cannot be fully described by the measured sulfite content, as drop in BE was 3.46 mEq/L for PMP and 5.75 mEq/L CA-PMP (Supplemental Table 5.2 & Table 5.3). Variations in the plasma electrolyte concentration, PCO_2 and total amount of weak acids can regulate blood pH [164]. The release of chloride ions from RBCs and albumin have reported in the literature, as a PCO_2 dependent change in the strong ion difference, which acidify the plasma to limit pH increase due to CO_2 removal [164,165]. This buffer and the polyprotic nature of sulfurous acid account for a portion of the observed drop in BE, but future work will quantify blood electrolytes to fully describe anions which impact drop in BE. Mixtures beyond 2.2% SO_2 were not possible as we were limited by the mass flow controllers, however the data suggests CO_2 removal could be further improved by increasing SO_2 concentration. No hemolysis due to the acidic sweep gas was observed by spectrophotometric assay of plasma free hemoglobin (data not shown).

At physiologic pH and temperature, the dissociated byproducts of SO_2 introduced into blood are in the sulfite and bisulfite ion form. These species are endogenous to biological systems from metabolism of sulfur amino acids. Sulfites are commonly used as antioxidant preservatives in cosmetics, food and pharmaceutical products [166]. Sulfite oxidase, found in the mitochondria of most mammalian tissues, catalyzes sulfur detoxification by oxidizing sulfite to sulfate for excretion through urine [167,168]. Various review articles have surveyed the literature for toxicology and safety of sulfites, finding no serious adverse effects as a result of chronically administered sulfite [161,167,169]. Roughly 1 – 5% of the population does present sulfite sensitivity, due to impaired sulfite oxidase activity, though most reactions are mild [166,168].

Additionally, recovery of sulfite oxidase activity has been reported in an infant with molybdenum cofactor deficiency through dosage of cyclic pyranopterin monophosphate [170]. In-vitro toxicology assessment of sulfite indicates potential to react with DNA causing mutagenesis, however these effects have not been replicated in-vivo at physiologic concentrations [161,169,171]. As a potentially protective mechanism, blood plasma proteins have been shown to reversibly react with sulfite to form s-sulfonate groups, mitigating insult of high sulfite concentrations on tissues [161,172,173]. Typical daily dietary sulfite intake can be up to 0.14 mmol/kg body weight and normal human serum sulfite can range from 0 – .01 mM [161,174]. Based upon urinary sulfate excretion, daily endogenous human sulfite generation is estimated at 0.3 – 0.4 mmol/kg [175]. Scaling the 0.28 mM sulfite concentration we observe with acidic sweep gas to a low blood flow CO_2 removal device at 500 mL/min, yields a theoretical sulfite infusion rate of 0.12 mmol/kg/hour or 2.88 mmol/kg/day for an average 70 kg adult. Studies have demonstrated the capacity of mammalian sulfite oxidase is extremely high compared with normal endogenous and exogenous sulfite loads [176]. Perfused dog livers tested for up to 3 hours oxidized sulfite at rates of at least 19 mmol/kg/day (559% more sulfite than the daily acidic sweep gas rate) [161,177]. In rhesus monkeys, Gunnison et al. estimated the biological half-life of sulfite at 10 minutes after intravenous doses of 0.3 – 0.6 mmol/kg sulfite (at least 208% more sulfite than the hourly acidic sweep gas rate), and the capacity to metabolize orally administered sulfite at 2.74 mmol/kg/day for 11 consecutive days (within 5% of the daily acidic sweep gas rate) [161,176]. In healthy human subjects, consumption of 0.21 mmol/kg sulfite (75% more sulfite than hourly acidic sweep gas rate) elevated serum sulfite concentration up to 0.112 mM within 30 minutes, which then returned to basal levels within 3 hours without any adverse reactions [178]. This data suggests the acidic sweep gas sulfite levels seen here (up to 2.88 mmol/kg/day) are tolerable, and could be

oxidized and excreted by the human body without serious adverse reaction. We conclude use of SO_2 acidic sweep gas has potential as a clinically viable approach to increasing HFM CO_2 removal efficiency.

Application of the acidic sweep gas and bioactive CA-HFMs to current $ECCO_2R$ devices yields a CO_2 removal device capable of removing a clinically significant 100 mL/min (50% of the metabolic needs of an adult patient [68]) with smaller surface areas. Model devices in this study utilized surface area (0.0151 m^2) and liquid flow rates (45 mL/min) appropriately scaled to mimic the mass transport environment of comparable human HFM devices under clinically relevant conditions (197 mL/min/m^2). We would expect similar performance by our approaches when translated to full scale commercial devices. For example, highly efficient low blood flow (< 500 mL/min) CO_2 removal devices such as the Hemolung RAS® (ALung Technologies, Pittsburgh PA) reported peak CO_2 removal rates of 121 mL/min with 0.6 m^2, for a comparable efficiency of 201 mL/min/m^2 [179]. Incorporation of an acidic sweep gas and bioactive CA-HFMs into this device could improve average efficiency up to 283 mL/min/m^2, thereby requiring just 0.35m^2 for 100 mL/min CO_2 removal support, at blood flow rates less than 500 mL/min.

In conclusion, development of highly efficient $ECCO_2R$ devices will facilitate minimally invasive vascular access (11-15 Fr cannula) for partial respiratory support (up to 50%) at low blood flow rates (200-500 mL/min). By mixing dilute concentrations of acidic SO_2 gas into the oxygen sweep gas, we acidified the blood in and around diffusional boundary layer, increasing the trans-HFM CO_2 pressure gradient to more than double CO_2 removal while maintaining near physiologic pH. Future work will focus on assessing the enzymatic coating stability over time and validating the SO_2 acidic sweep gas technique and sulfite byproduct safety in an animal model, elucidating the difference in BE and sulfite concentration and explore means of removing exogenous sulfite if

necessary. Bioactive CA coatings in combination with SO_2 acidic sweep gas could lead to next generation highly efficient CO_2 removal devices for the treatment of acute and acute-on-chronic lung failure.

6.0 SUMMARY & CONCLUSIONS

In patients suffering from acute respiratory failure, extracorporeal carbon dioxide removal is a powerful alternative or adjuvant therapy to avoid mechanical ventilation induced lung injury. The complexity and invasiveness of current respiratory assist devices used for $ECCO_2R$ has limited widespread use in ICUs. New technologies that facilitate accelerated CO_2 removal may lead to the development of smaller, more efficient respiratory assist devices that can be implemented by intensivists and other nonsurgical clinicians. Several novel respiratory assist devices have been developed and/or proposed which mechanically enhance gas exchange, however further improvement in efficiency is still desired. The work of this thesis develops and characterizes a novel carbonic anhydrase bioactive coating for HFMs which can be employed to substantially increase CO_2 exchange in blood.

In its current state, CA HFM technology will likely face many hurdles limiting its clinical potential. The first generation of this coating (Chapter 2) utilized CNBr/TEA conjugation chemistry, known to be both toxic and susceptible to leaching. This proof of principle study demonstrated the impact of CA-modified HFMs on both hemocompatibility and CO_2 removal from blood for improved respiratory assist devices. CA-immobilized HFMs increased blood CO_2 removal rate by 36% and decreased in platelet deposition by a 95% compared to unmodified HFMs. While highlighting the potential of bioactive HFMs, CNBr conjugation chemistry is not a clinically viable approach. We took steps towards addressing CA coating toxicity and stability with an amine based conjugation strategy utilizing chitosan polymers and glutaraldehyde crosslinkers (Chapter 3). Next generation CA coatings could further improve toxicity with biocompatible amine based crosslinkers such as genipin, however limitations in the lifespan of CA

enzyme coating remain. These bioactive HFMs will likely not have the stability to endure a medical device sterilization process, survive on the shelf for months to years, and then ultimately deliver sustained CA activity over a therapeutic window of days to weeks. Exploration of cross linked enzyme aggregates and single enzyme nanogels have demonstrated promise in the literature as paths to creating enzymes which can maintain activity for years on end. Additionally, some groups have developed highly stable CA variants for use in CO_2 sequestration in greenhouse gas emissions. A commercially viable bioactive HFM will probably employ engineered CA enzymes which can reliably deliver activity throughout the lifespan of a medical device.

Compared to our current 30 – 40% increase in blood CO_2 removal, we anticipated at least 100% increase will be necessary for the development of next-generation minimally invasive devices. Amine based CA HFMs (Chapter 3) increased CA loading by 561%, however the improvements in immobilized enzyme activity did not manifest in further increase in bioactive HFM CO_2 removal efficiency. In Chapter 4 we characterized the impact of bioactive HFMs on CO_2 removal and explain the mechanisms which govern the efficacy of these biocatalytic devices. We separated out the impact of individual blood components (plasma albumin, red blood cells or free carbonic anhydrase) and fluid flow rate on bioactive HFMs CO_2 removal efficiency. Based on our findings, we proposed a bicarbonate/CO_2 disequilibrium hypothesis to describe performance of CA-modified devices in blood. This work was the first study to characterize the CO_2 mass transport processes within these biocatalytic devices which impede CA coating efficacy and may serve as a basis towards developing approaches which improve bioactive HFM efficiency. In short, strategies which maximize CA loading on HFMs are not ideal avenues for improved efficiency of biocatalytic CO_2 removal devices.

Improvement in CO_2 removal rates using CA-modified devices in blood were realized by maximizing bicarbonate/CO_2 disequilibrium at the fiber surface via blood acidification (Chapter 5). We introduced dilute sulfur dioxide in oxygen sweep gas to acidify the blood in and around the diffusional boundary layer, thereby forcing dehydration of bicarbonate to CO_2. Our results demonstrated a dilute acidic sweep gas can increase CO_2 removal and when used in combination with bioactive CA-HFMs had a synergistic effect to more than double CO_2 removal efficiency while maintaining physiologic pH. While achieving our efficiency target, the use of sulfur dioxide as a blood acidification agent introduces tremendous complexity and risk to the patient, limiting our clinical potential. Engineering devices to deliver acidic gases in a manner that is safe and practical to implement in a hospital setting may be fruitful avenues towards introducing a device which utilizes this technology.

In conclusion, the work presented here summarizes the efforts to characterize the impact bioactive HFMs on CO_2 removal and explain the mechanisms which govern the efficacy of these biocatalytic devices. In its current state this technology will need to overcome the hurdles of shelf life and patient risk/complexity to see true clinical potential. The impact of this work is less a clinical solution, and rather an instrument in elucidating mechanisms which will enable highly efficient CO_2 removal devices. We hope understanding the mechanistic properties of CA HFMs may potentiate clinically useful technologies which will enable the next generation highly efficient and hemocompatible HFM-based artificial lungs.

BIBLIOGRAPHY

[1] Federspiel WJ, Henchir KA. Lung, artificial: basic principles and current applications. Encycl Biomater Biomed Eng 2004;9:910.

[2] Tremblay LN, Slutsky AS. Ventilator-induced lung injury: from the bench to the bedside. Intensive Care Med 2005;32:24–33. doi:10.1007/s00134-005-2817-8.

[3] Pesenti A, Patroniti N, Fumagalli R. Carbon dioxide dialysis will save the lung. Crit Care Med 2010;38:S549–54. doi:10.1097/CCM.0b013e3181f1fe0c.

[4] Terragni P, Maiolo G, Ranieri VM. Role and potentials of low-flow CO(2) removal system in mechanical ventilation. Curr Opin Crit Care 2012;18:93–8. doi:10.1097/MCC.0b013e32834f17ef.

[5] Kaushik M, Wojewodzka-Zelezniakowicz M, Cruz DN, Ferrer-Nadal A, Teixeira C, Iglesias E, et al. Extracorporeal Carbon Dioxide Removal: The Future of Lung Support Lies in the History. Blood Purif 2012;34:94–106. doi:10.1159/000341904.

[6] Cove M, MacLaren G, Federspiel W, Kellum J. Bench to bedside review: Extracorporeal carbon dioxide removal, past present and future. Crit Care 2012;16:232. doi:10.1186/cc11356.

[7] Batchinsky AI, Jordan BS, Regn D, Necsoiu C, Federspiel WJ, Morris MJ, et al. Respiratory dialysis: reduction in dependence on mechanical ventilation by venovenous extracorporeal CO2 removal. Crit Care Med 2011;39:1382–7. doi:10.1097/CCM.0b013e31820eda45.

[8] Wearden PD, Federspiel WJ, Morley SW, Rosenberg M, Bieniek PD, Lund LW, et al. Respiratory dialysis with an active-mixing extracorporeal carbon dioxide removal system in a chronic sheep study. Intensive Care Med 2012;38:1705–11. doi:10.1007/s00134-012-2651-8.

[9] Crotti S, Lissoni A, Tubiolo D, Azzari S, Tarsia P, Caspani L, et al. Artificial Lung as an Alternative to Mechanical Ventilation in COPD Exacerbation. Eur Respir J 2012;39:212–5. doi:10.1183/09031936.00021111.

[10] What is chronic obstructive pulmonary disease (COPD)? n.d. http://www.nhlbi.nih.gov/health/dci/Diseases/Copd/Copd_WhatIs.html.

[11] Fanelli V, Ranieri MV, Mancebo J, Moerer O, Quintel M, Morley S, et al. Feasibility and safety of low-flow extracorporeal carbon dioxide removal to facilitate ultra-protective ventilation in patients with moderate acute respiratory distress syndrome. Crit Care 2016;20:36. doi:10.1186/s13054-016-1211-y.

[12] Mannino DM, Braman S. The Epidemiology and Economics of Chronic Obstructive Pulmonary Disease. Proc Am Thorac Soc 2007;4:502–6. doi:10.1513/pats.200701-001FM.

[13] Trahanas JM, Lynch WR, Bartlett RH. Extracorporeal Support for Chronic Obstructive Pulmonary Disease: A Bright Future. J Intensive Care Med 2017;32:411–20. doi:10.1177/0885066616663119.

[14] Sullivan SD, Ramsey SD, Lee TA. The Economic Burden of COPD. CHEST 2000;117:5S-9S. doi:10.1378/chest.117.2_suppl.5S.

[15] Toy EL, Beaulieu NU, McHale JM, Welland TR, Plauschinat CA, Swensen A, et al. Treatment of COPD: Relationships between daily dosing frequency, adherence, resource use, and costs. Respir Med 2011;105:435–41. doi:10.1016/j.rmed.2010.09.006.

[16] Vestbo J, Hurd SS, Agustí AG, Jones PW, Vogelmeier C, Anzueto A, et al. Global Strategy for the Diagnosis, Management, and Prevention of Chronic Obstructive Pulmonary Disease. Am J Respir Crit Care Med 2013;187:347–65. doi:10.1164/rccm.201204-0596PP.

[17] Centers for Disease Control and Prevention (CDC). Chronic obstructive pulmonary disease among adults--United States, 2011. MMWR Morb Mortal Wkly Rep 2012;61:938–43.

[18] Forey BA, Thornton AJ, Lee PN. Systematic review with meta-analysis of the epidemiological evidence relating smoking to COPD, chronic bronchitis and emphysema. BMC Pulm Med 2011;11:36. doi:10.1186/1471-2466-11-36.

[19] Celli BR, Barnes PJ. Exacerbations of chronic obstructive pulmonary disease. Eur Respir J 2007;29:1224–38. doi:10.1183/09031936.00109906.

[20] Wells JM, Washko GR, Han MK, Abbas N, Nath H, Mamary AJ, et al. Pulmonary Arterial Enlargement and Acute Exacerbations of COPD. N Engl J Med 2012;367:913–21. doi:10.1056/NEJMoa1203830.

[21] Celli BR, Thomas NE, Anderson JA, Ferguson GT, Jenkins CR, Jones PW, et al. Effect of Pharmacotherapy on Rate of Decline of Lung Function in Chronic Obstructive Pulmonary Disease. Am J Respir Crit Care Med 2008;178:332–8. doi:10.1164/rccm.200712-1869OC.

[22] Quon BS, Gan WQ, Sin DD. Contemporary management of acute exacerbations of COPD: a systematic review and metaanalysis. Chest 2008;133:756–66. doi:10.1378/chest.07-1207.

[23] Berry CE, Wise RA. Mortality in COPD: causes, risk factors, and prevention. COPD J Chronic Obstr Pulm Dis 2010;7:375–382.

[24] on behalf of the ALIEN Network, Villar J, Blanco J, Añón JM, Santos-Bouza A, Blanch L, et al. The ALIEN study: incidence and outcome of acute respiratory distress syndrome in the era of lung protective ventilation. Intensive Care Med 2011;37:1932–41. doi:10.1007/s00134-011-2380-4.

[25] Thompson BT, Chambers RC, Liu KD. Acute Respiratory Distress Syndrome. N Engl J Med 2017;377:562–72. doi:10.1056/NEJMra1608077.

[26] Phua J, Badia JR, Adhikari NKJ, Friedrich JO, Fowler RA, Singh JM, et al. Has Mortality from Acute Respiratory Distress Syndrome Decreased over Time? Am J Respir Crit Care Med 2009;179:220–7. doi:10.1164/rccm.200805-722OC.

[27] Wheeler AP, Bernard GR. Acute lung injury and the acute respiratory distress syndrome: a clinical review. The Lancet 2007;369:1553–1564.

[28] Peniston Feliciano HL, Mahapatra S. Acute Respiratory Distress Syndrome (ARDS). StatPearls, Treasure Island (FL): StatPearls Publishing; 2017.

[29] Weinacker AB, Vaszar LT. Acute Respiratory Distress Syndrome: Physiology and New Management Strategies. Annu Rev Med 2001;52:221–37. doi:10.1146/annurev.med.52.1.221.

[30] Health NI of. ARDS Network. Ventilation with lower tidal volumes as compared with traditional tidal volumes for acute lung injury and the acute respiratory. N Engl J Med 2000;342:1301–1308.

[31] Ware LB, Matthay MA. The Acute Respiratory Distress Syndrome. N Engl J Med 2000;342:1334–49. doi:10.1056/NEJM200005043421806.

[32] Rubenfeld GD, Caldwell E, Peabody E, Weaver J, Martin DP, Neff M, et al. Incidence and Outcomes of Acute Lung Injury. N Engl J Med 2005;353:1685–93. doi:doi: 10.1056/NEJMoa050333.

[33] Annich G, Lynch W, MacLaren G, Wilson J, Bartlett R, editors. ECMO: Extracorporeal Cardiopulmonary Support in Critical Care. vol. 1. 4th ed. Ann Arbor, MI: Extracorporeal Life Support Organization; 2012.

[34] Ward NS, Dushay KM. Clinical concise review: Mechanical ventilation of patients with chronic obstructive pulmonary disease. Crit Care Med 2008;36:1614. doi:10.1097/CCM.0b013e318170f0f3.

[35] Lightowler JV, Wedzicha JA, Elliott MW, Ram FSF. Non-invasive positive pressure ventilation to treat respiratory failure resulting from exacerbations of chronic obstructive pulmonary disease: Cochrane systematic review and meta-analysis. BMJ 2003;326:185.

[36] Lund LW, Federspiel WJ. Removing extra CO2 in COPD patients. Curr Respir Care Rep 2013;2:131–8. doi:10.1007/s13665-013-0057-x.

[37] Crummy F, Buchan C, Miller B, Toghill J, Naughton MT. The use of noninvasive mechanical ventilation in COPD with severe hypercapnic acidosis. Respir Med 2007;101:53–61. doi:10.1016/j.rmed.2006.04.013.

[38] Moretti M, Cilione C, Tampieri A, Fracchia C, Marchioni A, Nava S. Incidence and causes of non-invasive mechanical ventilation failure after initial success. Thorax 2000;55:819–25. doi:10.1136/thorax.55.10.819.

[39] Confalonieri M, Garuti G, Cattaruzza MS, Osborn JF, Antonelli M, Conti G, et al. A chart of failure risk for noninvasive ventilation in patients with COPD exacerbation. Eur Respir J 2005;25:348–355.

[40] Chandra D, Stamm JA, Taylor B, Ramos RM, Satterwhite L, Krishnan JA, et al. Outcomes of Noninvasive Ventilation for Acute Exacerbations of Chronic Obstructive Pulmonary Disease in the United States, 1998–2008. Am J Respir Crit Care Med 2012;185:152–9. doi:10.1164/rccm.201106-1094OC.

[41] Phua J, Kong K, Lee KH, Shen L, Lim TK. Noninvasive ventilation in hypercapnic acute respiratory failure due to chronic obstructive pulmonary disease vs. other conditions: effectiveness and predictors of failure. Intensive Care Med 2005;31:533–9. doi:10.1007/s00134-005-2582-8.

[42] Vermeeren MA, Schols AM, Wouters EF. Effects of an acute exacerbation on nutritional and metabolic profile of patients with COPD. Eur Respir J 1997;10:2264–2269.

[43] Brower R, Matthay MA. Ventilation with Lower Tidal Volumes as Compared with Traditional Tidal Volumes for Acute Lung Injury and the Acute Respiratory Distress Syndrome. N Engl J Med 2000;342:1301–8.

[44] Rubenfeld GD, Cooper C, Carter G, Thompson BT, Hudson LD. Barriers to providing lung-protective ventilation to patients with acute lung injury. Crit Care Med 2004;32:1289–93. doi:10.1097/01.CCM.0000127266.39560.96.

[45] Kregenow DA, Rubenfeld GD, Hudson LD, Swenson ER. Hypercapnic acidosis and mortality in acute lung injury*. Crit Care Med 2006;34:1. doi:10.1097/01.CCM.0000194533.75481.03.

[46] Terragni PP, Rosboch G, Tealdi A, Corno E, Menaldo E, Davini O, et al. Tidal Hyperinflation During Low Tidal Volume Ventilation in Acute Respiratory Distress Syndrome. Am J Respir Crit Care Med 2006:200607-915OC. doi: 10.1164/rccm.200607-915OC .

[47] Terragni PP, Del Sorbo L, Mascia L, Urbino R, Martin EL, Birocco A, et al. Tidal volume lower than 6 ml/kg enhances lung protection: role of extracorporeal carbon dioxide removal. Anesthesiology 2009;111:826–35. doi:10.1097/ALN.0b013e3181b764d2.

[48] Hill JD, O'Brien TG, Murray JJ, Dontigny L, Bramson ML, Osborn JJ, et al. Prolonged extracorporeal oxygenation for acute post-traumatic respiratory failure (shock-lung syndrome) use of the Bramson membrane lung. N Engl J Med 1972;286:629–634.

[49] Marcolin R, Mascheroni D, Pesenti A, Bombino M, Gattinoni L. Ventilatory impact of partial extracorporeal CO2 removal (PECOR) in ARF patients. ASAIO J 1986;32:508–510.

[50] MacLaren G, Combes A, Bartlett RH. Contemporary extracorporeal membrane oxygenation for adult respiratory failure: life support in the new era. Intensive Care Med 2012;38:210–220.

[51] Rupprecht L, Lunz D, Philipp A, Lubnow M, Schmid C. Pitfalls in percutaneous ECMO cannulation. Heart Lung Vessels 2015;7:320–6.

[52] Vertrees RA, Nason R, Hold MD, Leeth AM, Schmalstieg FC, Boor PJ, et al. Smoke/Burn Injury-Induced Respiratory Failure Elicits Apoptosis in Ovine Lungs and Cultured Lung Cells, Ameliorated With Arteriovenous CO2 Removal*. Chest 2004;125:1472–82. doi:10.1378/chest.125.4.1472.

[53] Schmalstieg FC, Keeney SE, Rudloff HE, Palkowetz KH, Cevallos M, Zhou X, et al. Arteriovenous CO2 Removal Improves Survival Compared to High Frequency Percussive and Low Tidal Volume Ventilation in a Smoke/Burn Sheep Acute Respiratory Distress Syndrome Model. Ann Surg 2007;246:512–23. doi:10.1097/SLA.0b013e318148c6e6.

[54] Combes A, Pesenti A, Ranieri VM. Fifty Years of Research in ARDS.Is Extracorporeal Circulation the Future of Acute Respiratory Distress Syndrome Management? Am J Respir Crit Care Med 2017;195:1161–70. doi:10.1164/rccm.201701-0217CP.

[55] Peek GJ, Mugford M, Tiruvoipati R, Wilson A, Allen E, Thalanany MM, et al. Efficacy and economic assessment of conventional ventilatory support versus extracorporeal membrane oxygenation for severe adult respiratory failure (CESAR): a multicentre randomised controlled trial. The Lancet 2009;374:1351–63.

[56] Federspiel WJ, Svitek RG. Lung, artificial: current research and future directions. Encycl Biomater Biomed Eng 2004:922–931.

[57] Svitek RG, Federspiel WJ. A Mathematical Model to Predict CO2 Removal in Hollow Fiber Membrane Oxygenators. Ann Biomed Eng 2008;36:992–1003. doi:10.1007/s10439-008-9482-3.

[58] Mortensen JD, Berry G. Conceptual and design features of a practical, clinically effective intravenous mechanical blood oxygen/carbon dioxide exchange device (IVOX). Int J Artif Organs 1989;12:384–389.

[59] Mihelc KM, Frankowski BJ, Lieber SC, Moore ND, Hattler BG, Federspiel WJ. Evaluation of a Respiratory Assist Catheter that Uses an Impeller Within a Hollow Fiber Membrane Bundle: ASAIO J 2009;55:569–74. doi:10.1097/MAT.0b013e3181bc2655.

[60] Jeffries RG, Lund L, Frankowski B, Federspiel WJ. An extracorporeal carbon dioxide removal (ECCO2R) device operating at hemodialysis blood flow rates. Intensive Care Med Exp 2017;5. doi:10.1186/s40635-017-0154-1.

[61] Geers C, Gros G. Carbon Dioxide Transport and Carbonic Anhydrase in Blood and Muscle. Physiol Rev 2000;80:681–715.

[62] Longmuir IS, Forster RE, Woo C-Y. Diffusion of carbon dioxide through thin layers of solution. Nature 1966;209:393.

[63] Forster RE, Itada N. Carbonic anhydrase activity in intact red cells as measured by means of 18 O exchange between CO 2 and water. Biophys. Physiol. Carbon Dioxide, Springer; 1980, p. 177–183.

[64] Klocke RA. Potential role of endothelial carbonic anhydrase in dehydration of plasma bicarbonate. Trans Am Clin Climatol Assoc 1997;108:44–58.

[65] Zimmermann M, Bein T, Arlt M, Philipp A, Rupprecht L, Mueller T, et al. Pumpless extracorporeal interventional lung assist in patients with acute respiratory distress syndrome: a prospective pilot study. Crit Care 2009;13:R10. doi:10.1186/cc7703.

[66] Bein T, Weber F, Philipp A, Prasser C, Pfeifer M, Schmid F-X, et al. A new pumpless extracorporeal interventional lung assist in critical hypoxemia/hypercapnia*. Crit Care Med 2006;34:1372–7. doi:10.1097/01.CCM.0000215111.85483.BD.

[67] Jeffries RG, Mussin Y, Bulanin DS, Lund LW, Kocyildirim E, Zhumadilov ZZ, et al. Pre-clinical evaluation of an adult extracorporeal carbon dioxide removal system with active mixing for pediatric respiratory support. Int J Artif Organs 2014;37:888–99. doi:10.5301/ijao.5000372.

[68] Galletti P., Colton C. Artificial Lungs and Blood– Gas Exchange Devices. Biomed Eng Handb Bronzino JD Ed CRC Press LLC Boca Raton 2000:1–19.

[69] Snider MT, Chaudhari SN, Richard RB, Whitcomb DR, Russell GB. Augmentation of CO2 Transfer in Membrane Lungs by the Infusion of a Metabolizable Organic Acid. ASAIO J 1987;33.

[70] Zanella A, Patroniti N, Isgrò S, Albertini M, Costanzi M, Pirrone F, et al. Blood acidification enhances carbon dioxide removal of membrane lung: an experimental study. Intensive Care Med 2009;35:1484–7. doi:10.1007/s00134-009-1513-5.

[71] Zanella A, Giani M, Redaelli S, Mangili P, Scaravilli V, Ormas V, et al. Infusion of 2.5 meq/min of lactic acid minimally increases CO2 production compared to an isocaloric glucose infusion in healthy anesthetized, mechanically ventilated pigs. Crit Care 2013;17:R268. doi:10.1186/cc13098.

[72] Zanella A, Mangili P, Redaelli S, Scaravilli V, Giani M, Ferlicca D, et al. Regional Blood Acidification Enhances Extracorporeal Carbon Dioxide Removal: A 48-hour Animal Study. Anesthesiology 2014;120:416–24. doi:10.1097/ALN.0000000000000099.

[73] Zanella A, Mangili P, Giani M, Redaelli S, Scaravilli V, Castagna L, et al. Extracorporeal carbon dioxide removal through ventilation of acidified dialysate: An experimental study. J Heart Lung Transplant n.d. doi:10.1016/j.healun.2013.12.006.

[74] MIZOCK BA, FALK JL. Lactic acidosis in critical illness. Crit Care Med 1992;20.

[75] Mikkelsen ME, Miltiades AN, Gaieski DF, Goyal M, Fuchs BD, Shah CV, et al. Serum lactate is associated with mortality in severe sepsis independent of organ failure and shock*: Crit Care Med 2009;37:1670–7. doi:10.1097/CCM.0b013e31819fcf68.

[76] Khosravani H, Shahpori R, Stelfox HT, Kirkpatrick AW, Laupland KB. Occurrence and adverse effect on outcome of hyperlactatemia in the critically ill. Crit Care 2009;13:R90.

[77] Gutierrez G, Williams JD. The riddle of hyperlactatemia. Crit Care 2009;13:176.

[78] Fall PJ, Szerlip HM. Lactic Acidosis: From Sour Milk to Septic Shock. J Intensive Care Med 2005;20:255–71. doi:10.1177/0885066605278644.

[79] Demers P, Elkouri S, Martineau R, Couturier A, Cartier R. Outcome with high blood lactate levels during cardiopulmonary bypass in adult cardiac operation. Ann Thorac Surg 2000;70:2082–6. doi:10.1016/S0003-4975(00)02160-3.

[80] Zanella A, Castagna L, Salerno D, Scaravilli V, Abd El Aziz El Sayed Deab S, Magni F, et al. Respiratory Electrodialysis. A Novel, Highly Efficient Extracorporeal CO2 Removal Technique. Am J Respir Crit Care Med 2015;192:719–26. doi:10.1164/rccm.201502-0289OC.

[81] Zanella A, Castagna L, El Sayed SAEA, Scaravilli V, Ferlicca D, Magni F, et al. Extracorporeal CO2 Removal by Respiratory Electrodialysis: An In Vitro Study. ASAIO J 2016;62:143–149.

[82] Arazawa DT, Oh H-I, Ye S-H, Johnson Jr. CA, Woolley JR, Wagner WR, et al. Immobilized carbonic anhydrase on hollow fiber membranes accelerates CO2 removal from blood. J Membr Sci 2012;403–404:25–31. doi:10.1016/j.memsci.2012.02.006.

[83] Greene R. Pulmonary vascular obstruction in the adult respiratory distress syndrome. J Thorac Imaging 1986;1.

[84] Tomashefski JF, Davies P, Boggis C, Greene R, Zapol WM, Reid LM. The pulmonary vascular lesions of the adult respiratory distress syndrome. Am J Pathol 1983;112:112–26.

[85] Kaar JL, Oh H-I, Russell AJ, Federspiel WJ. Towards improved artificial lungs through biocatalysis. Biomaterials 2007;28:3131–9. doi:doi: DOI: 10.1016/j.biomaterials.2007.03.021.

[86] Ye S-H, Johnson CA Jr, Woolley JR, Snyder TA, Gamble LJ, Wagner WR. Covalent surface modification of a titanium alloy with a phosphorylcholine-containing copolymer for reduced thrombogenicity in cardiovascular devices. J Biomed Mater Res A 2009;91:18–28. doi:10.1002/jbm.a.32184.

[87] Ye S-H, Johnson Jr. CA, Woolley JR, Murata H, Gamble LJ, Ishihara K, et al. Simple surface modification of a titanium alloy with silanated zwitterionic phosphorylcholine or sulfobetaine modifiers to reduce thrombogenicity. Colloids Surf B Biointerfaces 2010;79:357–64. doi:10.1016/j.colsurfb.2010.04.018.

[88] Goddard JM, Hotchkiss JH. Polymer surface modification for the attachment of bioactive compounds. Prog Polym Sci 2007;32:698–725. doi:10.1016/j.progpolymsci.2007.04.002.

[89] Mao C, Qiu Y, Sang H, Mei H, Zhu A, Shen J, et al. Various approaches to modify biomaterial surfaces for improving hemocompatibility. Adv Colloid Interface Sci 2004;110:5–17. doi:10.1016/j.cis.2004.02.001.

[90] Florchinger B, Philipp A, Klose A, Hilker M, Kobuch R, Rupprecht L, et al. Pumpless Extracorporeal Lung Assist: A 10-Year Institutional Experience. Ann Thorac Surg 2008;86:410–7. doi:10.1016/j.athoracsur.2008.04.045.

[91] Michanetzis GPA, Katsala N, Missirlis YF. Comparison of haemocompatibility improvement of four polymeric biomaterials by two heparinization techniques. Biomaterials 2003;24:677–88. doi:10.1016/S0142-9612(02)00382-4.

[92] Kohn J, Wilchek M. A colorimetric method for monitoring activation of sepharose by cyanogen bromide. Biochem Biophys Res Commun 1978;84:7–14. doi:10.1016/0006-291X(78)90255-3.

[93] Tamada Y, Kulik EA, Ikada Y. Simple method for platelet counting. Biomaterials 1995;16:259–61. doi:doi: DOI: 10.1016/0142-9612(95)92126-Q.

[94] Grigat E, Pütter R. Chemie der Cyansäureester, I. Cyansäureester aus Hydroxylverbindungen und Halogencyan. Chem Ber 1964;97:3012–7. doi:10.1002/cber.19640971107.

[95] Kohn J, Wilchek M. A new approach (cyano-transfer) for cyanogen bromide activation of Sepharose at neutral pH, which yields activated resins, free of interfering nitrogen derivatives. Biochem Biophys Res Commun 1982;107:878–84. doi:10.1016/0006-291X(82)90604-0.

[96] Jurado LA, Mosley J, Jarrett HW. Cyanogen bromide activation and coupling of ligands to diol-containing silica for high-performance affinity chromatography: Optimization of conditions. J Chromatogr A 2002;971:95–104. doi:10.1016/S0021-9673(02)00964-0.

[97] Kohn J, Wilchek M. The use of cyanogen bromide and other novel cyanylating agents for the activation of polysaccharide resins. Appl Biochem Biotechnol 1984;9:285-305–305.

[98] Axéan R, Ernback S. Chemical Fixation of Enzymes to Cyanogen Halide Activated Polysaccharide Carriers. Eur J Biochem 1971;18:351–60. doi:10.1111/j.1432-1033.1971.tb01250.x.

[99] Duerksen PJ, Wilkinson KD. Immobilization of proteins via arginine residues. Anal Biochem 1987;160:444–54. doi:10.1016/0003-2697(87)90074-1.

[100] Schall CA, Wiencek JM. Stability of nicotinamide adenine dinucleotide immobilized to cyanogen bromide activated agarose. Biotechnol Bioeng 1997;53:41–8. doi:10.1002/(SICI)1097-0290(19970105)53:1<41::AID-BIT7>3.0.CO;2-Z.

[101] Zhou X, Loran DB, Wang D, Hyde BR, Lick SD, Zwischenberger JB. Seventy-two hour gas exchange performance and hemodynamic properties of NOVALUNG®iLA as a gas exchanger for arteriovenous carbon dioxide removal. Perfusion 2005;20:303–8. doi:10.1191/0267659105pf838oa.

[102] Wang Z-G, Wan L-S, Liu Z-M, Huang X-J, Xu Z-K. Enzyme immobilization on electrospun polymer nanofibers: An overview. J Mol Catal B Enzym 2009;56:189–95. doi:10.1016/j.molcatb.2008.05.005.

[103] Algar WR, Prasuhn DE, Stewart MH, Jennings TL, Blanco-Canosa JB, Dawson PE, et al. The Controlled Display of Biomolecules on Nanoparticles: A Challenge Suited to Bioorthogonal Chemistry. Bioconjug Chem 2011;22:825–58. doi:10.1021/bc200065z.

[104] Wong LS, Khan F, Micklefield J. Selective Covalent Protein Immobilization: Strategies and Applications. Chem Rev 2009;109:4025–53. doi:10.1021/cr8004668.

[105] Liu T-Y, Lin W-C, Huang L-Y, Chen S-Y, Yang M-C. Hemocompatibility and anaphylatoxin formation of protein-immobilizing polyacrylonitrile hemodialysis membrane. Biomaterials 2005;26:1437–44. doi:10.1016/j.biomaterials.2004.04.039.

[106] Sperling C, Houska M, Brynda E, Streller U, Werner C. In vitro hemocompatibility of albumin–heparin multilayer coatings on polyethersulfone prepared by the layer-by-layer technique. J Biomed Mater Res A 2006;76A:681–9. doi:10.1002/jbm.a.30519.

[107] Lin W-C, Liu T-Y, Yang M-C. Hemocompatibility of polyacrylonitrile dialysis membrane immobilized with chitosan and heparin conjugate. Biomaterials 2004;25:1947–57. doi:10.1016/j.biomaterials.2003.08.027.

[108] Oh H, Ye S, Johnson Jr CA, Woolley JR, Federspiel WJ, Wagner WR. Hemocompatibility Assessment of Carbonic Anhydrase Modified Hollow Fiber Membranes for Artificial Lungs. Artif Organs 2010;34:439–42. doi:10.1111/j.1525-1594.2009.00882.x.

[109] Aamand R, Dalsgaard T, Jensen FB, Simonsen U, Roepstorff A, Fago A. Generation of nitric oxide from nitrite by carbonic anhydrase: a possible link between metabolic activity and vasodilation. Am J Physiol - Heart Circ Physiol 2009;297:H2068–74. doi:10.1152/ajpheart.00525.2009.

[110] Frost MC, Reynolds MM, Meyerhoff ME. Polymers incorporating nitric oxide releasing/generating substances for improved biocompatibility of blood-contacting medical devices. Biomaterials 2005;26:1685–93. doi:10.1016/j.biomaterials.2004.06.006.

[111] Alp E, Voss A. Ventilator associated pneumonia and infection control. Ann Clin Microbiol Antimicrob 2006;5:7. doi:10.1186/1476-0711-5-7.

[112] Ranieri VM, Suter PM, Tortorella C, De Tullio R, Dayer JM, Brienza A, et al. Effect of mechanical ventilation on inflammatory mediators in patients with acute respiratory distress syndrome: a randomized controlled trial. JAMA J Am Med Assoc 1999;282:54–61.

[113] Conrad S, Zwischenberger J, Grier L, Alpard S, Bidani A. Total extracorporeal arteriovenous carbon dioxide removal in acute respiratory failure: a phase I clinical study. Intensive Care Med 2001;27:1340–51. doi:10.1007/s001340100993.

[114] Kimmel JD, Arazawa DT, Ye S-H, Shankarraman V, Wagner WR, Federspiel WJ. Carbonic anhydrase immobilized on hollow fiber membranes using glutaraldehyde activated chitosan for artificial lung applications. J Mater Sci Mater Med 2013;24:2611–21. doi:10.1007/s10856-013-5006-2.

[115] Hermanson GT. Bioconjugate Techniques. Academic Press; 2013.

[116] Hayakawa T, Yoshinari M, Nemoto K. Characterization and protein-adsorption behavior of deposited organic thin film onto titanium by plasma polymerization with hexamethyldisiloxane. Biomaterials 2004;25:119–27. doi:10.1016/S0142-9612(03)00484-8.

[117] Hamerli P, Weigel T, Groth T, Paul D. Surface properties of and cell adhesion onto allylamine-plasma-coated polyethylenterephtalat membranes. Biomaterials 2003;24:3989–99. doi:10.1016/S0142-9612(03)00312-0.

[118] Vickers NJ, McArthur SL, Shard AG, MacNeil S. Ceric Ammonium Nitrate Initiated Grafting of PEG to Plasma Polymers for Cell-Resistant Surfaces. Plasma Process Polym 2008;5:192–201. doi:10.1002/ppap.200700062.

[119] Calderon JG, Harsch A, Gross GW, Timmons RB. Stability of plasma-polymerized allylamine films with sterilization by autoclaving. J Biomed Mater Res 1998;42:597–603. doi:10.1002/(SICI)1097-4636(19981215)42:4<597::AID-JBM16>3.0.CO;2-R.

[120] Harsch A, Calderon J, Timmons RB, Gross GW. Pulsed plasma deposition of allylamine on polysiloxane: a stable surface for neuronal cell adhesion. J Neurosci Methods 2000;98:135–44. doi:10.1016/S0165-0270(00)00196-5.

[121] Ruiz J, St-Georges-Robillard A, Thérésy C, Lerouge S, Wertheimer MR. Fabrication and Characterisation of Amine-Rich Organic Thin Films: Focus on Stability. Plasma Process Polym 2010;7:737–53. doi:10.1002/ppap.201000042.

[122] Förch R, Zhang Z, Knoll W. Soft Plasma Treated Surfaces: Tailoring of Structure and Properties for Biomaterial Applications. Plasma Process Polym 2005;2:351–72. doi:10.1002/ppap.200400083.

[123] Eash HJ, Jones HM, Hattler BG, Federspiel WJ. Evaluation of Plasma Resistant Hollow Fiber Membranes For Artificial Lungs. ASAIO J 2004;50.

[124] Horbett TA. Principles underlying the role of adsorbed plasma proteins in blood interactions with foreign materials. Cardiovasc Pathol 1993;2:137–148.

[125] Wan J, Thomas MS, Guthrie S, Vullev VI. Surface-Bound Proteins with Preserved Functionality. Ann Biomed Eng 2009;37:1190–205. doi:10.1007/s10439-009-9673-6.

[126] A. Sheldon R, Pelt S van. Enzyme immobilisation in biocatalysis: why, what and how. Chem Soc Rev 2013;42:6223–35. doi:10.1039/C3CS60075K.

[127] Manta C, Ferraz N, Betancor L, Antunes G, Batista-Viera F, Carlsson J, et al. Polyethylene glycol as a spacer for solid-phase enzyme immobilization. Enzyme Microb Technol 2003;33:890–8. doi:10.1016/S0141-0229(03)00221-7.

[128] Soares AL, Guimar\ aes GM, Polakiewicz B, Pitombo RN., Abrah\ ao-Neto J. Effects of polyethylene glycol attachment on physicochemical and biological stability of E. coli-asparaginase. Int J Pharm 2002;237:163–170.

[129] Zalipsky S. Chemistry of polyethylene glycol conjugates with biologically active molecules. Adv Drug Deliv Rev 1995;16:157–182.

[130] Bindhu LV, Abraham ET. Immobilization of horseradish peroxidase on chitosan for use in nonaqueous media. J Appl Polym Sci 2003;88:1456–64. doi:10.1002/app.11815.

[131] Akkuş Çetinus Ş, Nursevin Öztop H. Immobilization of catalase into chemically crosslinked chitosan beads. Enzyme Microb Technol 2003;32:889–94. doi:10.1016/S0141-0229(03)00065-6.

[132] Cook AD, Pajvani UB, Hrkach JS, Cannizzaro SM, Langer R. Colorimetric analysis of surface reactive amino groups on poly(lactic acid-co-lysine):poly(lactic acid) blends. Biomaterials 1997;18:1417–24. doi:16/S0142-9612(97)00075-6.

[133] Abbas A, Vivien C, Bocquet B, Guillochon D, Supiot P. Preparation and Multi-Characterization of Plasma Polymerized Allylamine Films. Plasma Process Polym 2009;6:593–604. doi:10.1002/ppap.200900016.

[134] Di Mundo R, Ricci M, d'Agostino R, Fracassi F, Palumbo F. PECVD of Low Carbon Content Silicon Nitride-Like Thin Films with Dimethylaminosilanes. Plasma Process Polym 2007;4:S21–6. doi:10.1002/ppap.200730203.

[135] Nordell BJ, Keck CL, Nguyen TD, Caruso AN, Purohit SS, Lanford WA, et al. Tuning the properties of a complex disordered material: Full factorial investigation of PECVD-grown amorphous hydrogenated boron carbide. Mater Chem Phys 2016;173:268–84. doi:10.1016/j.matchemphys.2016.02.013.

[136] Beck AJ, Candan S, Short RD, Goodyear A, Braithwaite NSJ. The Role of Ions in the Plasma Polymerization of Allylamine. J Phys Chem B 2001;105:5730–6. doi:10.1021/jp0043468.

[137] Denis L, Cossement D, Godfroid T, Renaux F, Bittencourt C, Snyders R, et al. Synthesis of Allylamine Plasma Polymer Films: Correlation between Plasma Diagnostic and Film Characteristics. Plasma Process Polym 2009;6:199–208. doi:10.1002/ppap.200800137.

[138] Denis L, Marsal P, Olivier Y, Godfroid T, Lazzaroni R, Hecq M, et al. Deposition of Functional Organic Thin Films by Pulsed Plasma Polymerization: A Joint Theoretical and Experimental Study. Plasma Process Polym 2010;7:172–81. doi:10.1002/ppap.200900131.

[139] Silverman DN, Lindskog S. The catalytic mechanism of carbonic anhydrase: implications of a rate-limiting protolysis of water. Acc Chem Res 1988;21:30–6. doi:10.1021/ar00145a005.

[140] Lindskog S, Silverman DN. The catalytic mechanism of mammalian carbonic anhydrases. Carbonic Anhydrases, Birkhäuser, Basel; 2000, p. 175–95. doi:10.1007/978-3-0348-8446-4_10.

[141] Talbert JN, Goddard JM. Enzymes on material surfaces. Colloids Surf B Biointerfaces 2012;93:8–19.

[142] Lund LW, Hattler BG, Federspiel WJ. Gas permeance measurement of hollow fiber membranes in gas-liquid environment. AIChE J 2002;48:635–643.

[143] Fery A, Schöler B, Cassagneau T, Caruso F. Nanoporous Thin Films Formed by Salt-Induced Structural Changes in Multilayers of Poly(acrylic acid) and Poly(allylamine). Langmuir 2001;17:3779–83. doi:10.1021/la0102612.

[144] Saito R, Sato T, Ikai A, Tanaka N. Structure of bovine carbonic anhydrase II at 1.95 Å resolution. Acta Crystallogr D Biol Crystallogr 2004;60:792–5. doi:10.1107/S0907444904003166.

[145] Arazawa DT, Kimmel JD, Federspiel WJ. Kinetics of CO2 exchange with carbonic anhydrase immobilized on fiber membranes in artificial lungs. J Mater Sci Mater Med 2015;26. doi:10.1007/s10856-015-5525-0.

[146] Boone CD, Habibzadegan A, Tu C, Silverman DN, McKenna R. Structural and catalytic characterization of a thermally stable and acid-stable variant of human carbonic anhydrase II containing an engineered disulfide bond. Acta Crystallogr D Biol Crystallogr 2013;69:1414–22. doi:10.1107/S0907444913008743.

[147] Dodgson SJ, Forster RE. Carbonic Anhydrase Activity of Intact Erythrocytes from Seven Mammals. J Appl Physiol 1983;55:1292–8.

[148] ANSI/AAMI/ISO 7199:2009 -- Cardiovascular implants and artificial organs — Blood-gas exchangers (oxygenators) 2009.

[149] Gilmour KM. Perspectives on carbonic anhydrase. Comp Biochem Physiol - Part Mol Integr Physiol 2010;157:193–7. doi:10.1016/j.cbpa.2010.06.161.

[150] Thorslund A, Lindskog S. Studies of the Esterase Activity and the Anion Inhibition of Bovine Zinc and Cobalt Carbonic Anhydrases. Eur J Biochem 1967;3:117–23. doi:10.1111/j.1432-1033.1967.tb19504.x.

[151] Khalifah RG. Carbon dioxide hydration activity of carbonic anhydrase: paradoxical consequences of the unusually rapid catalysis. Proc Natl Acad Sci 1973;70:1986–1989.

[152] Hasinoff BB. Kinetics of carbonic anhydrase catalysis in solvents of increased viscosity: a partially diffusion-controlled reaction. Arch Biochem Biophys 1984;233:676–81.

[153] Truskey GA, Yuan F, Katz DF. Transport Phenomena in Biological Systems. 2 edition. Upper Saddle River, N.J.: Prentice Hall; 2009.

[154] Jeffries RG, Frankowski BJ, Burgreen GW, Federspiel WJ. Effect of Impeller Design and Spacing on Gas Exchange in a Percutaneous Respiratory Assist Catheter: Impeller Testing for a Respiratory Assist Catheter. Artif Organs 2014:n/a-n/a. doi:10.1111/aor.12308.

[155] Arazawa DT, Kimmel JD, Finn MC, Federspiel WJ. Acidic sweep gas with carbonic anhydrase coated hollow fiber membranes synergistically accelerates CO2 removal from blood. Acta Biomater 2015;25:143–9. doi:10.1016/j.actbio.2015.07.007.

[156] Terragni PP, Del Sorbo L, Mascia L, Urbino R, Martin EL, Birocco A, et al. Tidal volume lower than 6 ml/kg enhances lung protection: role of extracorporeal carbon dioxide removal. Anesthesiology 2009;111:826–35. doi:10.1097/ALN.0b013e3181b764d2.

[157] Calverley PMA. Respiratory failure in chronic obstructive pulmonary disease. Eur Respir J 2003;22:26s-30s. doi:10.1183/09031936.03.00030103.

[158] Budweiser S, Jörres RA, Pfeifer M. Treatment of respiratory failure in COPD. Int J Chron Obstruct Pulmon Dis 2008;3:605.

[159] Reddy RM, Guntupalli KK. Review of ventilatory techniques to optimize mechanical ventilation in acute exacerbation of chronic obstructive pulmonary disease. Int J Chron Obstruct Pulmon Dis 2007;2:441.

[160] BOND SJ, STEWART DL, NAGARAJ HS, WINSTON S, GROFF DB. Complicated Cannula Insertions and Cannula Dislodgments Associated With Extracorporeal Membrane Oxygenation. ASAIO J 1998;44.

[161] Gunnison AF. Sulphite toxicity: A critical review of in vitro and in vivo data. Food Cosmet Toxicol 1981;19:667–82. doi:10.1016/0015-6264(81)90519-8.

[162] Pocker Y, Beug MW. Kinetic studies of bovine carbonic anhydrase catalyzed hydrolyses of p-substituted phenyl esters. Biochemistry (Mosc) 1972;11:698–707. doi:10.1021/bi00755a005.

[163] Sander R. Compilation of Henry's law constants for inorganic and organic species of potential importance in environmental chemistry. Max-Planck Institute of Chemistry, Air Chemistry Department; 1999.

[164] Langer T, Scotti E, Carlesso E, Protti A, Zani L, Chierichetti M, et al. Electrolyte shifts across the artificial lung in patients on extracorporeal membrane oxygenation:

Interdependence between partial pressure of carbon dioxide and strong ion difference. J Crit Care 2015;30:2–6. doi:10.1016/j.jcrc.2014.09.013.

[165] Fogh-Andersen N, Bjerrum PJ, Siggaard-Andersen O. Ionic binding, net charge, and Donnan effect of human serum albumin as a function of pH. Clin Chem 1993;39:48–52.

[166] Vally H, Misso NLA, Madan V. Clinical effects of sulphite additives. Clin Exp Allergy 2009;39:1643–1651. doi:10.1111/j.1365-2222.2009.03362.x.

[167] Schweigert BS, Chichester CO, Mrak EM. ADVANCES IN FOOD RESEARCH. Academic Press; 1986.

[168] Lester MR. Sulfite sensitivity: significance in human health. J Am Coll Nutr 1995;14:229–32.

[169] B N, Ar E. Final report on the safety assessment of sodium sulfite, potassium sulfite, ammonium sulfite, sodium bisulfite, ammonium bisulfite, sodium metabisulfite and potassium metabisulfite. Int J Toxicol 2002;22 Suppl 2:63–88.

[170] Veldman A, Santamaria-Araujo JA, Sollazzo S, Pitt J, Gianello R, Yaplito-Lee J, et al. Successful Treatment of Molybdenum Cofactor Deficiency Type A With cPMP. Pediatrics 2010;125:e1249–54. doi:10.1542/peds.2009-2192.

[171] Shapiro R. Genetic effects of bisulfite (sulfur dioxide). Mutat Res Genet Toxicol 1977;39:149–75. doi:10.1016/0165-1110(77)90020-3.

[172] Gunnison AF, Farruggella TJ. Preferential S-sulfonate formation in lung and aorta. Chem Biol Interact 1979;25:271–7.

[173] Gunnison AF, Palmes ED. Species variability in plasma S-sulfonate levels during and following sulfite administration. Chem Biol Interact 1978;21:315–29. doi:10.1016/0009-2797(78)90029-7.

[174] Pundir CS, Rawal R. Determination of sulfite with emphasis on biosensing methods: a review. Anal Bioanal Chem 2013;405:3049–62. doi:10.1007/s00216-013-6753-0.

[175] Sulfites as Food Additives. Nutr Rev 1976;34:58–62. doi:10.1111/j.1753-4887.1976.tb05697.x.

[176] Gunnison AF, Bresnahan CA, Palmes ED. Comparative sulfite metabolism in the rat, rabbit, and rhesus monkey. Toxicol Appl Pharmacol 1977;42:99–109. doi:10.1016/0041-008X(77)90200-9.

[177] Jr WJ, Jr GJ, Jm W. Toxicity of intraperitoneal bisulfite. Clin Pharmacol Ther 1967;9:328–32.

[178] Ji AJ, Savon SR, Jacobsen DW. Determination of total serum sulfite by HPLC with fluorescence detection. Clin Chem 1995;41:897–903.

[179] Burki NK, Mani RK, Herth FJF, Schmidt W, Teschler H, Bonin F, et al. A novel extracorporeal CO2 removal system: Results of a pilot study in COPD patients with hypercapnic respiratory failure. CHEST J 2012. doi:10.1378/chest.12-0228.